The Role of the Collagen Receptor, Discoidin Domain Receptor 2 (DDR2) in Craniofacial Development

by

Fatma Faiez A. Mohamed

A dissertation submitted in partial fulfillment
of the requirements for the degree of
Doctor of Philosophy
(Oral Health Sciences)
in the University of Michigan
2019

Doctoral Committee:

Professor Renny T. Franceschi, Chair
Associate Professor Nan Hatch
Professor Vesa Kaartinen
Associate Professor Daniel Lucas-Alcaraz

Fatma Faiez A. Mohamed

fmohamed@umich.edu

ORCID iD: 0000-0003-1008-6541

DEDICATION

To my parents, my husband and my siblings

ACKNOWLEDGEMENTS

I would like to thank all people who have made this dissertation possible:

Dr. Renny Franceschi, my dissertation advisor. I am extremely grateful for your mentorship, invaluable guidance and support over the years of my doctoral studies. Thank you for all the opportunities you offered to me and for ongoing support to pursue a career in biomedical research.

My dissertation committee members: Dr. Vesa Kaartinen, Dr. Daniel Lucas-Alcaraz, and Dr. Nan Hatch. Thank you to your collaboration, valuable feedback and insightful suggestions.

Past and current Franceschi Lab members: Chunxi Ge, Yan Li, Abdulaziz Binrayes, and Hanshi Sun. Thank you for your contribution to this research, friendship and support. I do not think I could have done all this by myself. A special thanks to Chunxi Ge for fruitful discussion, providing necessary reagents, and developing $Ddr2^{fl/fl}$ and Ddr2-LacZ knock-in mouse models indispensable for this work, and to past lab member Guisheng Zhao who first taught me basic laboratory skills and methods in cellular and molecular biology.

The Oral Health Science (OHS) Program: The program director Dr. Vesa Kaartinen, past and current program staff Patricia Schultz, Manette London, Kimberly Smith, Amy Watson, Melissa Karby, and Sarah Gawne. Thank you for your dedication for the OHS

program, support, and administrative assistant. Thank you to all OHS faculty for contribution to the program success.

I am indebted and thankful to the former OHS program director and pre-candidate advisor, Dr. Jan Ching Chun Hu, for strong support, guidance, and encouragement during my years in the program.

Dean Laurie McCauley. Thank you for your support for OHS graduate students and for service and outstanding leadership.

The past and current OHS graduate students. Thank you for the wonderful friendship and peer support over the years in the program.

My thanks to Dr. David H. Kohn and Dr. Peter X. Ma laboratories for the great opportunity to get my first exposure to research in bone biology and tissue engineering. I am particularly thankful to Dr. Joseph Gardinier, a past postdoc in David Kohn's laboratory, for research training and directions as I co-authored my first publication.

I would also like to express my strong appreciation to: Dr. Yuji Mishina (University of Michigan, Ann Arbor, USA) for providing the Gli1-CreERT knock-in mice; Dr. Stina Schipani (University of Michigan, Ann Arbor, USA) for providing the Col2-Cre transgenic mice; Dr. Greenberg, B. H. (University of California-San Diego, La Jolla, California) for providing Ddr2$^{mer\text{-}iCre\text{-}mer}$ mice; and Dr. Noriaki Ono (University of Michigan, Ann Arbor, USA) for providing Ai14; tdTomato reporter mice.

I would also like to gratefully acknowledge the technical assistance and helpful advice from Christopher Strayhorn (Dental School Histology Core), Michelle Lynch (MicroCT Core) and from Taocong Jin (Office of Research).

I am extremely grateful for all funding sources for financial support throughout my graduate studies, including the Libyan Government Scholarship from the Libyan Ministry of Higher Education and Scientific Research, graduate student research assistantship from the University of Michigan, pre-candidate and candidate research grants, OHS block grants, Rackham Graduate School travel grants, NIH/NIDCR grant DE11723 and research funds from the Department of Periodontics and Oral Medicine-University of Michigan School of Dentistry (to R.T.F.), and the Michigan Musculoskeletal Health Core Center (NIH/NIAMS P30 AR069620).

I cannot begin to express my gratitude to my wonderful family: my parents, my husband, and my siblings for your tremendous support at many levels during the years of my life. My dear husband Abdalla Alaowami. Thank you very much for being very supportive and extremely patient. What I accomplished today would not have been possible without your love and relentless support.

TABLE OF CONTENTS

LIST OF FIGURES

LIST OF TABLES

ABSTRACT

Defects in cranial growth and development cause a wide range of disorders known to dramatically impact physical, social, and emotional development of affected children. An understanding of the critical molecules and pathways necessary for craniofacial development is necessary to successfully treat these patients. Development of craniofacial bones requires interactions between progenitor cells and the collagen-rich extracellular matrix. Cell-matrix interactions are critical for normal proliferation, differentiation, migration and remodeling, and required to maintain the shapes of individual bones and their relative proportions (reviewed in Chapter 1). DDR2 is a receptor tyrosine kinase that is activated by triple helical collagens abundant in the bone extracellular matrix (ECM). Inactivating mutations in DDR2 cause spondylo-meta-epiphyseal dysplasia, short limbs and abnormal calcification, a rare, autosomal inherited human disorder associated with distinct craniofacial defects including prominent forehead, wide open fontanels, hypertelorism, a short nose with a depressed nasal bridge, a long philtrum, micrognathia, and abnormal teeth. *Ddr2*-deficient mice also exhibited craniofacial abnormalities including eye protrusion, short snout, and impaired intramembranous ossification associated with delayed suture formation. However, the specific functions of DDR2 in craniofacial development have not been previously described. In Chapter 2, a detailed characterization of *Ddr2*-knockout skulls identified growth defects in calvarial and cranial base bones that were most dramatic in the anterior part of skull. *Ddr2*-deficient mice also exhibited features of delayed endochondral ossification at the cranial base due to chondrocyte disorganization,

deficient chondrocyte proliferation, and abnormalities in cartilage ECM distribution and turnover. As a perquisite for understanding its function, the distribution of *Ddr2* expression was examined using a *Ddr2*-LacZ knock-in mouse model. Using this approach, potential cellular sites of DDR2 action were identified in cranial sutures, periosteum, dura mater, and resting and proliferative chondrocytes of cranial base synchondroses, regions enriched in skeletal stem cells. However, *Ddr2*-LacZ expression could not be detected in terminally differentiated cells, such as hypertrophic chondrocytes and osteocytes, suggesting a potential role in stem/progenitor cell function. Intriguingly, our experiments showed that *Ddr2* and Gli1, a mediator of hedgehog signaling, are in overlapping cell populations. Gli1 is associated with sutural stem cells and mesenchymal metaphyseal osteoprogenitors in long bones. In support of our hypothesis that *Ddr2* functions in skeletal stem/progenitor cells, genetic labeling of *Ddr2*-expressing cells using *Ddr2*$^{\text{Mer-icre-Mer}}$ mice bred to Ai14 tdTomato reporter mice revealed the contribution of *Ddr2*-expressing cells to chondrocyte, osteoblast, osteocyte, and marrow-lining cell lineages. Additional experiments involving tissue-specific knockout approaches established a critical function of *Ddr2* in skeletal progenitors cells (Gli1- and Col2-expressing cells) to control chondrocyte and osteoblast differentiation during postnatal craniofacial bone formation. Collagen-mediated signaling is also critical for tissue differentiation and mineralization in tooth dentin and alveolar bone. In Chapter 3, in vivo and in vitro studies demonstrated the requirement for DDR2 signaling in tooth root development, periodontal ligament (PDL) integrity, and alveolar bone maintenance. Furthermore, *Ddr2*-LacZ expression identified *Ddr2* in dental follicle and dental papilla in developing tooth and in dentin-forming odontoblasts and PDL cells in mature teeth. Additional studies revealed DDR2 regulation of RUNX2 phosphorylation as a potential mechanism for tooth root development. Lastly, Chapter 4 summarizes the main findings of this dissertation and suggests future directions for this research. Together, this

dissertation advances our understanding of the roles of cell-matrix interactions in craniofacial development by establishing the functions of a new collagen receptor.

CHAPTER I

Introduction

Craniofacial abnormalities, which are among the most common birth defects, impact the physical, social, and emotional development of affected children (Fish 2016; Trainor and Richtsmeier 2015). Unfortunately, treatment modalities still remain limited due to our incomplete understanding of development and diseases of the craniofacial skeleton. Therefore, it is essential to advance our knowledge on signaling pathways and common mechanisms involved in regulation of craniofacial complex, as a basis for discovering new therapies for craniofacial diseases.

During craniofacial development, cells of skeletal elements interact with their surrounding extracellular matrix (ECM) through cell-surface receptors and their signaling pathways. The ECM-cell interaction regulates cell proliferation, migration, differentiation and remodeling to develop and maintain the shapes of individual bones and the relative proportions of the skeleton [reviewed in (Erlebacher et al. 1995)]. Therefore, understanding the contribution of ECM-mediated signaling is critical for understanding the development of craniofacial skeleton and disease. The goal of this dissertation is to elucidate the function of discoidin domain receptor 2 (DDR2) in postnatal development of craniofacial skeleton. DDR2 is a receptor tyrosine kinase that directly mediates the interaction of skeletal cells with triple helical collagens present in the bone ECM. Inactivating mutations in *DDR2* cause spondylo-meta-epiphyseal dysplasia, short limbs

and abnormal calcification (SMED, SL-AC), a rare, autosomal inherited human disorder associated with distinct skeletal and craniofacial defects, such as dwarfism, short limbs, low bone mass, dysmorphic face, midfacial hypoplasia, and open fontanels. This suggests that DDR2 is an important regulator of craniofacial and skeletal development and growth. To test this hypothesis, I use mouse models that share similar phenotypes with SMED, SL-AC patients, allowing me to systematically characterize craniofacial bone phenotypes and identify underlying signaling pathways involved in regulation of processes that modulate the development of craniofacial skeleton. In addition, I use reporter mice to determine where *Ddr2* is expressed in skeletal tissues as a prerequisite for a detailed targeted deletion analysis to understand tissue-specific functions of *Ddr2*. This research advances our understanding of the contribution of cell-matrix interactions to craniofacial development and disease by establishing the functions of a new collagen receptor in skeletal development.

In this chapter, I will provide an overview of craniofacial development, discuss the importance of cell-ECM interactions in development including the role of the collagen receptors, β1 integrin and discoidin domain receptors, in this process and link this background to the goals of this dissertation.

Part I: Craniofacial Development: Contribution of Cranial Sutures and Cranial Base

Development of the craniofacial skeleton is a complex process involving formation of the neurocranium and viscerocranium and interactions with surrounding developing tissues (Thorogood 1988). This process is highly regulated by several critical signaling pathways and matrix-mediated interactions (Neben and Merrill 2015; Thorogood 1988). Therefore, it is unsurprising that craniofacial abnormalities are among

most common birth defects in humans (Fish 2016; Trainor and Richtsmeier 2015). The skeletal system in all mammals develops through two distinct mechanisms: intramembranous ossification and endochondral ossification (Nakashima and de Crombrugghe 2003) **(Figure I.1)**. Intramembranous ossification occurs when mesenchymal progenitor cells condense and directly differentiate into bone-forming osteoblasts. Osteoblasts then contribute to bone formation by synthesizing and secreting bone-specific extracellular matrix proteins, including type I collagen, bone sialoprotein (BSP), osteopontin and osteocalcin. This process mainly takes place in the cranial vault **(Figure I.1)**, the clavicle, and in the periosteum of long bones. In contrast, endochondral ossification involves the initial formation of cartilage templates from the condensation of mesenchymal progenitor cells and differentiation into chondrocytes followed by the conversion of cartilage templates into bone. This process accounts for the initial formation of most bones of the axial and appendicular skeleton [reviewed in (Erlebacher et al. 1995; Nakashima and de Crombrugghe 2003)] **(Figure I.1)**.

The cranial vault, which arises from neurocranium, develops through osteogenic differentiation of mesenchymal progenitor cells of neural crest and mesoderm origin as well as bone formation at the edge of osteogenic fronts (Nakashima and de Crombrugghe 2003). As ossification proceeds, the bone edges between two opposing cranial bones form butt-ended or overlapping sutures **(Figure I.1)**. Sutures formed between more than two bones are called fontanels (Opperman 2000), including the anterior fontanel located between the two frontal and the two parietal bones of the developing cranium. The cranial vault is thus formed from membranous bones, namely frontal, parietal, temporal, and occipital bones, and in between cranial bones are cranial sutures. The cranial sutures primarily function as the major sites for intramembranous bone growth. They contain unossified, fibrous connective tissue that facilitates new bone

formation at the sutural edges of the osteogenic fronts. For normal development, sutures must remain open or patent to allow growth of the cranial vault to be synchronized with growth of the cranial base and developing brain.

Cranial sutures are thought to provide a niche for stem cells that contribute to craniofacial bone growth and regeneration (Lana-Elola et al. 2007; Maruyama et al. 2016; Wilk et al. 2017; Zhao et al. 2015). Several genetic markers have been associated with sutural stem cells (SuSCs) including glioma-associated oncogene 1 (Gli1), an intermediate in hedgehog signaling, Axin-related protein 2 (Axin2), an intermediate in Wnt signaling, and Paired related homeobox 1 (Prx1), reviewed in (Mohamed and Franceschi 2017). SuSCs have been postulated to present in mid sutural mesenchyme and, as they and their progeny differentiate into bone-forming osteoblasts, they become incorporated in the growing bones. Disruption in the function of SuSCs may underlie mechanisms responsible for suture dysmorphogenesis seen in several human syndromes. For example, ablation of SuSCs could lead to craniosynostosis, a premature closure of cranial sutures resulting in arrest of skull growth (Durham et al. 2019; Zhao et al. 2015), while impaired cell proliferation and osteogenic differentiation of SuSCs could lead wide-open fontanels due to reduced or delayed bone growth (Goto et al. 2004; Qin et al. 2019).

The cranial base, which also arises from neurocranium, is the most complex structure of the skeleton (Nie 2005). Cells of the cranial base arise from two distinct cell populations, neural crest and mesoderm. The anterior cranial base is entirely derived from neural crest, while the posterior cranial base is derived from paraxial mesoderm (Couly et al. 1993; Le Douarin et al. 1993; Le Lievre 1978; McBratney-Owen et al. 2008; Noden 1988; Thorogood 1988). The cranial base provides a platform to protect the brain and sense organs, and protect and support the pituitary gland in a saddle-shaped

depression (called stella turcia) in the superior surface of cranial base, as well as provide a foundation to support the growth of the facial skeleton (Lieberman et al. 2000). The importance of the cranial base to craniofacial development and disease is emphasized by its involvement in many human syndromes such as craniosynostosis, Down's syndrome, Turner syndrome, cleidocranial dysplasia (CCD), cleft palate, and osteogenesis imperfecta (Cheung et al. 2011; McGrath et al. 2012; Nie 2005; Paliga et al. 2014; Tahiri et al. 2014). Together, proper development and growth of the cranial base is critical for proper development of other craniofacial elements and associated organs.

Development of the cranial base begins early during development when three pairs of mesenchymal condensations differentiate into cartilage and fuse to form the cranial base template spanning the entire skull length. The cranial base cartilage then undergoes endochondral ossification to form various bones such as the ethmoid, presphenoid, basisphenoid, and basioccipital bones in midline and laterally from the auditory capsules of the temporal bones. The cranial base becomes interrupted with cartilaginous structures between each bone called synchondroses (Kjaer 1990). Cranial base synchondroses are important growth centers that are major contributors to craniofacial development (Teddy Cendekiawan 2010). There are three synchondroses present in the midline cranial base distributed anteroposteriorly: sphenoethmoidal synchondrosis, intersphenoid synchondrosis and spheno-occipital synchondrosis. Sphenoethmoidal and intersphenoid synchondroses are derivatives of neural crest cells, while spheno-occipital synchondrosis is derived from paraxial mesoderm. Each synchondrosis contributes to longitudinal skull growth at specific times during prenatal and postnatal development (Nie 2005). Premature fusion of synchondroses can lead to midface hypoplasia as seen in patients with syndromic craniosynostosis (Tahiri et al.

2014).

Histologically, the synchondrosis has an interesting structure as it is composed of mirror-image growth plates with resting chondrocytes in the central zone and proliferative, and hypertrophic chondrocytes on both sides (**Figure I.2**). Unlike long bone growth plates, synchondroses do not undergo secondary ossification, and do not have an articular synovial layer. Both long bone growth plates and synchondroses are under different mechanical stresses in vivo. Although cranial synchondroses are understudied, current work suggests that they share many properties with traditional growth plates including being regulated by several key pathways, including PTHrP, IHH, FGFs, BMPs, WNT/β-catenin, and primary cilia [reviewed in (Wei et al. 2016)], as well as being dependent on interactions with components of the surrounding extracellular matrix, particularly type II collagen, the predominant collagen species of cartilage (Thorogood 1988). It is assumed, but not proven, that long bone growth plates and cranial synchondroses are similar sites of endochondral bone formation.

In view of these similarities, a brief discussion of the long bone growth plate is instructive. Chondrocytes in the resting zone (resting chondrocytes) are round single or paired cells embedded in type II collagen-rich extracellular matrix (Abad et al. 2002). These cells make important contributions to endochondral bone formation (Abad et al. 2002). Within this population are skeletal stem cells that are capable of self-renewal and multipotent differentiation to many skeletally related cells including chondrocytes, osteoblasts and bone marrow stromal cells (Mizuhashi et al. 2018). Cells of the resting zone have the intrinsic ability to replenish the entire growth plate after surgical excision of proliferative and hypertrophic chondrocyte zones (Abad et al. 2002). The progeny of resting chondrocytes undergo active cell divisions to provide clones of proliferative chondrocytes -- very thin or flattened cells lined up in columns along the long axis of the

bone. The chondrocytes then stop proliferation and undergo hypertrophy and terminal differentiation. Hypertrophic chondrocytes synthesize and secrete type X collagen as a substrate for ossification and blood vessel invasion, a process that attracts bone cells and facilitates the replacement of cartilage with bone. A subpopulation of chondrocytes may also trans-differentiate into osteoblasts and osteocytes (Jing et al. 2017). Chondrocyte proliferation and differentiation are regulated by Indian hedgehog (Ihh) signaling via a negative feedback loop involving parathyroid hormone-related peptide (PTHrP) (Kronenberg and Chung 2001). However, the mechanism responsible for maintaining the stemness and cell fate of resting zone chondrocytes is not understood.

Resting chondrocytes also play an important role in directing the formation and spatial organization of the growth plate (Abad et al. 2002; Abad et al. 1999). It has been postulated that resting zone chondrocytes might produce a growth plate-orienting factor that directs the alignment of proliferative clones into columns parallel to the long axis of the bone (Abad et al. 2002). Although resting zone chondrocytes express PTHrP during fetal development, knockout of this gene in mice did not lead to chondrocyte disorganization (Schipani et al. 1997). In addition, PTHrP expression was reported in prehypertrophic and hypertrophic chondrocytes in the postnatal growth plate (Kindblom et al. 2002; van der Eerden et al. 2000). This suggests that PTHrP is unlikely to be responsible for maintaining chondrocyte organization. Abnormal chondrocyte organization was seen in growth plates of Ihh-deficient mice; however, Ihh is spatially restricted to early hypertrophic zone, not in the resting zone so is also unlikely to be a primary chondrocyte orienting factor (St-Jacques et al. 1999). Identifying growth plate-orienting factors that maintain the hierarchical organization of the growth plate is crucial for a better understanding of cartilage development and disease.

Part II: Extracellular Matrix Signaling in Craniofacial and Skeletal Development

Extracellular matrix (ECM) signaling plays a critical role in skeletal development and growth, and has been implicated in a wide spectrum of human skeletal disorders such as skeletal dysplasias, chondrodysplasias, osteoarthritis, and osteoporosis (Erlebacher et al. 1995; Kuivaniemi et al. 1997; Lu et al. 2011; Velleman 2000). Several fundamental aspects during skeletal development depend on a reciprocal interaction between skeletal cells and their ECM. The ECM-cell interaction regulates cell proliferation, migration, differentiation and remodeling to develop and maintain the shapes of individual bones and the relative proportions of the skeleton [reviewed in (Erlebacher et al. 1995)]. The skeletal ECM is composed of collagens, non-collagenous proteins and proteoglycans. Collagens are the most abundant proteins in mammalian tissues where at least 25 distinct collagens have been identified. These collagens can be divided into two general groups based on structure, fibrillar collagens and non-fibrillar collagens. Fibrillar collagens, which include collagen types I-III, V, and XI all exist in a characteristic triple-helical conformation (Kuivaniemi et al. 1997), while type X non-fibrillar collagen is spatially restricted in the hypertrophic cartilage of growth plates. The collagen-rich ECM maintains the structural integrity and cellular organization of developing tissues, controls the spatial and temporal response to growth factors and can activate several signal transduction pathways (Kim et al. 2011; Leitinger and Kwan 2006; Rozario and DeSimone 2010).

Collagen signaling plays a critical role in many aspects of craniofacial and skeletal development. For example, fibrillar type I collagen is the predominant collagen in bone, tooth and periodontal ligaments, where it regulates various cellular processes. Type I collagen is required for osteoblast differentiation and mineralization (Lynch et al. 1995; Mizuno et al. 2000) since inhibition of collagen synthesis blocks osteoblast

differentiation and inhibits osteoblast marker gene expression (Franceschi and Iyer 1992; Shi et al. 1996). Mutations in the two type I collagen genes, COL1A1 and COL1A2, cause multiple disorders of bones and teeth including osteogenesis/dentinogensis imperfecta (OI/DI), osteoporosis, bone weakness and fracture, and Ehlers-Danlos syndrome (EDS) that are all associated with abnormal craniofacial growth, cranial base abnormalities, dental malocclusion, and dentinogenesis imperfecta (Andersson et al. 2017; Cheung et al. 2011; Eimar et al. 2016; Kuivaniemi et al. 1997). *Col1a1* mutant mice showed multiple craniofacial and dental phenotypes characterized by short skull length, a mandibular side shift, malocclusion, wide periodontal space, and defects in the dentin matrix and mineralization, similar to those observed in OI an EDS syndromes (Eimar et al. 2016).

Type II collagen, which is the core protein in the cartilage extracellular matrix, is important for normal chondrogenesis as well as for maintaining the structural integrity and cellular organization of developing tissues (Brown et al. 1981; Pace et al. 1997; Seegmiller et al. 1971; Spranger et al. 1994; Vikkula et al. 1994). Mutations in type II collagen cause chondrodysplasias, cartilage disorders affecting the formation of skeletal and craniofacial bones (Brown et al. 1981; Rintala et al. 1997; Rittenhouse et al. 1978; Savontaus et al. 2004; Seegmiller et al. 1971; Spranger et al. 1994; Vikkula et al. 1994). For example, a mutation in the region encoding the C-propeptide globular domain of *Col2a1* in mice (*Dmm/Dmm* mice) results in lethal dwarfism, shortened vertebral column, small rib cage, and craniofacial defects characterized by skull dismorphogenesis, reduced skull length, reduced cranial base length, cleft palate and short mandible (Brown et al. 1981; Pace et al. 1997). The mutation in the C-propeptide domain results in defects in the assembly and folding of type II collagen and alteration of collagen distribution within the cartilage extracellular matrix. These extracellular matrix defects

impact the structural integrity of the tissue and lead to loss of columnar organization of proliferative chondrocytes (Brown et al. 1981).

Part III: Collagen Cell-Surface Receptors

Interactions between collagens and cells are mediated by cell-surface receptors such as β1 integrins and discoidin domain receptors (Harburger and Calderwood 2009; Leitinger and Hohenester 2007).

Integrins

Integrins are heterodimeric transmembrane receptors composed of α and β subunits that mediate cell-cell and cell-matrix interactions during development and disease (for review see (Bouvard et al. 2001; Legate et al. 2009; Lowell and Mayadas 2012; Wickstrom et al. 2011). The β1 integrin subfamily, including α1β1, α2β1, α10β1, and α11β1, primarily functions as collagen receptors (Leitinger 2011). They are widely expressed in skeletal bone cells, such as bone marrow precursor cells, chondrocytes, osteoblasts, osteocytes-- terminally differentiated osteoblasts, and osteoclasts (Gronthos et al. 2001; Hughes et al. 1993; Nesbitt et al. 1993). β1 integrin expression is also seen in regions of dental basement membrane, dental mesenchyme and dental epithelium, where its interaction with ECM is important during tooth development (Saito et al. 2015; Salmivirta et al. 1996). Integrin signaling is known to play critical roles in regulating cell adhesion, proliferation, survival and cell polarity. Germline deletion of the β1 integrin subunit gene in mice is embryonic lethal due to inner mass failure during early development (Stephens et al. 1995). To gain insight into the function of β1 integrins during skeletal and tooth development, conditional knockout strategies were employed. β1 integrin disruption in various osteoblast lineages exhibited skeletal and craniofacial

phenotypes with varying severity (Shekaran et al. 2014; Zimmerman et al. 2000). Mice with β1 integrin knockout in mesenchymal progenitors died at birth due to severe skeletal and craniofacial defects. β1 integrin disruption in pre-osteoblasts using Osx-Cre resulted in viable mice with moderate early defects, which became milder with age. These mice exhibited defects in calvarial ossification, incisor eruption and growth as well as femoral bone properties. In contrast, knockout in mature osteoblasts had only minor effects on skeletal phenotype (Shekaran et al. 2014).

In cartilage, lack of the β1-integrin subunit led to a chondroplasia characterized by loss of columnar organization of the growth plate, reduced chondrocyte proliferation and increased chondrocyte apoptosis, which was shown to be responsible for bone shortening and dwarfism (Aszodi et al. 2003). These phenotypes are similar to what was seen in knockouts of type II collagen, the main protein species in cartilage. In contrast to β1 integrin knockouts, deletion of individual α subunits of collagen-binding integrins exhibited relatively mild phenotypes (Bengtsson et al. 2005; Chen et al. 2002; Gardner et al. 1996; Popova et al. 2007; Pozzi et al. 1998), suggesting redundancy among collagen-binding integrins or other collagen receptors being involved.

β1 integrins interact with collagens by binding a specific amino acid sequence (GFOGER) within collagen triple-helical regions [reviewed in (Leitinger and Hohenester 2007)]. This binding mediates outside-in and inside-out signaling to initiate specific signaling pathways (for review, see (Harburger and Calderwood 2009). Previous work from the Franceschi laboratory demonstrated that the β1 integrin-collagen interaction is necessary for activation of RUNX2, a transcriptional activator of osteoblast differentiation and chondrocyte maturation during early skeletal development. In pre-osteoblasts, it was demonstrated that the interaction between α2β1 integrins and type I collagen–containing ECM is required for RUNX2 phosphorylation and activation via an ERK/MAPK-

dependent pathway, as well as, for induction of osteoblast-specific gene expression (Franceschi and Iyer 1992; Franceschi et al. 1994; Xiao et al. 2000; Xiao et al. 1998). Blocking α2β1 integrins using either DGEA-containing peptides or anti- α2 antibodies abolished both binding of RUNX2 to OSE2 DNA and OSE2 enhancer activity and inhibited osteoblast-specific gene expression (Xiao et al. 1998). In addition, Ge and colleagues demonstrated that MAP kinase-dependent RUNX2 phosphorylation occurs at two sites at Ser (301) and Ser (319) within the proline/serine/threonine domain of RUNX2 (Ge et al. 2009). The specific requirement of the ERK/MAPK pathway in RUNX2 phosphorylation, osteoblast differentiation and skeletal development has been demonstrated both in vitro and in vivo (Ge et al. 2007; Xiao et al. 2000). The current state of knowledge suggests that, upon binding with collagen-rich ECM, α2β1 integrin activates the MAPK kinase pathway leading to RUNX2 activation and phosphorylation. Active RUNX2 then binds to OSE2 elements in the osteocalcin promoter to activate transcription and promote osteoblast differentiation (Takeuchi et al. 1997).

Discoidin Domain Receptor 2 (DDR2): A Unique Receptor for Collagens

Discoidin domain receptors, DDR1 and DDR2, are members of an unusual class of receptor tyrosine kinases (RTKs) that are activated by multiple triple-helical collagens (Leitinger and Hohenester 2007; Shrivastava et al. 1997; Vogel et al. 1997). Unlike integrins that are devoid of intrinsic tyrosine kinase activity, DDRs are receptor tyrosine kinases that undergo tyrosine autophosphorylation upon binding to several collagens. Both DDR1 and DDR2 are widely expressed in several tissues in mammals and have important roles in embryo development and human disease (Leitinger 2014; Vogel et al. 2006). While DDR1 expression is high in epithelial cells, DDR2 is mainly expressed by cells of mesenchymal origin (Alves et al. 1995).

Unlike canonical RTKs that bind to soluble ligands, DDRs bind to fibrillar and non-fibrillar collagens with varying specificities and affinities: while both DDR1 and DDR2 bind to fibrillar collagens, type I-III and V; only DDR1 binds to the basement membrane type IV collagen and only DDR2 binds to non-fibrillar type X collagen (Leitinger and Kwan 2006; Shrivastava et al. 1997; Vogel et al. 1997). Structurally, DDRs consist of a discoidin (DS) domain, followed a DS-like domain, an extracellular juxtramembrane domain, a transmembrane (TM) domain, an intracellular juxtramembrane domain, and conserved cytoplasmic tyrosine kinase domain **(Figure I.3)**. The DS domain, a 160-amino acid motif in the extracellular region, structurally distinguishes DDRs from other RTKs and is required for recognition and binding to fibrillar collagens (Leitinger 2003; Leitinger et al. 2004). The DS domain binds a GVMGFO motif (O is hydroxproline) within type I-III fibrillar collagens **(Figure I.4)**. This GVMGFO binding site is distinct from integrin binding sites in collagen such as the GFOGER sequence (Konitsiotis et al., 2008). Although it is activated by non-fibrillar type X collagen, the DS domain of DDR2 does not recognize type X collagen, indicating that a unique binding mechanism is employed for interactions with this collagen (Leitinger and Kwan, 2006). However, the biological significance in the differential binding specificity of DDR2 toward fibrillar and non-fibrillar collagens is not clear (Leitinger and Kwan 2006). Elucidating the mechanisms of differential collagen recognition by DDR2 is crucial for understanding which collagen ligands activate DDR2 during fundamental processes of bone formation and development.

Upon collagen binding, DDR2 undergoes autophosphorylation of tyrosine residues on the cytoplasmic kinase domain, creating docking sites for adaptor proteins involved in downstream signaling. Interestingly, the collagen-induced autophosphorylation is unusually slow and sustain for several hours (Shrivastava et al.

1997; Vogel et al. 1997). DDR2 signaling is transduced through the Src non-receptor tyrosine kinase and the adaptor molecule Shc, both of which are required for full activation of DDR2 (Ikeda et al. 2002). DDR2 is shown to signal through several pathways including ERK1/2 and P38 MAPK pathways (Ge et al. 2016; Lin et al. 2010; Zhang et al. 2011). Like other RTKs, DDR2 signaling controls many fundamental cellular processes, such as proliferation, differentiation, migration, and remodeling of the extracellular matrix (Herrera-Herrera and Quezada-Calvillo 2012; Labrador et al. 2001; Lin et al. 2010; Olaso et al. 2001; Olaso et al. 2002; Zhang et al. 2011). Upregulation of DDR2 activity is implicated in many human diseases, such as fibrotic diseases of the lung, kidney and liver, atherosclerosis, osteoarthritis and several types of cancers (Vogel et al. 2006).

Skeletal Expression of DDR2 During Embryonic and Postnatal Development

DDR2 is expressed in many mesenchymal cells under a variety of physiological and pathological conditions such as in dermal fibroblasts during wound healing (Olaso et al. 2002), hepatic stellate cells during hepatic fibrosis (Olaso et al. 2011), articular chondrocytes during osteoarthritis (Lin et al. 2010), mesenchymal stromal cells during breast carcinogenesis (Gonzalez et al. 2017), and cardiac fibroblast during heart development (Cowling et al. 2014). While it is expressed in several tissues, the growth defects due to *Ddr2* loss of function are largely manifested in the skeletal tissues. However, little information is available on where DDR2 is actually expressed during embryonic and postnatal skeletal development. Using PCR analysis, *Ddr*2 mRNA was detected in E11 day-old mouse embryos coincident with the appearance of *Runx2*, the master transcription factor of skeletogenesis (Lin et al. 2010). However, the tissue-specific expression of *Ddr2* was missing in this study. Another study reported *Ddr*2

mRNA expression in hypertrophic chondrocytes of 17-day-old embryonic chick tibial epiphyses (Leitinger and Kwan 2006), but the tissue and cellular expression of *Ddr2* has not been systemically examined during embryonic development.

With regard with *Ddr2* expression in the postnatal skeleton, results from the previous studies were inconclusive due to discrepancies in experimental methodology. Using *in situ* hybridization, Labrador and colleagues reported expression of *Ddr2* mRNA in tibial growth plates of 1-week old mice, specifically in the chondrocyte columns in the proliferative chondrocyte of the growth plate, in the calcified cartilage at the cartilage-bone junction, and in the trabecular bone surface (Labrador et al. 2001). Using immunohistochemistry (IHC) analysis; however, a subsequent study could not detect DDR2 expression in the proliferative chondrocytes. Instead, IHC results revealed DDR2 expression in all articular cartilage chondrocytes and hypertrophic chondrocytes, but not in proliferative chondrocytes of the growth plate of 5 week-old mouse knee joint (Leitinger and Kwan 2006). Lin and colleagues analyzed human osteoarthritic knee using immunohistochemistry and showed DDR2 expression only in the superficial zone of articular cartilage (Lin et al. 2010), but not in middle and deep zones as previously reported (Leitinger and Kwan 2006), and in osteoblastic lineage cells of subchondral bone of human osteoarthritic knee: in osteocytes, bone lining cells, and active osteoblasts within the subchondral bone, but not in chondrocytes in the calcified cartilage (Lin et al. 2010). Despite previous efforts to localize DDR2 in the skeletal long bone, the identity of *Ddr2*-expressing cells in the skeleton is not well defined. Taken together, results from previous studies point to a potential role of DDR2 in cartilage and bone development. However, determining its expression is a perquisite for understanding DDR2 function during craniofacial and skeletal development.

Part IV: The role of DDR2 of Craniofacial and Skeletal Development

Human and animal genetic studies indicate that DDR2 is an important regulator of skeletal development and bone growth. The role of DDR2 in skeletal development was emphasized by identifying missense mutations in *DDR2* as the genetic etiology of spondylo-meta-epiphyseal dysplasia (SMED) with short limbs and abnormal calcifications (SMED, SL-AC) (Al-Kindi et al. 2014; Ali et al. 2010; Bargal et al. 2009; Mansouri et al. 2016; Urel-Demir et al. 2018). SMED, SL-AC is a rare, autosomal recessive human growth disorder characterized by disproportionate short stature, short limbs, short broad fingers, abnormal metaphyses and epiphyses, platyspondyly and abnormal calcifications -- a characteristic feature of the disease. SMED, SL-AC patients also have distinct craniofacial abnormalities including a prominent forehead, wide open fontanelle, hypertelorism, sparse eyebrows, a short nose with a depressed nasal bridge, a long philtrum and micrognathia (Al-Kindi et al. 2014; Mansouri et al. 2016; Rozovsky et al. 2011; Smithson et al. 2009; Urel-Demir et al. 2018). In addition, SMED, SL-AC patients have abnormal pear-shaped vertebral bodies and small rib cages, and those patients often die of respiratory insufficiency due to inadequate expansion of the chest wall and difficulty breathing (Fano et al. 2001; Urel-Demir et al. 2018). SMED, SL-AC syndrome arises from inactivating mutations in exons encoding the extracellular domain, cytosolic TM domain and tyrosine kinase domain of DDR2. These mutations including missense, nonsense, and splice junction mutations are summarized in **Table I.1**. The consequence of these mutations is manifested by defects in intramembranous and endochondral bones and further suggests a potential role for DDR2-mediated signaling in craniofacial and skeletal development.

Importantly, the abnormalities in the SMED, SL-AC patients are phenocopied by *Ddr2* deficiency in mice. A spontaneous 150-kb deletion in the *Ddr2* locus resulted in a

dwarf and infertile phenotype designated *smallie* or *slie* (Kano et al. 2008). At birth, *slie* mutant mice are indistinguishable from their wild-type littermates, but exhibit abnormal growth retardation to become dwarf by adulthood (Kano et al. 2008). They exhibited a small body size and reduced weight that became obvious 10 days after birth (Kano et al. 2008). *Slie/slie* mice also developed skeletal abnormalities characterized by reduced bone mass in axial and appendicular skeletons that were attributed to defective osteoblast differentiation and mineralization (Ge et al. 2016; Kano et al. 2008). Craniofacial abnormalities were also observed including eye protrusion, short snout, and impaired intramembranous ossification associated with delayed suture formation (Ge et al. 2016; Kano et al. 2008). In a prior study, *Ddr2*-deficient mice generated by disrupting the kinase activity of *Ddr2* gene also exhibited a progressive skeletal phenotype characterized by irregular growth of flat bones of the skull, a shorter snout, and shortening of long bones (12 to 15% reduction in length by 4 months of age) due to reduction in growth plate chondrocyte proliferation (Labrador et al. 2001). In another study, germline deletion of *Ddr2* due to a frameshift mutation resulting from knock-in of a MerCreMer gene into exon 3 also caused skeletal growth defects similar to those noted in the previously described *Ddr2*-deficient mice (Cowling et al. 2014). Regardless of the genetic basis for the *Ddr2* null allele, these studies consistently showed that loss of *Ddr2* led to a reduction in body weight, dwarfism, short limbs and abnormal axial and craniofacial bones. In addition to skeletal phenotypes, *slie/slie* mice were infertile as a consequence of gonadal dysfunction and showed a significant increase in levels of plasma glucose and adiponectin, and a significant decrease in levels of leptin (adipokine) and blood urea nitrogen (Ge et al. 2016; Kano et al. 2008). It is not known if these systemic effects of Ddr2 deficiency could indirectly affect the skeleton. To address this issue, a tissue-specific conditional knockout strategy is needed.

DDR2 Signaling in Osteoblast and Chondrocyte Proliferation and Differentiation

Cell proliferation and differentiation of chondrocytes and osteoblasts are essential prerequisites for proper skeletal development and bone formation. Several lines of evidence support the importance of DDR2 in chondrocyte and osteoblast proliferation and differentiation. Osteogenic induction of undifferentiated mesenchymal cells and osteoblast precursors stimulated *Ddr2* mRNA expression during early stages of differentiation (Lin et al. 2010; Zhang et al. 2011). Western blot analysis of DDR2 activity also showed a gradual increase in the levels of DDR2 phosphorylation over the course of differentiation (Zhang et al. 2011). During induced osteogenesis, knockdown of endogenous DDR2 through specific shRNA significantly suppressed osteoblast marker gene expression, osteogenic differentiation and mineralization while overexpression of DDR2 increased osteoblast markers in both undifferentiated and differentiated cells (Lin et al. 2010; Zhang et al. 2011). Consistent with these results, calvaria and bone marrow primary cells isolated from *Ddr2*$^{slie/slie}$ mice formed fewer mineralized nodules and expressed lower levels of osteoblast marker mRNAs under induced osteogenesis (Ge et al, 2016). In contrast, they formed increased numbers of lipid droplet-containing cells and expressed higher levels of adipocyte markers (Ge et al. 2016).

Mechanistically, DDR2 promotes osteoblast and chondrocyte differentiation at least in part by stimulating ERK and p38 MAP kinase-dependent phosphorylation of RUNX2, a master transcriptional factor required for skeletal development (Lin et al. 2010; Zhang et al. 2011). Previous studies from the Franceschi laboratory showed that MAP kinases phosphorylate RUNX2 at serine residues S301 and S319 (Ge et al. 2009). Gain of function experiments using RUNX2 S301, 319E phosphomimetic mutant that had enhanced transcriptional activity rescued the impaired osteogenic phenotype observed in *Ddr2*-silenced cells, while a S301,319A mutant RUNX2 that is unresponsive

to ERK MAPK regulation inhibited DDR2 induction of osteogenesis (Zhang et al. 2011). The relationship between DDR2 and RUNX2 phosphorylation/activation was further demonstrated in primary calvarial osteoblasts (Ge et al. 2016). In cells isolated from wild type mice, transfection with a wild type RUNX2 expression vector up-regulated osteoblast-specific gene expression while this RUNX2-dependent transcription was inhibited by approximately 50 percent in *Ddr2*$^{slie/slie}$ cells. The requirement for *Ddr2* was not seen when wild type or *Ddr2*$^{slie/slie}$ cells were transfected with phosphorylation-deficient S301,319A mutant RUNX2 (Ge et al. 2016). Results also showed that a constitutively active phosphomimetic RUNX2 mutant (S301,319E) could rescue the decrease in osteoblast gene expression seen in *Ddr2*-deficient cells (Ge et al. 2016). In addition to its function in osteogenesis, DDR2 facilitated RUNX2 phosphorylation and type X collagen expression in hypertrophic chondrocytes (Zhang et al. 2011). Together, these studies indicate that DDR2 plays an essential role in osteoblast and chondrocyte differentiation in vitro; however, the function of DDR2 in osteoblasts and chondrocytes has not been established in in vivo.

Ddr2 is upregulated by activating transcription factor 4 (ATF4), a leucine zipper transcription factor that is a critical regulator of skeletal development, osteoblast differentiation, and function (Yang et al. 2004). ATF4 deficiency in mice resulted in delayed bone formation during embryonic development and low bone mass throughout postnatal life (Yang et al. 2004). During osteoblast differentiation, ATF4 cooperates with CCAAT/enhancer binding protein b (C/EBPb) to enhance osteocalcin gene expression (Yang et al. 2004). Lin and colleagues demonstrated that ATF4 enhanced DDR2 mRNA expression, whereas knockdown of ATF4 expression delayed DDR2 induction during osteoblast differentiation (Lin et al. 2010). Results from this study suggest that ATF cooperates with C/EBPb to bind a CCAAT/enhancer binding protein-(C/EBP) binding site

at -1150bp in the DDR2 promoter to stimulate DDR2 transcription, since ATF4 mutants deficient in C/EBPb binding were incapable of activating DDR2 (Lin et al. 2010). Once activated, DDR2, in turn, stimulates p38 MAPK, which is responsible for subsequent RUNX2 activation and osteoblast gene expression (Lin et al. 2010).

Cell proliferation of osteoblasts and chondrocytes is important for cell expansion and bone growth before differentiation. Zhang and colleagues found that DDR2 could regulate osteoblast and chondrocyte proliferation in vitro (Zhang et al. 2011). Knockdown of DDR2 in pre-osteoblast (MC3T3-E1) or in chondrocyte (ADTC5) cell lines reduced cell growth in culture. Other studies also reported proliferative effects of DDR2 in additional cell types (Olaso et al. 2001; Olaso et al. 2002). DDR2 regulation of osteoblast and chondrocyte proliferation may not be dependent on RUNX2 phosphorylation (Zhang et al. 2011). However, the molecular mechanisms responsible for proliferative actions of DDR2 need to be determined.

Part V: Summary and Problem Statement

In this chapter, we established the importance of collagen-cell interactions during craniofacial and skeletal development, with emphasis on possible roles of the cell-surface collagen receptor, discoidin domain receptor 2 (DDR2), in this process. This emphasis is justified because DDR2, unlike integrins, is a direct mediator of collagen signaling via activation of its intrinsic tyrosine kinase activity. In addition, previous human and mouse genetic studies established an important function for DDR2 in craniofacial and skeletal development, with loss of DDR2 function causing multiple bone defects in axial and appendicular bones as well as skull. However, this crucial function is not well understood. Our incomplete understanding is partially because the identity of *Ddr2*-expressing cells in skeleton is not well defined, and thus cellular actions of DDR2 remain

unknown. While previous studies reported craniofacial phenotypes in human SMED, SL-AC patients and *Ddr2*-knockout mice, the function of *Ddr2* in craniofacial development has not been previously investigated. This dissertation will explore the hypothesis that *Ddr2* is an important cell autonomous regulator of craniofacial development. We base our hypothesis on prior studies establishing the importance of collagen extracellular signaling for proper bone and tooth formation. We will test this hypothesis by achieving the following specific aims: 1) Characterize the craniofacial phenotype of *Ddr2* knockout mice, 2) Determine the spatial and temporal pattern of *Ddr2* expression in craniofacial bone and tooth, and 3) Elucidate cellular actions of *Ddr2* in the craniofacial skeleton using tissue-specific conditional knockouts. In Chapter 2 the importance of *Ddr2* in postnatal craniofacial development will be established through detailed analysis of craniofacial phenotypes of *Ddr2* knockout mice. As will be shown, germline *Ddr2*-deficient mice have defects in intramembranous bone formation as manifested by delayed suture formation in calvaria as well as abnormal chondrogenesis characterized by significant widening in resting zone and loss of columnar organization of proliferative chondrocytes in cranial base synchondroses. *Ddr2*-LacZ reporter mice along with lineage tracing approaches will be used to identify *Ddr2*-expressing cells in cranial sutures, periosteum, dura mater and resting and proliferative chondrocytes of cranial base synchondroses as well as reveal the contribution of *Ddr2*-expressing cells to osteoblast lineages and osteocytes in calvaria and to chondrocyte lineages and cortical and trabecular bones in the cranial base. These studies suggest *Ddr2* may function in skeletal progenitor cells. Additional experiments involving tissue-specific knockout strategies will establish a critical function of *Ddr2* in skeletal progenitors cells to control chondrocyte and osteoblast differentiation during cartilage growth and postnatal craniofacial bone formation. Collagen-mediated signaling is also critical for tissue differentiation and mineralization in tooth dentin and alveolar bone. In Chapter 3, in vivo

and in vitro studies will establish the requirement for DDR2 signaling in tooth root development, periodontal ligament (PDL) integrity and alveolar bone maintenance. The spatial and temporal expression of *Ddr2* in dental follicle and dental papilla in developing tooth and in dentin-forming odontoblasts and PDL cells in mature tooth will be established using LacZ reporter mice. Additional studies will reveal DDR2 regulation of Runx2 phosphorylation as a potential mechanism for tooth root development, as well as possible DDR2 regulation of PDL extracellular matrix. Lastly, Chapter 4 suggests future directions for this research, with emphasis on the role of DDR2 in regulating the assembly and turnover of collagen-rich extracellular matrix, osteoblast function and chondrocyte polarity -- important mechanisms required for proper bone formation. Experiments to further elucidate the function for *Ddr2* in tooth root development are also proposed. Together, this dissertation advances our understanding of the roles of cell-matrix interactions in craniofacial development and disease by establishing the functions of a new collagen receptor.

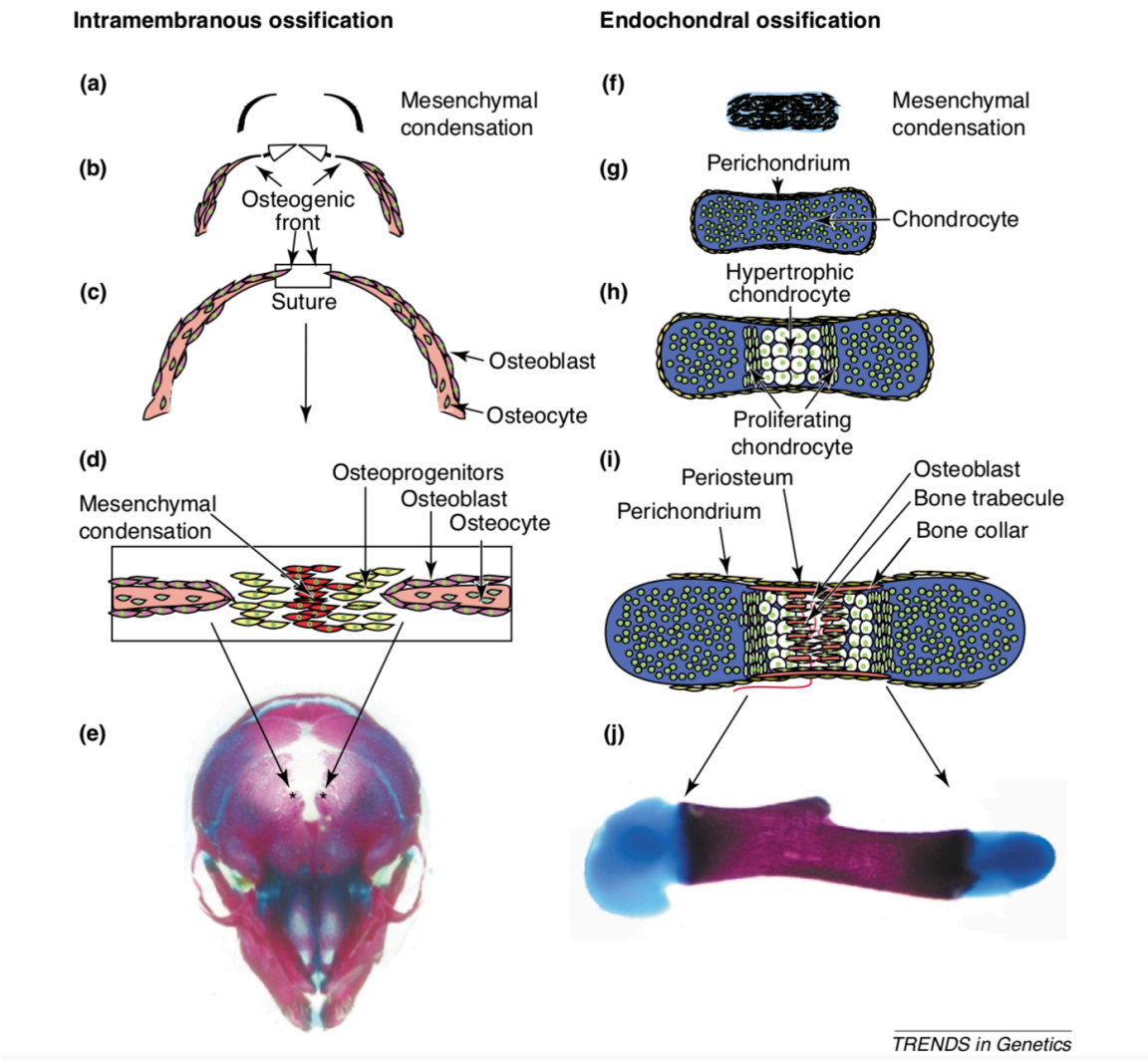

Figure I.1: Principle mechanisms of skeletal development (Nakashima and de Crombrugghe 2003).

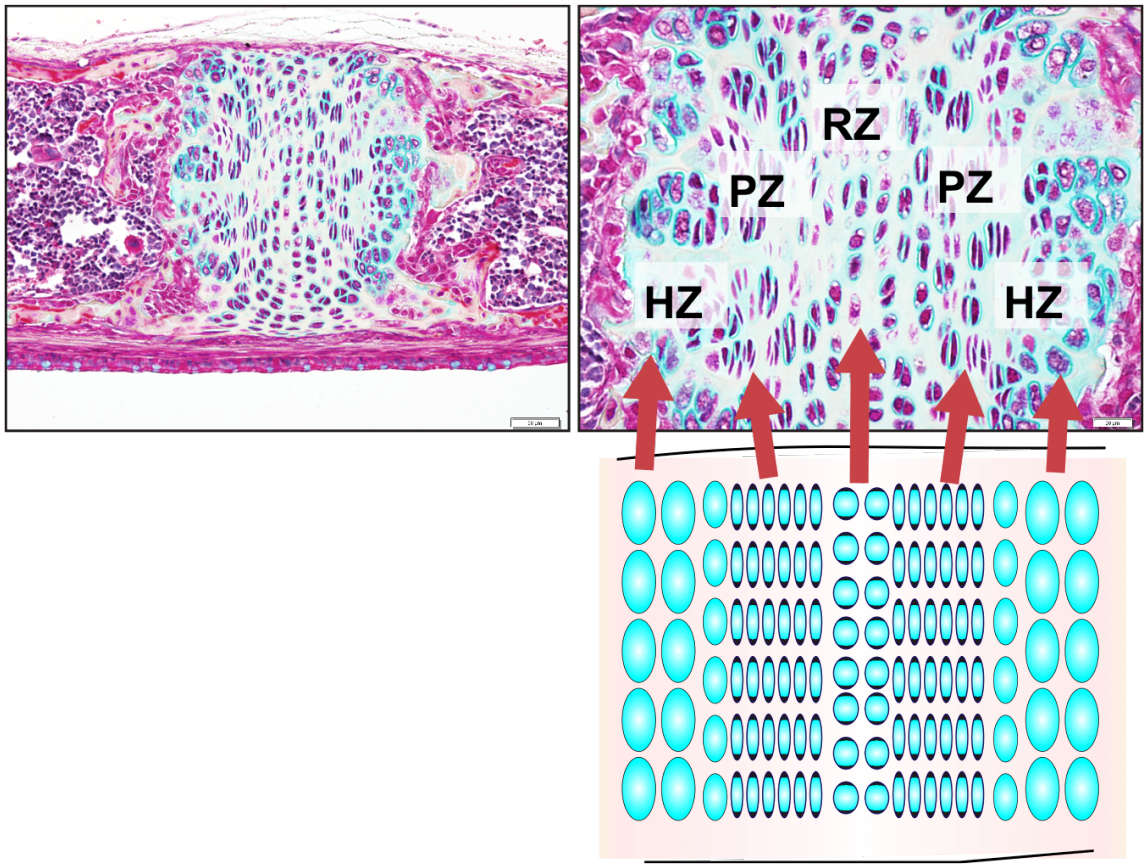

Figure I.2: Structure of cranial base synchondrosis. Cranial base synchondrosis has a mirror-image growth plates with resting chondrocytes in the central zone and proliferative and hypertrophic chondrocytes on both sides. RZ: Resting chondrocyte zone; PZ: Proliferative chondrocyte zone; HZ: Hypertrophic chondrocyte zone.

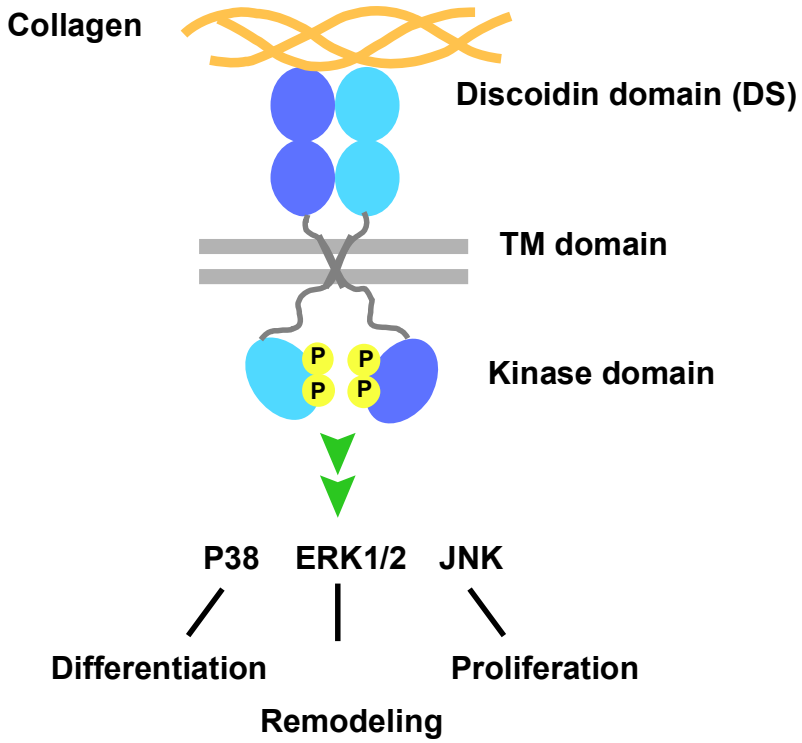

Figure I.3: **Schematic representations of the DDR2 structure and signaling pathway.** DDR2 has a unique extracellular structure characterized by presence of discoidin (DS), the DS-like domain, the TM domain, and the tyrosine kinase domain. The DS domain includes the collagen binding sequence preferentially binds to fibrillar collagens, but not to non-fibrillar basement membrane collagen. Upon collagen binding, DDR2 undergoes autophosphorylation to trigger downstream signaling, mainly through P38, ERK1/2, and JNK collectively to regulate cell differentiation, proliferation, and remodeling.

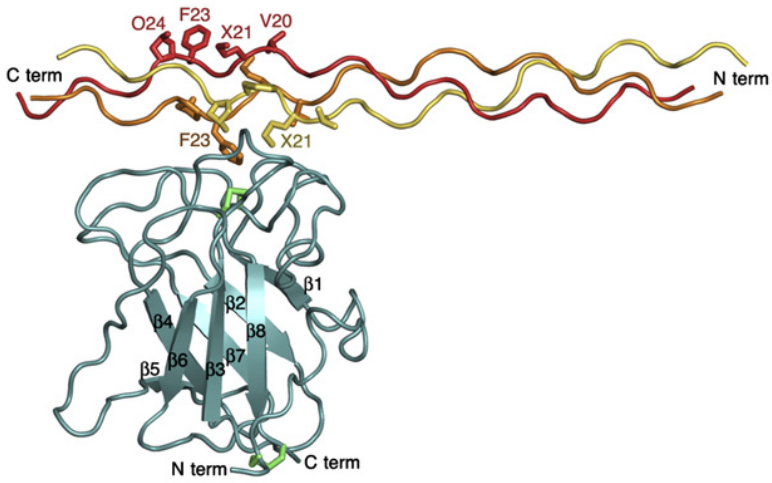

α1(I) …GPOGARGQA**GVMGFO**GPK…
α1(II)…GPQGARGQO**GVMGFO**GPK…
α1(III)...GPSGPRGQO**GVMGFO**GPK…

Figure I.4: Crystal Structure of the DDR2 DS Domain-Collagen Complex. Cartoon representation of the DS domain (cyan) and the collagen peptide (yellow, leading chain; orange, middle chain; red, trailing chain). The b strands of the DS domain are numbered sequentially. Disulfide bonds are in green. The side chains of the collagen GVMGFO motif are shown as sticks. Selected residues are labeled. X denotes norleucine. Adopted from (Carafoli et al. 2009).

Table I.1: Mutations reported in patients with spondylo-meta-epiphyseal dysplasia, short limb-abnormal calcification type.

Patient origin (no)	Mutations	Encoding region	References
Jerusalem (6)	c.2177T > G Ile726Arg Exon 17 c.2138C > T Thr713Ile Exon 17 c.2283 þ 1G > A SJM (splice site mutation) Exon 17 c.2254C > T Arg752Cys Exon 17	The tyrosine kinase domain of the DDR2 gene	(Bargal et al. 2009)
Egypt (2)	c.2254C > T Arg752Cys Exon 17	The tyrosine kinase domain of the DDR2 gene	(Ali et al. 2010)
UAE (2)	c.337G > A Glu113Lys Exon 5	The extracellular domain	(Ali et al. 2010)
Oman (2)	c.2468_2469delCT p.S823Cfs*2 Exon18		(Al-Kindi et al. 2014)
Morocco (1)	c.370C > T (p.Arg124Trp) Exon 5	The extracellular domain	(Mansouri et al. 2016)
Not reported (1)	c.1465 C > T p.R489* Exon13	The cytosolic JM domain	(Urel-Demir et al. 2018)
India (1)	c.2422C > T p.Gln808Ter	-	(Gupta et al. 2019)

References

Abad V, Meyers JL, Weise M, Gafni RI, Barnes KM, Nilsson O, Bacher JD, Baron J. 2002. The role of the resting zone in growth plate chondrogenesis. Endocrinology. 143(5):1851-1857.

Abad V, Uyeda JA, Temple HT, De Luca F, Baron J. 1999. Determinants of spatial polarity in the growth plate. Endocrinology. 140(2):958-962.

Al-Kindi A, Kizhakkedath P, Xu H, John A, Sayegh AA, Ganesh A, Al-Awadi M, Al-Anbouri L, Al-Gazali L, Leitinger B et al. 2014. A novel mutation in ddr2 causing spondylo-meta-epiphyseal dysplasia with short limbs and abnormal calcifications (smed-sl) results in defective intra-cellular trafficking. BMC Med Genet. 15:42.

Ali BR, Xu H, Akawi NA, John A, Karuvantevida NS, Langer R, Al-Gazali L, Leitinger B. 2010. Trafficking defects and loss of ligand binding are the underlying causes of all reported ddr2 missense mutations found in smed-sl patients. Hum Mol Genet. 19(11):2239-2250.

Alves F, Vogel W, Mossie K, Millauer B, Hofler H, Ullrich A. 1995. Distinct structural characteristics of discoidin i subfamily receptor tyrosine kinases and complementary expression in human cancer. Oncogene. 10(3):609-618.

Andersson K, Dahllof G, Lindahl K, Kindmark A, Grigelioniene G, Astrom E, Malmgren B. 2017. Mutations in col1a1 and col1a2 and dental aberrations in children and adolescents with osteogenesis imperfecta - a retrospective cohort study. PLoS One. 12(5):e0176466.

Aszodi A, Hunziker EB, Brakebusch C, Fassler R. 2003. Beta1 integrins regulate chondrocyte rotation, g1 progression, and cytokinesis. Genes Dev. 17(19):2465-2479.

Bargal R, Cormier-Daire V, Ben-Neriah Z, Le Merrer M, Sosna J, Melki J, Zangen DH, Smithson SF, Borochowitz Z, Belostotsky R et al. 2009. Mutations in ddr2 gene cause smed with short limbs and abnormal calcifications. Am J Hum Genet. 84(1):80-84.

Bengtsson T, Aszodi A, Nicolae C, Hunziker EB, Lundgren-Akerlund E, Fassler R. 2005. Loss of alpha10beta1 integrin expression leads to moderate dysfunction of growth plate chondrocytes. J Cell Sci. 118(Pt 5):929-936.

Bouvard D, Brakebusch C, Gustafsson E, Aszodi A, Bengtsson T, Berna A, Fassler R. 2001. Functional consequences of integrin gene mutations in mice. Circ Res. 89(3):211-223.

Brown KS, Cranley RE, Greene R, Kleinman HK, Pennypacker JP. 1981. Disproportionate micromelia (dmm): An incomplete dominant mouse dwarfism with abnormal cartilage matrix. J Embryol Exp Morphol. 62:165-182.

Carafoli F, Hohenester E. 2013. Collagen recognition and transmembrane signalling by discoidin domain receptors. Biochim Biophys Acta. 1834(10):2187-2194.

Chen J, Diacovo TG, Grenache DG, Santoro SA, Zutter MM. 2002. The alpha(2) integrin subunit-deficient mouse: A multifaceted phenotype including defects of branching morphogenesis and hemostasis. Am J Pathol. 161(1):337-344.

Cheung MS, Arponen H, Roughley P, Azouz ME, Glorieux FH, Waltimo-Siren J, Rauch F. 2011. Cranial base abnormalities in osteogenesis imperfecta: Phenotypic and genotypic determinants. J Bone Miner Res. 26(2):405-413.

Couly GF, Coltey PM, Le Douarin NM. 1993. The triple origin of skull in higher vertebrates: A study in quail-chick chimeras. Development. 117(2):409-429.

Cowling RT, Yeo SJ, Kim IJ, Park JI, Gu Y, Dalton ND, Peterson KL, Greenberg BH. 2014. Discoidin domain receptor 2 germline gene deletion leads to altered heart structure and function in the mouse. Am J Physiol Heart Circ Physiol. 307(5):H773-781.

Durham E, Howie RN, Larson N, LaRue A, Cray J. 2019. Pharmacological exposures may precipitate craniosynostosis through targeted stem cell depletion. Stem Cell Res. 40:101528.

Eimar H, Tamimi F, Retrouvey JM, Rauch F, Aubin JE, McKee MD. 2016. Craniofacial and dental defects in the col1a1jrt/+ mouse model of osteogenesis imperfecta. J Dent Res. 95(7):761-768.

Erlebacher A, Filvaroff EH, Gitelman SE, Derynck R. 1995. Toward a molecular understanding of skeletal development. Cell. 80(3):371-378.

Fano V, Lejarraga H, Barreiro C. 2001. Spondylo-meta-epiphyseal dysplasia, short limbs, abnormal calcification type: A new case with severe neurological involvement. Pediatr Radiol. 31(1):19-22.

Fish JL. 2016. Developmental mechanisms underlying variation in craniofacial disease and evolution. Dev Biol. 415(2):188-197.

Franceschi RT, Iyer BS. 1992. Relationship between collagen synthesis and expression of the osteoblast phenotype in mc3t3-e1 cells. J Bone Miner Res. 7(2):235-246.

Franceschi RT, Iyer BS, Cui Y. 1994. Effects of ascorbic acid on collagen matrix formation and osteoblast differentiation in murine mc3t3-e1 cells. J Bone Miner Res. 9(6):843-854.

Gardner H, Kreidberg J, Koteliansky V, Jaenisch R. 1996. Deletion of integrin alpha 1 by homologous recombination permits normal murine development but gives rise to a specific deficit in cell adhesion. Dev Biol. 175(2):301-313.

Ge C, Wang Z, Zhao G, Li B, Liao J, Sun H, Franceschi RT. 2016. Discoidin receptor 2 controls bone formation and marrow adipogenesis. J Bone Miner Res.

Ge C, Xiao G, Jiang D, Franceschi RT. 2007. Critical role of the extracellular signal-regulated kinase-mapk pathway in osteoblast differentiation and skeletal development. J Cell Biol. 176(5):709-718.

Ge C, Xiao G, Jiang D, Yang Q, Hatch NE, Roca H, Franceschi RT. 2009. Identification and functional characterization of erk/mapk phosphorylation sites in the runx2 transcription factor. J Biol Chem. 284(47):32533-32543.

Gonzalez ME, Martin EE, Anwar T, Arellano-Garcia C, Medhora N, Lama A, Chen YC, Tanager KS, Yoon E, Kidwell KM et al. 2017. Mesenchymal stem cell-induced ddr2 mediates stromal-breast cancer interactions and metastasis growth. Cell Rep. 18(5):1215-1228.

Goto T, Aramaki M, Yoshihashi H, Nishimura G, Hasegawa Y, Takahashi T, Ishii T, Fukushima Y, Kosaki K. 2004. Large fontanelles are a shared feature of haploinsufficiency of runx2 and its co-activator cbfb. Congenit Anom (Kyoto). 44(4):225-229.

Gronthos S, Simmons PJ, Graves SE, Robey PG. 2001. Integrin-mediated interactions between human bone marrow stromal precursor cells and the extracellular matrix. Bone. 28(2):174-181.

Gupta N, Correa ARE, Jana M, Kabra M. 2019. Report of a novel homozygous nonsense ddr2 mutation in an indian adult male with spondylo-meta-epiphyseal dysplasia, short limb-abnormal calcification type. J Pediatr Genet. 8(3):153-156.

Harburger DS, Calderwood DA. 2009. Integrin signalling at a glance. J Cell Sci. 122(Pt 2):159-163.

Herrera-Herrera ML, Quezada-Calvillo R. 2012. Ddr2 plays a role in fibroblast migration independent of adhesion ligand and collagen activated ddr2 tyrosine kinase. Biochem Biophys Res Commun. 429(1-2):39-44.
Hughes DE, Salter DM, Dedhar S, Simpson R. 1993. Integrin expression in human bone. J Bone Miner Res. 8(5):527-533.
Ikeda K, Wang LH, Torres R, Zhao H, Olaso E, Eng FJ, Labrador P, Klein R, Lovett D, Yancopoulos GD et al. 2002. Discoidin domain receptor 2 interacts with src and shc following its activation by type i collagen. J Biol Chem. 277(21):19206-19212.
Jing Y, Jing J, Ye L, Liu X, Harris SE, Hinton RJ, Feng JQ. 2017. Chondrogenesis and osteogenesis are one continuous developmental and lineage defined biological process. Sci Rep. 7(1):10020.
Kano K, Marin de Evsikova C, Young J, Wnek C, Maddatu TP, Nishina PM, Naggert JK. 2008. A novel dwarfism with gonadal dysfunction due to loss-of-function allele of the collagen receptor gene, ddr2, in the mouse. Mol Endocrinol. 22(8):1866-1880.
Kim SH, Turnbull J, Guimond S. 2011. Extracellular matrix and cell signalling: The dynamic cooperation of integrin, proteoglycan and growth factor receptor. J Endocrinol. 209(2):139-151.
Kindblom JM, Nilsson O, Hurme T, Ohlsson C, Savendahl L. 2002. Expression and localization of indian hedgehog (ihh) and parathyroid hormone related protein (pthrp) in the human growth plate during pubertal development. J Endocrinol. 174(2):R1-6.
Kjaer I. 1990. Ossification of the human fetal basicranium. J Craniofac Genet Dev Biol. 10(1):29-38.
Kronenberg HM, Chung U. 2001. The parathyroid hormone-related protein and indian hedgehog feedback loop in the growth plate. Novartis Found Symp. 232:144-152; discussion 152-147.
Kuivaniemi H, Tromp G, Prockop DJ. 1997. Mutations in fibrillar collagens (types i, ii, iii, and xi), fibril-associated collagen (type ix), and network-forming collagen (type x) cause a spectrum of diseases of bone, cartilage, and blood vessels. Hum Mutat. 9(4):300-315.
Labrador JP, Azcoitia V, Tuckermann J, Lin C, Olaso E, Manes S, Bruckner K, Goergen JL, Lemke G, Yancopoulos G et al. 2001. The collagen receptor ddr2 regulates proliferation and its elimination leads to dwarfism. EMBO Rep. 2(5):446-452.
Lana-Elola E, Rice R, Grigoriadis AE, Rice DP. 2007. Cell fate specification during calvarial bone and suture development. Dev Biol. 311(2):335-346.
Le Douarin NM, Ziller C, Couly GF. 1993. Patterning of neural crest derivatives in the avian embryo: In vivo and in vitro studies. Dev Biol. 159(1):24-49.
Le Lievre CS. 1978. Participation of neural crest-derived cells in the genesis of the skull in birds. J Embryol Exp Morphol. 47:17-37.
Legate KR, Wickstrom SA, Fassler R. 2009. Genetic and cell biological analysis of integrin outside-in signaling. Genes Dev. 23(4):397-418.
Leitinger B. 2003. Molecular analysis of collagen binding by the human discoidin domain receptors, ddr1 and ddr2. Identification of collagen binding sites in ddr2. J Biol Chem. 278(19):16761-16769.
Leitinger B. 2011. Transmembrane collagen receptors. Annu Rev Cell Dev Biol. 27:265-290.
Leitinger B. 2014. Discoidin domain receptor functions in physiological and pathological conditions. Int Rev Cell Mol Biol. 310:39-87.
Leitinger B, Hohenester E. 2007. Mammalian collagen receptors. Matrix Biol. 26(3):146-155.

Leitinger B, Kwan AP. 2006. The discoidin domain receptor ddr2 is a receptor for type x collagen. Matrix Biol. 25(6):355-364.
Leitinger B, Steplewski A, Fertala A. 2004. The d2 period of collagen ii contains a specific binding site for the human discoidin domain receptor, ddr2. J Mol Biol. 344(4):993-1003.
Lieberman DE, Ross CF, Ravosa MJ. 2000. The primate cranial base: Ontogeny, function, and integration. Am J Phys Anthropol. Suppl 31:117-169.
Lin KL, Chou CH, Hsieh SC, Hwa SY, Lee MT, Wang FF. 2010. Transcriptional upregulation of ddr2 by atf4 facilitates osteoblastic differentiation through p38 mapk-mediated runx2 activation. J Bone Miner Res. 25(11):2489-2503.
Lowell CA, Mayadas TN. 2012. Overview: Studying integrins in vivo. Methods Mol Biol. 757:369-397.
Lu P, Takai K, Weaver VM, Werb Z. 2011. Extracellular matrix degradation and remodeling in development and disease. Cold Spring Harb Perspect Biol. 3(12).
Lynch MP, Stein JL, Stein GS, Lian JB. 1995. The influence of type i collagen on the development and maintenance of the osteoblast phenotype in primary and passaged rat calvarial osteoblasts: Modification of expression of genes supporting cell growth, adhesion, and extracellular matrix mineralization. Exp Cell Res. 216(1):35-45.
Mansouri M, Kayserili H, Elalaoui SC, Nishimura G, Iida A, Lyahyai J, Miyake N, Matsumoto N, Sefiani A, Ikegawa S. 2016. Novel ddr2 mutation identified by whole exome sequencing in a moroccan patient with spondylo-meta-epiphyseal dysplasia, short limb-abnormal calcification type. Am J Med Genet A. 170A(2):460-465.
Maruyama T, Jeong J, Sheu TJ, Hsu W. 2016. Stem cells of the suture mesenchyme in craniofacial bone development, repair and regeneration. Nat Commun. 7:10526.
McBratney-Owen B, Iseki S, Bamforth SD, Olsen BR, Morriss-Kay GM. 2008. Development and tissue origins of the mammalian cranial base. Dev Biol. 322(1):121-132.
McGrath J, Gerety PA, Derderian CA, Steinbacher DM, Vossough A, Bartlett SP, Nah HD, Taylor JA. 2012. Differential closure of the spheno-occipital synchondrosis in syndromic craniosynostosis. Plast Reconstr Surg. 130(5):681e-689e.
Mizuhashi K, Ono W, Matsushita Y, Sakagami N, Takahashi A, Saunders TL, Nagasawa T, Kronenberg HM, Ono N. 2018. Resting zone of the growth plate houses a unique class of skeletal stem cells. Nature. 563(7730):254-258.
Mizuno M, Fujisawa R, Kuboki Y. 2000. Type i collagen-induced osteoblastic differentiation of bone-marrow cells mediated by collagen-alpha2beta1 integrin interaction. J Cell Physiol. 184(2):207-213.
Mohamed FF, Franceschi RT. 2017. Skeletal stem cells: Origins, functions and uncertainties. Curr Mol Biol Rep. 3(4):236-246.
Neben CL, Merrill AE. 2015. Signaling pathways in craniofacial development: Insights from rare skeletal disorders. Curr Top Dev Biol. 115:493-542.
Nesbitt S, Nesbit A, Helfrich M, Horton M. 1993. Biochemical characterization of human osteoclast integrins. Osteoclasts express alpha v beta 3, alpha 2 beta 1, and alpha v beta 1 integrins. J Biol Chem. 268(22):16737-16745.
Nie X. 2005. Cranial base in craniofacial development: Developmental features, influence on facial growth, anomaly, and molecular basis. Acta Odontol Scand. 63(3):127-135.
Noden DM. 1988. Interactions and fates of avian craniofacial mesenchyme. Development. 103 Suppl:121-140.

Olaso E, Arteta B, Benedicto A, Crende O, Friedman SL. 2011. Loss of discoidin domain receptor 2 promotes hepatic fibrosis after chronic carbon tetrachloride through altered paracrine interactions between hepatic stellate cells and liver-associated macrophages. Am J Pathol. 179(6):2894-2904.

Olaso E, Ikeda K, Eng FJ, Xu L, Wang LH, Lin HC, Friedman SL. 2001. Ddr2 receptor promotes mmp-2-mediated proliferation and invasion by hepatic stellate cells. J Clin Invest. 108(9):1369-1378.

Olaso E, Labrador JP, Wang L, Ikeda K, Eng FJ, Klein R, Lovett DH, Lin HC, Friedman SL. 2002. Discoidin domain receptor 2 regulates fibroblast proliferation and migration through the extracellular matrix in association with transcriptional activation of matrix metalloproteinase-2. J Biol Chem. 277(5):3606-3613.

Opperman LA. 2000. Cranial sutures as intramembranous bone growth sites. Dev Dyn. 219(4):472-485.

Pace JM, Li Y, Seegmiller RE, Teuscher C, Taylor BA, Olsen BR. 1997. Disproportionate micromelia (dmm) in mice caused by a mutation in the c-propeptide coding region of col2a1. Dev Dyn. 208(1):25-33.

Paliga JT, Goldstein JA, Vossough A, Bartlett SP, Taylor JA. 2014. Premature closure of the spheno-occipital synchondrosis in pfeiffer syndrome: A link to midface hypoplasia. J Craniofac Surg. 25(1):202-205.

Popova SN, Barczyk M, Tiger CF, Beertsen W, Zigrino P, Aszodi A, Miosge N, Forsberg E, Gullberg D. 2007. Alpha11 beta1 integrin-dependent regulation of periodontal ligament function in the erupting mouse incisor. Mol Cell Biol. 27(12):4306-4316.

Pozzi A, Wary KK, Giancotti FG, Gardner HA. 1998. Integrin alpha1beta1 mediates a unique collagen-dependent proliferation pathway in vivo. J Cell Biol. 142(2):587-594.

Qin X, Jiang Q, Miyazaki T, Komori T. 2019. Runx2 regulates cranial suture closure by inducing hedgehog, fgf, wnt and pthlh signaling pathway gene expressions in suture mesenchymal cells. Hum Mol Genet. 28(6):896-911.

Rintala M, Metsaranta M, Saamanen AM, Vuorio E, Ronning O. 1997. Abnormal craniofacial growth and early mandibular osteoarthritis in mice harbouring a mutant type ii collagen transgene. J Anat. 190 (Pt 2):201-208.

Rittenhouse E, Dunn LC, Cookingham J, Calo C, Spiegelman M, Dooher GB, Bennett D. 1978. Cartilage matrix deficiency (cmd): A new autosomal recessive lethal mutation in the mouse. J Embryol Exp Morphol. 43:71-84.

Rozario T, DeSimone DW. 2010. The extracellular matrix in development and morphogenesis: A dynamic view. Dev Biol. 341(1):126-140.

Rozovsky K, Sosna J, Le Merrer M, Simanovsky N, Koplewitz BZ, Bar-Ziv J, Cormier-Daire V, Raas-Rothschild A. 2011. Spondyloepimetaphyseal dysplasia, short limb-abnormal calcifications type: Progressive radiological findings from fetal age to adolescence. Pediatr Radiol. 41(10):1298-1307.

Saito K, Fukumoto E, Yamada A, Yuasa K, Yoshizaki K, Iwamoto T, Saito M, Nakamura T, Fukumoto S. 2015. Interaction between fibronectin and beta1 integrin is essential for tooth development. PLoS One. 10(4):e0121667.

Salmivirta K, Gullberg D, Hirsch E, Altruda F, Ekblom P. 1996. Integrin subunit expression associated with epithelial-mesenchymal interactions during murine tooth development. Dev Dyn. 205(2):104-113.

Savontaus M, Rintala-Jamsa M, Morko J, Ronning O, Metsaranta M, Vuorio E. 2004. Abnormal craniofacial development and expression patterns of extracellular matrix components in transgenic del1 mice harboring a deletion mutation in the type ii collagen gene. Orthod Craniofac Res. 7(4):216-226.

Schipani E, Lanske B, Hunzelman J, Luz A, Kovacs CS, Lee K, Pirro A, Kronenberg HM, Juppner H. 1997. Targeted expression of constitutively active receptors for parathyroid hormone and parathyroid hormone-related peptide delays endochondral bone formation and rescues mice that lack parathyroid hormone-related peptide. Proc Natl Acad Sci U S A. 94(25):13689-13694.

Seegmiller R, Fraser FC, Sheldon H. 1971. A new chondrodystrophic mutant in mice. Electron microscopy of normal and abnormal chondrogenesis. J Cell Biol. 48(3):580-593.

Shekaran A, Shoemaker JT, Kavanaugh TE, Lin AS, LaPlaca MC, Fan Y, Guldberg RE, Garcia AJ. 2014. The effect of conditional inactivation of beta 1 integrins using twist 2 cre, osterix cre and osteocalcin cre lines on skeletal phenotype. Bone. 68:131-141.

Shi S, Kirk M, Kahn AJ. 1996. The role of type i collagen in the regulation of the osteoblast phenotype. J Bone Miner Res. 11(8):1139-1145.

Shrivastava A, Radziejewski C, Campbell E, Kovac L, McGlynn M, Ryan TE, Davis S, Goldfarb MP, Glass DJ, Lemke G et al. 1997. An orphan receptor tyrosine kinase family whose members serve as nonintegrin collagen receptors. Mol Cell. 1(1):25-34.

Smithson SF, Grier D, Hall CM. 2009. Spondylo-meta-epiphyseal dysplasia, short limb-abnormal calcification type. Clin Dysmorphol. 18(1):31-35.

Spranger J, Winterpacht A, Zabel B. 1994. The type ii collagenopathies: A spectrum of chondrodysplasias. Eur J Pediatr. 153(2):56-65.

St-Jacques B, Hammerschmidt M, McMahon AP. 1999. Indian hedgehog signaling regulates proliferation and differentiation of chondrocytes and is essential for bone formation. Genes Dev. 13(16):2072-2086.

Stephens LE, Sutherland AE, Klimanskaya IV, Andrieux A, Meneses J, Pedersen RA, Damsky CH. 1995. Deletion of beta 1 integrins in mice results in inner cell mass failure and peri-implantation lethality. Genes Dev. 9(15):1883-1895.

Tahiri Y, Paliga JT, Vossough A, Bartlett SP, Taylor JA. 2014. The spheno-occipital synchondrosis fuses prematurely in patients with crouzon syndrome and midface hypoplasia compared with age- and gender-matched controls. J Oral Maxillofac Surg. 72(6):1173-1179.

Takeuchi Y, Suzawa M, Kikuchi T, Nishida E, Fujita T, Matsumoto T. 1997. Differentiation and transforming growth factor-beta receptor down-regulation by collagen-alpha2beta1 integrin interaction is mediated by focal adhesion kinase and its downstream signals in murine osteoblastic cells. J Biol Chem. 272(46):29309-29316.

Teddy Cendekiawan RWKWaABMR. 2010. Relationships between cranial base synchondroses and craniofacial development: A review The Open Anatomy Journal.67-75.

Thorogood P. 1988. The developmental specification of the vertebrate skull. Development. 103 Suppl:141-153.

Trainor PA, Richtsmeier JT. 2015. Facing up to the challenges of advancing craniofacial research. Am J Med Genet A. 167(7):1451-1454.

Urel-Demir G, Simsek-Kiper PO, Akgun-Dogan O, Gocmen R, Wang Z, Matsumoto N, Miyake N, Utine GE, Nishimura G, Ikegawa S et al. 2018. Further expansion of the mutational spectrum of spondylo-meta-epiphyseal dysplasia with abnormal calcification. J Hum Genet. 63(9):1003-1007.

van der Eerden BC, Karperien M, Gevers EF, Lowik CW, Wit JM. 2000. Expression of indian hedgehog, parathyroid hormone-related protein, and their receptors in the

postnatal growth plate of the rat: Evidence for a locally acting growth restraining feedback loop after birth. J Bone Miner Res. 15(6):1045-1055.
Velleman SG. 2000. The role of the extracellular matrix in skeletal development. Poult Sci. 79(7):985-989.
Vikkula M, Metsaranta M, Ala-Kokko L. 1994. Type ii collagen mutations in rare and common cartilage diseases. Ann Med. 26(2):107-114.
Vogel W, Gish GD, Alves F, Pawson T. 1997. The discoidin domain receptor tyrosine kinases are activated by collagen. Mol Cell. 1(1):13-23.
Vogel WF, Abdulhussein R, Ford CE. 2006. Sensing extracellular matrix: An update on discoidin domain receptor function. Cell Signal. 18(8):1108-1116.
Wei X, Hu M, Mishina Y, Liu F. 2016. Developmental regulation of the growth plate and cranial synchondrosis. J Dent Res. 95(11):1221-1229.
Wickstrom SA, Radovanac K, Fassler R. 2011. Genetic analyses of integrin signaling. Cold Spring Harb Perspect Biol. 3(2).
Wilk K, Yeh SA, Mortensen LJ, Ghaffarigarakani S, Lombardo CM, Bassir SH, Aldawood ZA, Lin CP, Intini G. 2017. Postnatal calvarial skeletal stem cells expressing prx1 reside exclusively in the calvarial sutures and are required for bone regeneration. Stem Cell Reports. 8(4):933-946.
Xiao G, Jiang D, Thomas P, Benson MD, Guan K, Karsenty G, Franceschi RT. 2000. Mapk pathways activate and phosphorylate the osteoblast-specific transcription factor, cbfa1. J Biol Chem. 275(6):4453-4459.
Xiao G, Wang D, Benson MD, Karsenty G, Franceschi RT. 1998. Role of the alpha2-integrin in osteoblast-specific gene expression and activation of the osf2 transcription factor. J Biol Chem. 273(49):32988-32994.
Yang X, Matsuda K, Bialek P, Jacquot S, Masuoka HC, Schinke T, Li L, Brancorsini S, Sassone-Corsi P, Townes TM et al. 2004. Atf4 is a substrate of rsk2 and an essential regulator of osteoblast biology; implication for coffin-lowry syndrome. Cell. 117(3):387-398.
Zhang Y, Su J, Yu J, Bu X, Ren T, Liu X, Yao L. 2011. An essential role of discoidin domain receptor 2 (ddr2) in osteoblast differentiation and chondrocyte maturation via modulation of runx2 activation. J Bone Miner Res. 26(3):604-617.
Zhao H, Feng J, Ho TV, Grimes W, Urata M, Chai Y. 2015. The suture provides a niche for mesenchymal stem cells of craniofacial bones. Nat Cell Biol. 17(4):386-396.
Zimmerman D, Jin F, Leboy P, Hardy S, Damsky C. 2000. Impaired bone formation in transgenic mice resulting from altered integrin function in osteoblasts. Dev Biol. 220(1):2-15.

CHAPTER II

The Role of Discoidin Domain Receptor 2 (DDR2) in Craniofacial Development

Introduction

Defects in cranial growth and development cause a wide range of disorders known to dramatically impact physical, social, and emotional development of affected children. An understanding of the critical molecules and pathways necessary for craniofacial development is necessary to successfully treat these patients. The craniofacial skeleton develops through two distinct mechanisms: intramembranous ossification and endochondral ossification to form cranial vault and the cranial base, respectively. The intramembranous ossification occurs in the cranial vault when progenitor cells of neural crest and mesodermal origin condense and differentiate into bone-forming osteoblasts. The developing osteoblasts synthesize and secrete specialized extracellular matrix proteins, including type I collagen, bone sialoprotein, osteopontin, and osteocalcin. As new bone is deposited in the cranium, the edges of osteogenic fronts approximate each other to form cranial sutures. The cranial sutures contain unossified, fibrous connective tissue proposed to provide a niche for stem cells (Lana-Elola et al. 2007; Maruyama et al. 2016; Wilk et al. 2017; Zhao et al. 2015). Sutural stem cells (SuSCs) are associated with several genetic markers, including glioma-associated oncogene 1 (Gli1), an intermediate in hedgehog signaling, Axin-related protein 2 (Axin2), an intermediate in Wnt signaling, and paired related homeobox 1 (Prx1), reviewed in (Mohamed and Franceschi 2017). The current paradigm suggests

that SuSCs are present in mid sutural mesenchyme. As these cells differentiate into bone-forming osteoblasts, they facilitate new bone formation at sutural edges of the osteogenic fronts; a process that allows growth of the cranial vault in coordination with growth of the developing brain and cranial base.

In contrast, the endochondral ossification of the cranial base occurs through condensation and chondrogenic differentiation of mesenchymal progenitor cells to initially form cartilage templates, which are then replaced with bone. The mid-cranial base is composed from ethmoid, presphenoid, basisphenoid, and spheno-occipital bones separated by cartilaginous structures called synchondroses (i.e. sphenoethmoidal synchondrosis, intersphenoid synchondrosis, and spheno-occipital synchondrosis (Kjaer 1990). The sphenoethmoidal synchondrosis and intersphenoid synchondrosis are derivatives of neural crest, while the spheno-occipital synchondrosis is derived from paraxial mesoderm. Cranial base synchondroses are important growth centers that largely contribute to craniofacial development (Teddy Cendekiawan 2010). Histologically, the synchondrosis is a mirror-image growth plate with resting chondrocytes in the central zone and proliferative, and hypertrophic chondrocytes on both sides. The importance of the cranial base to craniofacial development and disease is emphasized by its involvement in many human syndromes such as craniosynostosis (premature closure of cranial sutures), Down's syndrome, Turner syndrome, cleidocranial dysplasia (CCD), cleft palate, and osteogenesis imperfecta (Cheung et al., 2011; McGrath et al., 2012; Nie, 2005; Paliga et al., 2014; Tahiri et al., 2014). Therefore, proper development and growth of the cranial base is critical for proper development of other craniofacial elements and associated organs.

During craniofacial development, several receptor tyrosine kinases (RTKs) have been identified as key regulators of critical cellular process, such as proliferation,

differentiation, migration, and cell survival (Lemmon and Schlessinger 2010). Examples include fibroblast growth factor receptors (FGFRs), epidermal growth factor receptor (EGFR), and receptor tyrosine kinase-like orphan receptor 2 (ROR2) (Miettinen et al. 1999; Rice et al. 2000; Schwabe et al. 2004). Mutations in these RTKs could cause a wide range of craniofacial abnormalities, such as craniosynostosis, broad prominent forehead, hypertelorism, cleft lip and palate, midface hypoplasia, a short nose, a long philtrum, and micrognathia (Afzal et al. 2000; Miettinen et al. 1999; Robin et al. 1993; Schwabe et al. 2004), suggesting the pivotal roles of RTK signaling in many fundamental aspects of craniofacial development. All RTKs share a common molecular architecture characterized by the extracellular ligand-binding domain, transmembrane domain, cytosolic juxtramembrane and tyrosine kinase domains (Lemmon and Schlessinger 2010). Upon binding growth factors or other signaling proteins, RTKs undergo conformational changes and autophosphorylation of tyrosine residues in the kinase domain creating docking sites for downstream signaling adaptors that mediate subsequent phosphorylation events and downstream signaling pathways (Lemmon and Schlessinger 2010).

Discoidin domain receptors (DDR1 and DDR2) are members of an unusual class of RTKs that are activated by triple-helical collagens (Leitinger and Hohenester 2007; Shrivastava et al. 1997; Vogel et al. 1997). DDRs are structurally distinct from other RTKs in having a unique extracellular structure characterized by the presence of a discoidin (DS) domain homologous to the discoidin I-like domain of the slime mold, Dictyostelium discoideum. DDR2 binds to fibril-forming (type I-III, V) and non-fibrillar (type X) collagens (Leitinger and Kwan 2006; Shrivastava et al. 1997; Vogel et al. 1997) -- an unusual characteristic of canonical RTKs known to bind to soluble growth factors. The DS domain determines the collagen recognition and binding specificity of DDR2. It

binds a GVMGFO motif (O is hydroxproline) within type I-III fibrillar collagens **(Figure I.4)** (Carafoli et al. 2009), but not to non-fibrillar basement membrane type IV collagen, which is exclusively recognized by DDR1 (Xu et al. 2011). Intriguingly, activation of DDRs is unusually slow and sustained for several hours after binding collagens (up to 18-24 hr) (Shrivastava et al. 1997; Vogel et al. 1997). However, the biological significance of such activation kinetics is not understood.

Human and animal genetic studies indicate that DDR2 is an important regulator for craniofacial development. In humans, *DDR2* loss of function mutations result in craniofacial abnormalities as part of a rare, autosomal recessive growth disorder called spondylo-meta-epiphyseal dysplasia (SMED) with short limbs and abnormal calcifications (SMED, SL-AC) (Al-Kindi et al., 2014; Ali et al., 2010; Bargal et al., 2009; Mansouri et al., 2016; Urel-Demir et al., 2018). Missense mutations in the extracellular domain and cytosolic tyrosine kinase domain of DDR2 have been identified which cause trafficking defects and loss of ligand binding leading to DDR2 loss-of-function in SMED, SL-AC disease (Ali et al. 2010). *DDR2* deficiency results in several defects in intramembranous and endochondral bone formation. Specifically, the craniofacial abnormalities in SMED, SL-AC patients include prominent forehead, wide-open fontanelle, hypertelorism, sparse eyebrows, a short nose with a depressed nasal bridge and long philtrum, micrognathia, and dental abnormalities (Al-Kindi et al., 2014; Mansouri et al., 2016; Rozovsky et al., 2011; Smithson et al., 2009; Urel-Demir et al., 2018). *Ddr2*-deficient mice exhibit similar phenotypes to those described in SMED, SL-AC patients (Cowling et al. 2014; Ge et al. 2016; Kano et al. 2008; Labrador et al. 2001). In the craniofacial region, these include eye protrusion, short snout, and impaired intramembranous ossification associated with delayed suture formation (Cowling et al. 2014; Ge et al. 2016; Kano et al. 2008; Labrador et al. 2001). *Ddr2* deficiency also

affects the axial and appendicular skeleton resulting in dwarfism, short limbs, and reduced bone mass (Ge et al. 2016; Kano et al. 2008; Labrador et al. 2001). While *Ddr2* clearly affects development of cranial, axial, and appendicular skeletons, little is known about how it functions, particularly in the craniofacial region. Furthermore, since *Ddr2* also functions in non-skeletal sites, it is possible that it could alter skeletal development via an indirect route.

In view of these considerations, in the present study, we performed detailed analysis of the craniofacial function of *Ddr2* with the goals of determining which portions of the craniofacial complex are affected, the distribution of DDR2 and its cellular sites of action. As will be shown, *Ddr2* has cell autonomous functions in putative skeletal progenitor cells of sutures and the cranial base where it affects these two cranial regions to dramatically alter cranial morphology.

Material and Methods

Mice

Ddr2-LacZ and *Ddr2*$^{fl/fl}$ mice were generated from "knockout-first" ES cell clone *Ddr2*$^{tm1a(EUCOMM)Wtsi}$(EPD0607__B01; European Mutant Mouse Repository) (https://www.eummcr.org). We developed *Ddr2*-LacZ knock-in mice by crossing founder mice harboring the Frt- flanked β-galactosidase (LacZ)-neo cassette with constitutive Sox2-Cre mice **(Figure II.6A)**, which result in Cre recombination in epiblast-derived tissues early during embryo development**.** *Ddr2*$^{fl/fl}$ mice were generated by crossing founder mice harboring the loxp- flanked coding exon 8 (exon 8) with the FLPo delete mice **(Figure II.6A)**. The *Ddr2*$^{fl/fl}$ mice were backcrossed onto C57BL/6 for at least six generations. *Ddr2* tissue-specific conditional knockouts were generated by crossing

mice carrying the *Ddr2* flox allele with Cre driver mouse lines, including Col2-Cre (Ovchinnikov et al. 2000) and Gli1-CreERT (Ahn and Joyner 2004). Other mice used in our experiments include *Ddr2*$^{mer\text{-}iCre\text{-}mer}$ mice obtained from Dr. Barry Greenburg (University of California-San Diego). *Ddr2*$^{mer\text{-}iCre\text{-}mer}$ mice harbor a MerCreMer cassette knocked in-frame into exon 2 of the *Ddr2* locus. To obtain *Ddr2*$^{mer\text{-}iCre\text{-}mer}$; Ai14 tdTomato reporter mice, we crossed *Ddr2*$^{mer\text{-}iCre\text{-}mer}$ heterozygous mice with Ai14 tdTomato line, which was previously described (Madisen et al. 2010). Cre-driver lines and Ai14 tdTomato were generous gifts (see acknowledgements). We also used *slie* homozygote mice, *Ddr2*$^{slie/slie}$, carrying a spontaneous 150-kb deletion mutation of *Ddr2* exons 1-17 resulting in a null allele (Kano et al. 2008). Homozygous *slie* mice were obtained from intercrossing heterozygous (*Ddr2*$^{+/slie}$) mice. Most mice used in our experiments were bred on C57BL/J6 background, except Col2-Cre; *Ddr2*$^{fl/fl}$ mice were bred on mixed background.

Genotyping

Genomic DNA was prepared from tail snips and ear punches using DNA REDExtract-N-Amp™ Tissue PCR Kit (Sigma-Aldrich, St. Louis, MO) according to the manufacturer's instructions. Polymerase chain reaction (PCR) analysis was then used to genotype the mice. Information about primers used for genotyping is presented in **Table II.1**. The genotyping of *Ddr2*$^{slie/slie}$ mice was performed by qRT-PCR with TaqMan probes on an ABI 7500 (Applied BioSystems) according to the provider's instructions. Production and genotyping of *Ddr2*$^{mer\text{-}iCre\text{-}mer}$, Col2-Cre, Gli1-CreERT, and Ai14 tdTomato reporter mice have been described previously (Ahn and Joyner 2004; Cowling et al. 2014; Madisen et al. 2010; Ovchinnikov et al. 2000; Zhang et al. 2002). All mice were housed under a 12-hour light cycle in compliance with the Guidelines for the Care and Use of Animals for Scientific Research. All protocols for mouse experiments were

approved by the Institutional Animal Care and Use Committee of the University of Michigan.

Whole-Mount Skeletal Staining

Whole-mount skeletal staining of mice was performed as described previously (McLeod 1980) with modification. Briefly, skin and internal organs were removed and skeletal tissues were fixed in 95% ethanol for 6 days at room temperature. Skulls of 2-week old mice were stained in 0.015% Alcian blue 8GX (Sigma A3157) solution in 80% ethanol and 20% acetic acid for 24 h and then cleared in 2% potassium hydroxide (KOH) for 1-2 days to remove soft tissues. Samples were then stained with 0.005% alizarin sodium sulphate (Sigma, A-3757) solution in 1%KOH for 12-14 h and cleared in 1% KOH and 20% glycerol to remove all soft tissues. Samples were stored in 50% glycerol: 50% ethanol and imaged using a dissection microscope (Nikon SMZ 745T) equipped with a Nikon DS-fi1 camera.

Micro-Computed Tomography (MicroCT) Analysis

Ten skulls from 3 month-old male and female mice were harvested and fixed in 10% formalin overnight at 4°C. Using microCT Scanco Model 100 (Scanco Medical), mouse skulls were scanned and reconstructed with voxel size of 12 μm, 70 kVp, 114 μA, 0.5-mm aluminum filter, and integration time of 500 ms. For craniofacial characterization, skull scans in VFF files were reoriented and cropped in MicroView software (version 2.5.0) and a total of 21 linear craniofacial measurements were made on 2D reoriented CT images using ImageJ software (version 1.51). We conducted the linear measurements according to previously published craniofacial landmarks (Vora et al. 2015). Thickness of cranial bones was measured on 2D reoriented CT images using a defined position on orthogonal views of MicroView software. Values for frontal and

parietal bone thickness represent the average of bone thickness from right and left measurements around frontal and sagittal sutures, respectively. Values for occipital bone thickness represents the average of bone thickness from side measurements of occipital bone. The morphology and patency of the main four cranial sutures (frontal, sagittal, coronal, and occipital) were assessed using the 2D reoriented CT images using ImageJ software. Each sample was given a unique number to avoid specification of mouse genotype during data analysis, thereby avoiding examiner bias.

Histology and Immunostaining

The whole skulls were fixed in 4% paraformaldehyde (PFA) for 48 h at 4°C. Specimens were decalcified in 10% ethylenediaminetetracetic acid (EDTA) (pH 7.2) (Fisher, S316-212) and were then processed for paraffin embedding. Specimens were sectioned at 5 µm using a microtome, deparaffinized and hydrated in ethanol series (100%, 95%, 70%) and in distilled water. For histological analysis, the sections were stained with hematoxylin and eosin according to the standard procedures. For immunofluorescence, the sections were subjected to heat-induced antigen retrieval using 1X Diva Decloaker (Biocare medical) following the manufacturer' instructions, washed with 1X PBS and then incubated with blocking buffer containing 5-10% normal donkey serum, 1% bovine serum albumin (BSA), 0.01% tween in 1X BSP for 1h at room temperature in a humid box. After blocking, the sections were then incubated at 4°C overnight using the following primary antibodies: Anti-COL2 (1:100, ab34712, Abcam); Anti-COL10 (1:100, ab58632, Abcam); Anti-SOX9 (1:100, sc-17341, Santa Cruz Biotechnology); Anti-GM130 (1:100, 610822, BD Biosciences); anti-MMP13 (1:100, ab39012, Abcam). For Anti-GLI1 (1:100, NBP1-78259, Novus biological), sections were retrieved using citrate buffer (target retrieval solution, Dako) and heated to 60 °C for 1 h. The sections were incubated with species-matched secondary antibodies for 1 h at room

temperature. The slides were rinsed three times with 1X PBS, and the cover slip was mounted using ProLong™ Gold Antifade Mountant with DAPI (Life technologies) for cell nuclei staining. The sections were then imaged with a Nikon Eclipse 55i microscope and an Olympus DP72 camera.

LacZ (β-galactosidase) Staining

LacZ staining of heterozygous *Ddr2*-LacZ ($Ddr2^{+/LacZ}$) skulls was performed according to standard protocols (Nagy 2007). Samples were fixed in 2% paraformaldehyde and 0.2% glutaraldehyde in 0.1 M, phosphate buffer pH 7.3 plus 5mM EGTA and 2mM $MgCl_2$ at 4 °C. For whole-mount staining, samples were rinsed after fixation 3 times in 1X PBS plus $MgCl_2$, and then incubated overnight at 37 °C in a freshly prepared X-gal solution containing an X-gal substrate (UltraPure X-Gal, Invitrogen), 2mM $MgCl_2$, 5mM potassium fericyanide (III) (702587, Sigma), 5mM potassium hexacyanoferrate (II) (P3289, sigma), 0.01% sodium deoxycholate, 0.02% NP-40. The samples were then visualized using a dissection microscope (Nikon SMZ 745T), and images were captured using a Nikon DS-fi1 camera. Wild-type littermates were used as controls. For frozen sections, samples were decalcified with 20% EDTA (pH 7.2) for up to 2 weeks according to the mouse age, rinsed in 1X PBS, then placed in 30% sucrose in 0.1M phosphate buffer with 2mM $MgCl_2$ at 4 °C overnight. Samples were then embedded in optimal cutting temperature compound (Tissue-Tek), cryosectioned at 12 µm thickness at -20 °C and mounted on glass histological slides (Fisherbrand™ ColorFrost™ Plus). For LacZ staining of frozen sections, samples were post-fixed in 0.2% PFA in 0.1 phosphate buffer pH 7.2 for 10 min on ice, washed 3 times in $MgCl_2$-containing PBS, and stained with an X-gal substrate (UltraPure X-Gal, Invitrogen), 2mM $MgCl_2$, 5mM potassium fericyanide (III) (702587, Sigma) and 5mM potassium hexacyanoferrate (II) (P3289, sigma) for overnight at 37°C. The sections were washed 3

times in 1X PBS followed by distilled water, counterstained with Vector Nuclear Fast Red staining, and dehydrated through ethanol series and xylene and mounted with an Acrytol mounting medium (Leica).

Proliferation and Apoptosis Assay

To assay cell proliferation, mice were injected intraperitoneally with 5-ethynyl-2'-deoxyuridine and sacrificed 4h after injection. EdU-labeled cells were detected using Click-iT® EdU Alexa Fluor® 488 Imaging Kit (Invitrogen, # C10337). Briefly, after deparaffinization and hydration, the tissue sections were incubated with Click-it reaction mixture for 30 min in a dark humid chamber. The sections were washed with 1X PBS 3 times for 2 minutes each, mounted with ProLong™ Gold Antifade Mountant with DAPI (Life technologies) (358 nm/461 nm) and imaged with a Nikon Eclipse 55i microscope and an Olympus DP72 camera. To assay cell apoptosis, we performed terminal deoxynucleotidyl transferase dUTP nick end labeling (TUNEL) assay according to the manufacturer instructions (FragEL™ DNA Fragmentation Detection Kit, Colorimetric-Klenow Enzyme, Calbiochem). Briefly, after deparaffinization and rehydration, the tissue sections were rinsed in 1X tris-buffered saline (TBS), permeabilized with Proteinase K and the endogenous peroxidase activity was blocked with 3% hydrogen peroxide for 5 minutes at room temperature. The sections then were incubated with Klenow Labeling reaction mixture in a humidified chamber at 37 °C for 1.5 h. For labeling detection, the sections were incubated with peroxidase streptavidin conjugate and subsequently with DAB solution. The sections were counterstained with methyl green solution and imaged with a Nikon Eclipse 55i microscope and an Olympus DP72 camera

Fluorescence-Based ELF97 TRAP for Osteoclasts

Frozen sections were fixed with 4% paraformaldehyde for 10 min and washed with PBS and subsequently with deionized water (ddH2O). Fixed sections were subjected to tartrate-resistant acid phosphatase (TRAP) staining using an ELF97 endogenous phosphatase detection kit (Invitrogen) combined with reagents from acid phosphatase, Leukocyte (TRAP) Kit (Sigma-Aldrich). Briefly, ELF97 endogenous phosphatase substrate was added to a mixture of 11 mM sodium nitrate, 112 mM sodium acetate, and 76 mM sodium tartrate solutions in ddH_2O. Sections were incubated with the TRAP mixture in a dark humid chamber for 15min at room temperature, washed with PBS, mounted with mounting medium, and visualized with DAPI channel using a Nikon Eclipse 55i microscope and an Olympus DP72 camera.

Statistical Analysis

Graphing of data and statistical analysis was performed using GraphPad Prism software (version 6.0e, La Jolla California USA). All values are presented as mean ± S.D. Unpaired, two-tailed Student's t test was used to analyze the difference between the two experimental groups. For categorical data, Fisher's exact test was used to analyze the significance of the observed frequencies of the defects in cranial sutures. * $P < 0.05$; ** $P < 0.01$, *** $P < 0.001$, **** $P < 0.0001$; n.s. not significant.

Results

Ddr2 knockout results in impaired bone growth dramatically manifested in the anterior craniofacial skeleton

While previous studies using *Ddr2*-deficient mice reported that they have craniofacial abnormalities including reduced mineralization and altered skull shape

(Cowling et al. 2014; Ge et al. 2016; Kano et al. 2008; Labrador et al. 2001), the basis of these changes has not been investigated. To understand the craniofacial phenotype of these animals, we first sought to define which parts of the skull are altered and then to determine the cellular basis for these changes. To characterize craniofacial abnormalities of *Ddr2*$^{slie/slie}$ mice, we performed linear measurements on micro-CT scans of 3 month-old skulls (n=10) using MicroView (version 2.5.0) and ImageJ software (NIH, version 1.51), and followed previously published landmarks for linear skull measurements (Vora et al. 2015). Our analysis along the anteroposterior axis revealed a significant reduction in the skull length (12%, P <0.0001) mainly due to shortening of nasal bone (19%, P <0.0001) as oppose to the cranial vault (8%, P <0.001) (**Figure II.1A and B**). The length of the cranial base in *Ddr2*$^{slie/slie}$ mice was also shorter than that in WT controls. Interestingly, the basisphenoid bone that forms the mid-posterior cranial base was mostly affected in the knockout mice (14%, P <0.0001) (**Figure II.1B**). The intersphenoid (ISS) and spheno-occipital synchondroses (SOS) form anterior and posterior borders of the basiosphenoid bone, respectively, and were both altered in *Ddr2*-deficient mice although changes were most dramatic in the ISS; the width of the ISS increased by 187% (P <0.0001) versus 23% (P <0.05) for the SOS (**Figure II.1C and 1D**). An increase in SOS height was also seen (12%, P <0.05) (**Figure II.1C and 1D**). Interestingly, defects due to *Ddr2* knockout were most obvious in the anterior craniofacial skeletal elements such as the nasal bones and ISS.

In addition to the shortened skull length, we also observed a significant increase in the anterior skull width (17%, P <0.0001), but did not detect differences in the posterior skull (data not shown), further indicating that *Ddr2* is preferentially active in the anterior skull. No significant differences were observed in anterior facial height or in anterior, middle, and posterior cranial heights between the knockout and WT mice.

However, the skull height and skull width in relation to the skull length was higher in *Ddr2*$^{slie/slie}$ mice than in the WT littermates, which could explain the dysmorphic skull shape (**Figure II.1E and 1F**). For further analysis of cranial bones, we selected orthogonal planes in the MicroView software (highlighted in different colors) to quantify if there is difference in thickness of frontal, parietal, and occipital bones between knockout and WT mice (**Figure II.2A**). The value for bone thickness represents the average of two measurements made in on each side of a corresponding cranial suture, as shown in (**Figure II.2A**). Strikingly, the thickness of frontal bone was significantly reduced (55% reduction, P <0.0001) in *Ddr2*$^{slie/slie}$ mice compared with WT mice (**Figure II.2B and 2C)**; however, no significant differences were observed in the thickness of parietal bone (**Figure II.2D and 2E)** or occipital bone (**Figure II.2F and 2G)**. The frontal bone defect in *Ddr2*$^{slie/slie}$ calvariae was associated with wide-open suture defect (**Figure II.2H**). While both DDRs, DDR1 and DDR2, share similarities in terms of molecular structure and ligand binding specificity, *Ddr1*-knockout mice did not have any of the craniofacial abnormalities we report for *Ddr2* (data not shown), suggesting a specific role of DDR2 in the development of craniofacial skeleton. In summary, *Ddr2* knockout mice exhibited defects in intramembranous and endochondral bones with major manifestations in the anterior craniofacial skeleton.

Ddr2 Knockout Exhibited Delayed Intramembranous and Endochondral Ossification

To further characterize the craniofacial abnormalities of *Ddr2*-knockout mice, we performed histological analysis on 2 week-old skulls using alcian blue (cartilage) and alizarin red S (mineral) and hematoxylin and eosin staining. Interestingly, alcian blue and alizarin red S staining showed abnormal cranial suture morphology and delayed formation of the frontal suture (yellow arrowhead) in the knockout calvariae **(Figure**

II.3A). Histological analysis also revealed that the midline cranial sutures (the frontal suture) were wider in the knockout mice than in WT controls, and the flanking bones were not well developed (**Figure II.3B).** However, no major differences were observed in the transverse cranial sutures, including coronal and lambdoid sutures.

We also examined the cranial base synchondroses focusing on ISS and SOS. Using alcian blue and alizarin red S staining, we found both synchondroses in *Ddr2*$^{slie/slie}$ mice were abnormally wide, but the increase of the width was more dramatic in ISS than in SOS (**Figure II.3C)**. Histological analysis revealed that the *Ddr2*-null synchondroses, particularly ISS, showed severe defects characterized by abnormal chondrocyte organization, wide resting zone, and loss of the columnar arrangement of proliferative chondrocytes (**Figure II.3D and 3E)**. This preferential enlargement of the ISS in *Ddr2*-deficient mice is consistent with the μCT data shown in **Figure II.1C**.

During endochondral bone development, resting chondrocytes in the growth plate undergo sequential proliferation, hypertrophic differentiation, and apoptosis before being replaced by bone. We therefore sought to assess whether *Ddr2* affects any of these parameters. To examine chondrocyte proliferation, we injected 2 week-old mice with EdU intraperitoneally 4 h before analysis, and the EdU-labeled cells were expressed as a percentage of total cells in the synchondrosis. EdU staining (green) showed labeling predominantly in the proliferative zone of ISS and SOS (**Figure II.4A)**; however, EdU+ chondrocytes were significantly reduced in *Dd2*-deficinet synchondroses: 55% reduction in ISS (P<0.0001) and 26% reduction in SOS (P <0.001) compared with WT controls (**Figure II.4B)**. These results indicate that *Ddr2* is required for normal synchondrosis chondrocyte proliferation. We also performed TUNEL assay to measure any change in apoptotic levels in synchondroses lacking *Ddr2* versus WT controls (**Figure II.4C)**. However, we did not observe any difference in TUNEL staining

in both the ISS and SOS (**Figure II.4D)**. While these results demonstrate a requirement for DDR2 in chondrocyte proliferation, they do not directly explain why the synchondrosis-resting zone is widened in the absence of *Ddr2*.

To gain further insight into changes occurring in synchondroses of *Ddr2*-deficient mice, we performed immunostaining of type II collagen (COL2) for undifferentiated chondrocytes, type X collagen (COL10) for hypertrophic chondrocytes, and matrix metalloproteinase 13 (MMP13) for late hypertrophic chondrocytes. In wild type synchondroses, immunofluorescent staining of type II collagen showed a homogenous distribution within the cartilage matrix around chondrocytes. In contrast, type II collagen was unevenly distributed in *Ddr2*-null synchondroses where it exhibited an intense ring-like distribution around chondrocytes that diminished in the adjacent interterritorial extracellular matrix (**Figure II.5A).** This suggests that DDR2 may regulate COL2 processing and/or distribution within the cartilage ECM. As expected, type X collagen immunostaining showed a specific signal in hypertrophic chondrocyte zone. We did not observe any change in the pattern of the type X collagen immunostaining between WT and $Ddr2^{slie/slie}$ mice. However, the later showed a slight enlargement of the hypertrophic zone of cranial base synchondroses both in ISS and SOS (**Figure II.5B)**, suggesting that the transition between hypertrophic chondrocytes and endochondral bone formation may be delayed. Consistent with this concept, we also observed decreased MMP13 immunostaining in *Ddr2*-null synchondroses (**Figure II.5C)**. Since type X collagen is a substrate of MMP13, we might speculate that the decrease in MMP13 levels in $Ddr2^{slie/slie}$ mice results in defective remodeling of type X collagen matrix in the hypertrophic zone, causing delayed endochondral ossification. Additional immunostaining for SOX9, a transcriptional factor essential for chondrogenesis, revealed immunoreactivity in resting chondrocytes and hypertrophic chondrocytes in WT

synchondroses (**Figure II.5D)**; however, SOX9 immunostaining was reduced in *Ddr2*$^{slie/slie}$ synchondroses. In long bone growth plates, *Sox9* is required to maintain chondrocyte proliferation, since *Sox9* knockout mice had shortened growth plates (Dy et al. 2012). Our observation of chondrocyte proliferation is reduced in *Ddr2*$^{slie/slie}$ synchondroses is consistent with this decreased in SOX9 immunostaining. However, the exact mechanisms remain to be identified. Taken together, our results suggest that *Ddr2* knockout resulted in abnormal chondrogenesis due to chondrocyte disorganization, deficient chondrocyte proliferation and abnormalities in cartilage extracellular matrix distribution and turnover.

Ddr2 is Expressed in Craniofacial Regions Enriched with Skeletal Stem/Progenitor Cells

Ddr2 deficiency results in growth defects in the craniofacial skeleton; however, no information is available on where *Ddr2* is actually expressed. To address this question, we used a *Ddr2*-lacZ Knock-in mouse model to determine the spatial and temporal expression of *Ddr2* during craniofacial development. Development of the *Ddr2*-lacZ knock-in mouse model is described in **Figure II.6A** and Methods. The expression pattern of *Ddr2* was examined using a combination of whole mount and frozen sections of *Ddr2*$^{+/LacZ}$ heterozygous mice at embryonic and postnatal stages. During fetal development, LacZ staining was first detected at E11.5 (not seen in the initial E9.5 time point) (**Figure II.6B)**. The whole mount staining of E11.5 revealed a broad *Ddr2* expression in the developing midface including the median and lateral nasal process (MNP and LNP), maxillary and mandibular processes, and supraorbital region (**Figure II.6B)**. Similar expression pattern was seen in E13.5 (**Figure II.6B)** and E16.5 embryo (data not shown). No LacZ staining was detected in the developing brain, but we noted a specific staining at the boundary between developing brain hemispheres corresponding

to the future cranial sutures (**Figure II.6B)**. Using frozen sections of the E13.5 embryonic head, LacZ staining was detected in cartilage primordia of the cranial base and in tongue mesenchyme, in addition to intense LacZ staining surrounding nasal septum, developing tooth buds, and surrounding Meckel's cartilages in the developing mandible (**Figure II.6C).** We confirmed that this staining was specific as no LacZ staining was observed in the wild-type *Ddr2*$^{+/+}$ embryos.

Postnatally, we found that *Ddr2* is expressed in multiple regions of craniofacial skeleton. The whole mount staining of *Ddr2*$^{+/LacZ}$ skulls from newborn mice showed broad *Ddr2* expression in the whole calvaria with most intense staining in the suture regions **(Figure II.7A, left)**. *Ddr2* expression became more restricted in cranial sutures as mice became older (3 months is the time point examined in adult mice) (**Figure II.7A right)**. Frozen sections of neonatal *Ddr2*$^{+/LacZ}$ skulls revealed *Ddr2* expression in the suture mesenchyme, in the periosteum and dura mater of flanking bones (**Figure II.7B)**. In adult calvaria frozen sections, LacZ staining was evident in the suture mesenchyme, dura mater, periosteum, and the lining of calvarial bone marrow (**Figure II.7C)**. However, we could not detect LacZ staining in osteocytes in the calvarial bones. This may suggest that *Ddr2* expression is highest during early stages of osteoblast differentiation. *Ddr2* expression was also detected in synchondroses in cranial bases, primarily located in the resting (RZ) and proliferative chondrocyte (PZ) zone, but could not be detected in hypertrophic chondrocytes (HZ) (**Figure II.7D)**. Additional positive cells were associated with trabecular bone and bone marrow as well as the periosteum (**Figure II.7D)**. In most of the tissues we examined, the pattern of neonatal expression of *Ddr2* was maintained throughout the adult life, but more interestingly, *Ddr2* expression was highest in regions enriched with skeletal stem/progenitor cells including cranial sutures, periosteum, dura mater, and resting chondrocytes. This observation suggests that *Ddr2* is in skeletal

progenitor cells that could contribute to the development of craniofacial skeleton.

Ddr2-Expressing Cells Contribute to Craniofacial Bones

Prior studies hypothesized that craniofacial stem cells reside within cranial sutures (Lana-Elola et al. 2007; Maruyama et al. 2016; Wilk et al. 2017; Zhao et al. 2015). These cells are of great interest because of their contribution to the development of craniofacial bones. Given that *Ddr2*-LacZ expression was detected in cranial sutures, we asked if *Ddr2* is in a suture cell population having properties of skeletal progenitors. To address this question, we used a lineage-tracing approach by breeding heterozygous *Ddr2*$^{Mer\text{-}icre\text{-}Mer}$ female mice (provided by Dr. Barry Greenberg, (University of California-San Diego, and described in Methods) with male homozygous Ai14 tdTomato reporter mice (provided by Dr. Ono Noriaki, University of Michigan). This approach allows us to genetically label *Ddr2*-expressing cells, trace their progeny and identify their location and differentiation status. Ai14 tdTomato mice have a flanked STOP cassette that interferes with transcription of tdTomato red fluorescent protein. Upon tamoxifen administration, Cre expression driven by *Ddr2* promoter excises the LoxP flanked STOP cassette resulting in tdTomato fluorescent protein only in *Ddr2*-expressing cells and their progeny. Cre-mediated recombination in *Ddr2*$^{Mer\text{-}icre\text{-}Mer}$*;* Ai14 tdTomato mice was induced with intragastric tamoxifen injections given for 4 days after birth and then skulls were harvested and analyzed at day 5, 2 weeks, and 2 months of age (**Figure II.8A)**. Whole mount of calvaria showed tdTomato labeling in all cranial sutures (i.e. frontal, sagittal, coronal and occipital sutures, **Figure II.8B)**. At day 5, frozen sections revealed labeling in select cells in cranial suture mesenchyme, periosteum, and dura mater of flanking calvarial bones. This distribution was similar to that seen for *Ddr2*-lacZ staining in **Figure II.7** indicating that these are mostly *Ddr2*-expressing cells (**Figure II.8C)**. Again in

agreement with the LacZ staining, we did not detect any labeling in osteocytes. Over a two-month trace, tdTomato labeling initially expanded throughout the suture mesenchyme and periosteal regions (P14) and by P60 was detected in osteocytes and lining cells in the bone marrow of flanking calvarial bones (**Figure II.8C)**. These data suggests that osteocytes and bone marrow-lining cells are progeny of *Ddr2*-expressing cells and establish the contribution of *Ddr2*-expressing cells to calvarial bone formation.

Examining the cranial base synchondroses at day 5, initial tdTomato labeling was detected in select cells in resting and proliferative zones, but not in hypertrophic chondrocytes (**Figure II.8D)**. These results are in agreement with *Ddr2-LacZ* expression, and suggest that the tdTomato-label is in *Ddr2*-expressing cells in resting and proliferating zone chondrocytes. It should be noted that the resting zone, at least in long bone growth plates, is known to contain chondroprogenitor cells (Abad et al. 2002; Mizuhashi et al. 2018). By two weeks, the tdTomato-labeled cells expanded to all chondrocyte lineages (resting, proliferative, and hypertrophic). By 2 months as growth declines in the cranial base, tdTomato labeling was retained in resting chondrocyte zone, consistent with this being a slow cycling progenitor population (**Figure II.8D)**. At this time, the label was also seen on the surface of trabecular bone in the bone marrow and in osteocytes within the cortical bone of the cranial base (**Figure II.8D)**. Together, these results are consistent with the hypothesis that *Ddr2* is expressed in stem/progenitor populations in cranial sutures and synchondroses that are precursors to differentiated cartilage and bone cell types. However, the identity of these cells needs to be determined.

Lineage Tracing Identifies Ddr2 in Osteoblast Lineages, including Gli1+ Osteoprogenitors, but not in Osteoclasts

Previous lineage-tracing experiments showed that Gli1, a mediator of hedgehog signaling, is associated with stem/progenitor cells in cranial sutures (Zhao et al. 2015). We asked if there is overlap between *Ddr2*- and *Gli1*-expressing cells. To address this question, we verified the activity of inducible Gli1-CreERT under our experimental conditions by breeding with Ai14 tdTomato reporter mice. Newborn mice heterozygous for inducible Gli1 and Ai14 alleles were injected intragastrically with four tamoxifen injections and analyzed for TdTomato distribution after two weeks (**Figure II.9A)**. Upon tamoxifen injection, Gli1 promoter-driven Cre recombination activates tdTomato red fluorescence only in Gli1-expressing cells and their progeny. TdTomato cells were identified mainly in cranial sutures in agreement with the previous study (Zhao et al. 2015) and with a pattern similar to that seen with *Ddr2* labeling (**Figure II.9B)**. Also similar to the $Ddr2^{Mer\text{-}icre\text{-}Mer}$ mice 2 weeks after tamoxifen injection, the Gli1-CreERT labeled all chondrocyte lineages in the cranial base (**Figure II.9B)**. These observations indicate that there is a large overlap between *Ddr2*- and *Gli1*- expressing cells and their progeny. In support of this hypothesis, we confirmed co-expression in synchondroses with anti-GLI1 immunofluorescence on $Ddr2^{Mer\text{-}icre\text{-}Mer}$*;* Ai14 tdTomato skulls (**Figure II.9C)**. At P5, we found that most of *Ddr2*+ tdTomato cells (red) in resting and proliferative zone of synchondrosis where it colocalized with GLI1 (green) (**Figure II.9C)**, additional evidence of co-expression of Ddr2 and Gli1 in many of the same cells.

Osteoclasts, a second type of bone cell, are multinucleated giant cells involved in bone resorption during development and remodeling of the skeleton and during tooth eruption (Jacome-Galarza et al. 2019). One the basis of cell culture studies, it was previously proposed that DDR2 is expressed in osteoclasts as well as

osteoblasts/osteoprogenitors (Zhang et al. 2015; Zhang et al. 2011). To address the possibility that *Ddr2*-tdTomato-labeled cells are osteoclasts, we performed fluorescent-based TRAP staining to mark TRAP+ multinucleated cells on frozen sections from *Ddr2*$^{Mer\text{-}icre\text{-}Mer}$*;* Ai14 tdTomato mice. Cre-recombination in *Ddr2*$^{Mer\text{-}icre\text{-}Mer}$*;* Ai14 tdTomato mice was induced at birth with four tamoxifen injections, as previously described and tissues were examined after 2 months. Multinucleated TRAP+ cells (green) appeared in cranial sutures, on the bone surface of osteogenic fronts and in the bone marrow of calvaria (**Figure II.9D)** and cranial base bones (data not show); however, the spatial distribution of these cells was distinct from that of *Ddr2* tdTomato-labeled cells (red) (**Figure II.9D)**, indicating that there is no overlap between TRAP+ osteoclasts and *Ddr2* tdTomato-labeled cells or their progeny.

Loss of Ddr2 in Gli1-expressing cells resulted in a craniofacial phenotype similar to Ddr2$^{slie/slie}$ *mice*

Our studies with globally *Ddr2*-deficient mice (*Ddr2*$^{slie/slie}$) clearly established the importance of *Ddr2* in craniofacial development. However, they do not provide any information concerning its cellular sites of action. In fact, based on current knowledge, *Ddr2* could affect craniofacial development indirectly. For example, *Ddr2*$^{slie/slie}$ mice exhibit gonadal insufficiency accompanied by reduced circulating levels of sex steroids, which could systemically affect bone formation. This emphasizes the importance of using a conditional deletion approach to determine if *Ddr2* has cell-autonomous functions in skeletal cells. The localization of *Ddr2* expression in cranial regions known to contain stem/progenitor populations and its colocalization with Gli1, a stem cell marker, suggest possible functions of *Ddr2* in a Gli1-positive progenitor population. To address this possibility, we initially choose to use an inducible Gli1-CreERT to conditionally delete *Ddr2* in Gli1-expressing cells and examine the effect of *Ddr2* loss of

function on cranial bone formation. In this study, we bred inducible Gli1-CreERT with mice carrying floxed *Ddr2* allele, which includes exon 8 flanked by LoxP sites (**Figure II.6A)** to generate conditional knockout mice (later referred to as Gli1-CreER; $Ddr2^{fl/fl}$ mice). In order to disrupt the *Ddr2* gene, we injected Gli1-CreER; $Ddr2^{fl/fl}$ newborn mice and their control littermates ($Ddr2^{fl/fl}$) intragastrically with tamoxifen for four days and analyzed them at 3 months of age (**Figure II.10A)**. PCR analysis of genomic DNA extracted from ear punches was performed to evaluate the efficiency of recombination after tamoxifen injections (**Figure II.10B)**. Gli1-CreER; $Ddr2^{fl/fl}$ mice exhibited a growth retardation that was first apparent at P10 (data not shown). By three months, conditional knockout of *Ddr2* in Gli1-expressing cells resulted in dwarfism to a magnitude similar to global *Ddr2* knockout (**Figure II.10C)**. Gli1-CreER; $Ddr2^{fl/fl}$ mice exhibited a significant reduction in the body length and body weight both in males and females (**Figure II.10D and 10E)**. Gli1-CreER; $Ddr2^{fl/fl}$ mice also showed stunted skull growth (**Figure II.11A).** To investigate the contribution of *Ddr2* in Gli1-expressing cells to the development of craniofacial skeleton, we performed anteroposterior linear skull measurements on MicroView oriented images, as was done with $Ddr2^{slie/slie}$ mice. Our results showed the skull length was relatively shorter in Gli1-CreER; $Ddr2^{fl/fl}$ mice (11% reduction, P <0.0001) versus control littermates (**Figure II.11B)**. The skull length is predominantly determined by endochondral ossification at the cranial base. Accordingly, conditional knockout mice showed shortening in cranial base bones, including presphenoid (13%, P <0.001), basisphenoid (14.6%, P<0.0001), and basioccipital bones (11%, P<0.001), suggesting impaired endochondral ossification. We also observed widening in cranial base synchondroses in Gli1-CreER; $Ddr2^{fl/fl}$ mice compared with control littermates (**Figure II.11C and 11D)**. This phenotype is quantitatively and qualitatively similar to that seen in $Ddr2^{slie/slie}$ mice. The abnormal skull shape in conditional knockout mice was due increased in skull width (**Figure II.11E)** and height (**Figure II.11F)** in relation to skull

length. In Gli1-CreER; *Ddr2*$^{fl/fl}$ mice, the skull abnormalities was associated with delayed suture formation manifested as a wide opening in the skull (**Figure II.11A)**. Together, these results are consistent with Gli1 distribution in cranial sutures and cranial base, and suggest that *Ddr2* functions in Gli1-expressing cells to control intramembranous and endochondral bone formation.

Discrimination between functions of Ddr2 in sutures and the cranial base

As described above, cranial base synchondroses are important growth centers contributing to craniofacial endochondral bone development. It has been proposed that deficient growth at the cranial base is responsible for craniofacial defects involving cranial sutures (Kreiborg et al. 1993). This suggests that cranial vault defects seen in *Ddr2*-deficient mice (both *Ddr2*$^{slie/slie}$ and Gli1-CreER; *Ddr2*$^{fl/fl}$ mice) could reflect cell-autonomous mechanisms of *Ddr2* in cranial vault (i.e. sutures) or could be a secondary consequence of deficient growth at the cranial base. To test this hypothesis, we sought to dissect the role of *Ddr2* in the cranial base from that in cranial suture. To this end, we conditionally deleted *Ddr2* in chondrocytes of the cranial base using a Col2-Cre. To develop Col2-Cre; *Ddr2*$^{fl/fl}$ conditional knockout mice, we sequentially bred mice for two generations: we first bred male Col2-Cre mice with female *Ddr2*$^{fl/fl}$ to generate Col2-Cre*; Ddr2fl/+* mice that were then with *Ddr2*$^{fl/fl}$ mice. This breeding strategy resulted in a conditional knockout mouse that is homozygous for the floxed *Ddr2* allele and heterozygous for Col2-Cre. The conditional knockout mice and their littermates were bred on a mixed background. PCR analysis of genomic DNA extracted from ear punches confirmed the Cre-mediated recombination of *Ddr2* (**Figure II.12A)**. Conditional knockout mice were born at the expected Mendelian frequency. At birth, Col2-Cre; *Ddr2*$^{fl/fl}$ mice were viable and indistinguishable from their control littermates, but as they

developed, Col2-Cre; *Ddr2*$^{fl/fl}$ mice exhibited growth defects compared with their littermate controls (*Ddr2*$^{fl/fl}$) (**Figure II.12B)**. Col2-Cre; *Ddr2*$^{fl/fl}$ mice displayed a significant reduction in the body length (**Figure II.12C)**, body weight (**Figure II.12D)**, and had a dysmorphic skull shape with short snout (**Figure II.12B)**. To quantify the craniofacial phenotype of Col2-Cre; *Ddr2*$^{fl/fl}$ mice and compare it with that of *Ddr2*$^{slie/slie}$ mice, we performed linear skull measurements on micro-CT scans of 3 month-old skulls (n=10) using the craniofacial landmarks described previously. In this study, the two experimental groups were matched for both gender and the genetic background of mice. Our analysis along the anteroposterior axis revealed a significant reduction in skull length (7%, *P* <0.0001) compared with the control littermates (*Ddr2fl/fl*) (**Figure II.13A and 13B)**; but this did not reach the magnitude seen in *Ddr2*$^{slie/slie}$ or Gli1-CreER; *Ddr2*$^{fl/fl}$ skulls (12 and 11% respectively -see **Figures II.1 and II.11**). The nasal bone was also significantly reduced (15.3%, *P* <0.0001) (**Figure II.13B).** The length of cranial vault that is mostly membranous bone was minimally affected (decreased by 2.5%, *P* <0.01) in Col2-Cre; *Ddr2*$^{fl/fl}$ mice (**Figure II.13B)**. Conditional knockout of *Ddr2* in chondrocytes also results in shortening in the posterior cranial base (11%, *P* <0.0001) mainly due to shortening in the length of basiosphenoid bone (15 %, *P* <0.0001) as oppose to reduction in the presphenoid bone or basioccipital bone (**Figure II.13B)**. The basisphenoid bone is unique in that it is mostly derived from neural crest cells but also has some mesodermal contribution to its caudal portion (McBratney-Owen et al. 2008). Cranial base growth defects could be explained by abnormalities in growth plate synchondroses, similar to *Ddr2*$^{slie/slie}$ and Gli1-CreER; *Ddr2*$^{fl/fl}$ mice. The intersphenoid synchondrosis (ISS) was significantly wider (270%, *P* <0.0001) and had increased height (32%, *P* <0.01) in Col2-Cre; *Ddr2*$^{fl/fl}$ mice than in *Ddr2*$^{fl/fl}$ control mice (**Figure II.13C and 13D)**. The width (17%, *P* <0.01) and height (23%, *P* <0.0001) of spheno-occipital

synchondrosis (SOS) in Col2-Cre; *Ddr2*$^{fl/fl}$ mice was also increased but to lesser extent than that of ISS.

Analyzing Col2-Cre; *Ddr2*$^{fl/fl}$ skulls on the frontal plane, we found increased anterior width (12%, *P* <0.0001), but a mild change in the posterior cranial width (2%, *P* <0.0001), consistent with our previous observations on the effects of *Ddr2* deficiency on the anterior part of skull. We did not detect any difference in facial or cranial heights; however, Col2-Cre; *Ddr2*$^{fl/fl}$ mice exhibited increased skull width (**Figure II.13E)** and height (**Figure II.13F)** in relation to skull length. This phenotype is similar to that seen in *Ddr2*$^{slie/slie}$ skulls and Gli1-CreER; *Ddr2*$^{fl/fl}$ mice. In contrast, conditional knockout of *Ddr2* in Col2-expressing chondrocytes did not affect cranial sutures. This clearly resolves functions of *Ddr2* in cranial base from functions in cranial sutures. Interestingly, when calvarial bone thickness was examined in selected orthogonal planes (**Figure II.14A)**, Col2-Cre; *Ddr2*$^{fl/fl}$ mice exhibited significant thinning in the frontal bone (56%, *P* <0.0001) as compared with controls (**Figure II.14B and 14C)**. Surprisingly, the parietal bone (11.4%, *P* <0.05) (**Figure II.14D and 14E)** and occipital bone (11.8% *P* <0.05*)* (**Figure II.14F and 14G)** also showed moderate decrease in thickness, suggesting some activity of Col2-Cre in parietal bone and occipital bones. This defect could not be detected in *Ddr2*$^{slie/slie}$ (**Figure II.2)** or Gli1-CreER*; Ddr2*$^{fl/fl}$ mice (data not shown). Taken together, these studies show that conditional deletion of *Ddr2* in chondrocytes results in craniofacial abnormalities characterized by shortened skull length, short snout, unexpected thinning in calvarial bones, and growth defects at the cranial base due to abnormal growth plate synchondroses, but no suture defects. From this, we can conclude that *Ddr2* has separate cell-autonomous functions in cranial base synchondroses and suture mesenchyme.

Loss of Ddr2 in chondrocytes causes deficient proliferation, ectopic hypertrophy and disrupted cell polarity

Anterior-posterior skull growth requires chondrocyte proliferation and hypertrophy in cranial base synchondroses. Disruption of these processes leads to a reduction in skull length. As our previous analysis revealed, the changes in cranial base synchondroses that were responsible for the short skull length were also accompanied by an increase in the height of mutant synchondroses. One explanation for this would be if cartilage growth were occurring in a dorsal-ventral direction. To address this issue, we sought to assess the onset and evolution of abnormal base chondrogenesis using time-course histological analysis. Our results showed no significant changes in growth plate synchondroses between Col2-Cre; *Ddr2*$^{fl/fl}$ conditional knockout newborns and control littermates. As endochondral ossification of cranial base progressed over a two-week period; the resting zone in control mice (highlighted with red line) became progressively narrower with time (**Figure II.15A)**. In contrast, this region progressively expanded at the expense of the proliferative and hypertrophic zone of synchondroses in Col2-Cre; *Ddr2*$^{fl/fl}$ mice (**Figure II.15A and 15B)**. The widening in cranial base synchondrosis could be due to defective chondrocyte function that possibly resulted in cell retention in resting zone and a delay in transitioning to proliferative chondrocytes. To assess cell proliferation, we injected mice with EdU intraperitoneally 4 h before analysis, and quantified EdU-labeled cells as a percentage of EdU+ cells (green) to the total cells in synchondrosis. EdU labeling was mostly displayed in the proliferative zone of synchondroses (**Figure II.16A)**. However, Col2-Cre; *Ddr2*$^{fl/fl}$ mice showed a 53% reduction off EdU+ cells in ISS (P<0.0001) and a 29% reduction in SOS, suggesting decreased chondrocyte proliferation (**Figure II.16B)**. In spite of this reduced proliferation rate, mutant synchondroses were enlarged and exhibited an increase in total cell number, suggesting chondrocytes proliferated less or at a lower rate, but they were retained in Col2-Cre;

Ddr2$^{fl/fl}$ synchondroses without progressing to proliferative and hypertrophic zones, possibly due to extracellular matrix abnormalities such those seen in *Ddr2*$^{slie/slie}$ mice.

These data are consistent with our LacZ localization studies that showed *Ddr2* being highly expressed in the resting zone, thus suggesting a critical function in regulation of extracellular matrix organization and turnover. To address this hypothesis, we performed type II collagen immunostaining to evaluate its distribution and organization within the cartilage matrix. Consistent to what was seen in *Ddr2*$^{slie/slie}$ mice **(Figure II.5A)**, type II collagen immunostaining showed uneven distribution around chondrocytes with diminished staining in the interterritorial matrix (**Figure II.16D)**. In addition, the spacing between chondrocytes in resting zone was increased in Col2-Cre; *Ddr2*$^{fl/fl}$ mice, possibly reflecting extracellular matrix abnormalities. Spacing between chondrocytes was measured by drawing lines between resting chondrocytes using ImageJ software (**Figure II.16C)**.

Intriguingly, Col2-Cre; *Ddr2*$^{fl/fl}$ mice also showed ectopic chondrocyte hypertrophy in the ventral side of cranial base synchondroses, particularity in the ISS (**Figure II.15A)**. It appeared as if the resting chondrocytes shifted their organization to establish a new gradient of proliferative and hypertrophic chondrocytes on the ventral side of cranial base synchondrosis. This suggests growth in the dorsal-ventral direction and may explain the increased height in Col2-Cre; *Ddr2*$^{fl/fl}$ synchondroses. MicroCT images of 3 month-old mice also showed W-shaped synchondroses (dotted line) in Col2-Cre; *Ddr2*$^{fl/fl}$ mice **(Figure II.13C)**, suggesting that ectopic endochondral ossification had taken a place on the ventral side of ISS (Note: these changes were not seen in SOS). The shift in chondrocyte organization suggests a possible role of *Ddr2* in regulating cell polarity and organization. To test this hypothesis, we evaluated chondrocyte organization in the ISS using GM130 immunofluorescence, a marker for Golgi

apparatus. Immunostaining of GM130 showed well defined, localized cytoplasmic staining on one side or the other of chondrocytes, indicating that these cells are normally polarized within synchondroses (**Figure II.16E)**. In Col2-Cre; *Ddr2*$^{fl/fl}$ mice; however, GM130 immunostaining became diffuse and not well defined, suggesting the polarization of chondrocytes was disrupted (**Figure II.16E)**. These results were also seen in Gli1-CreER; *Ddr2*$^{fl/fl}$ synchondroses (not shown). This indicates proper DDR2 signaling is required to maintain chondrocyte polarization. Together, our results suggest that *Ddr2* in resting chondrocytes plays an important role for specification of polarity through the interaction with the cartilage extracellular matrix; however, a direct role of *Ddr2* in chondrocyte polarization cannot be excluded.

Discussion

In this study, we demonstrated an important function of DDR2 in regulating development of the craniofacial skeleton. Detailed analysis of craniofacial phenotypes of *Ddr2* knockout mice revealed defects in anterior-posterior skull growth that were partially explained by a delay in endochondral ossification at the cranial base. This was attributed to a *Ddr2* deficiency in resting chondrocytes resulting in deficient chondrocyte proliferation, disrupted chondrocyte polarity/ organization and abnormal cartilage matrix deposition. These findings suggest a novel function for *Ddr2* in regulating cranial base development. This important structure provides a platform to protect the brain and sense organs in the skull, supports the pituitary gland, provides a foundation to support growth of the facial skeleton, articulates with the vertebral column and forms the roof of the nasopharynx (Lieberman et al. 2000). The importance of the cranial base is highlighted functionally from the role it plays in craniofacial growth through integrating different patterns of growth in various adjoining regions of the skull (Lieberman et al. 2000).

Therefore, proper growth of cranial base is important for the development of other skeletal elements and associated structures. Consistent with our findings, SMED, SL-AC patients who carry inactivating mutations in *DDR2* exhibit severe craniofacial abnormalities, including a prominent forehead, wide open fontanelle, hypertelorism, sparse eyebrows, a short nose with a depressed nasal bridge, a long philtrum, micrognathia, and dental abnormalities (Al-Kindi et al. 2014; Mansouri et al. 2016; Rozovsky et al. 2011; Smithson et al. 2009; Urel-Demir et al. 2018). The delayed endochondral ossification could be responsible for shortening in the cranial base and midface hypoplasia in SMED, SL-AC patients and for growth defects in other craniofacial structures.

Interestingly, defects in skull growth were profoundly manifested in the anterior craniofacial skeletal elements. *Ddr2*-deficient mice showed dramatic changes in ISS, nasal and frontal bones as oppose to SOS and other cranial bones, which are mostly posterior. Anterior craniofacial structures, including ISS, nasal and frontal bones, are typically derived from neural crest cells, while posterior structures, including SOS, parietal, and occipital bones, have a separate embryonic origin in paraxial mesoderm (Couly et al. 1993; Le Douarin et al. 1993; Le Lievre 1978; McBratney-Owen et al. 2008; Noden 1988; Thorogood 1988). This may suggest that a critical function for *Ddr2* in neural crest-derived tissues. Perhaps related to this function, our study showed that prenatal *Ddr2*-LacZ expression initially identified in the developing midface at E11.5 was coincident with the appearance of neural crest-derived mesenchymal tissues. This expression was localized to cartilage primordia of nasal septum, cranial base and Mackle's cartilages in the developing mandible. *Ddr2*-LacZ staining was strongest in developing tooth buds and mesenchymal condensations around Meckel's cartilages. However, neural crest-specific knockouts are required to address whether *Ddr2*

selectively functions in this cell population.

During bone formation, cells destined to form skeletal elements interact with their collagen-rich ECM to regulate proliferation, differentiation, remodeling and migration. Fibrillar type II collagen, the predominant collagen species of cartilage matrix and one of the ligands for DDR2, is important for normal chondrocyte proliferation, structural integrity and cellular organization (Brown et al., 1981; Pace et al., 1997; Seegmiller et al., 1971; Spranger et al., 1994; Vikkula et al., 1994). In this study, we evaluated type II collagen expression using immunofluorescence and showed homogenous and uniform staining throughout the cartilage matrix. However, the mutant cranial base synchondroses showed a discontinuous staining pattern, predominantly in pericellular space adjacent to chondrocytes. Interestingly, similar results were observed in *Dmm/Dmm* mice harboring a mutation in the C-propeptide globular domain of type II collagen (*Col2a1*), which is responsible for collagen assembly (Pace et al. 1997). The mutation in the C-propeptide domain results in defects in the assembly and folding of type II collagen, alteration of collagen distribution and collagen-proteoglycan interactions in the cartilage extracellular matrix (Brown et al. 1981; Pace et al. 1997). *Dmm/Dmm* mice exhibited dwarfism, shortened vertebral column, small rib cage and craniofacial defects characterized by skull dysmorphogenesis, reduced skull length, reduced cranial base length, cleft palate, and short mandible (Brown et al. 1981; Pace et al. 1997). These phenotypes are similar to that seen in *Ddr2*-deficient mice. It is possible that *Ddr2* plays critical roles in cartilage matrix organization by controlling the assembly, folding and secretion of type II collagen and/or by regulating collagen-proteoglycan interactions. Determining how DDR2 regulates various aspects of collagen fibrillogenesis is beyond the goal of this study. However, our findings are in agreement with previous studies showing abnormal collagen deposition and/or crosslinking in *Ddr2*-deficient heart and

postnatal testicular tissues (Cowling et al. 2014; Zhu et al. 2015). In addition, our characterization of *Ddr2* function in tooth development showed atypical collagen fibers in periodontal ligaments surrounding tooth roots in *Ddr2*$^{slie/slie}$ mice **(Figure III.2 and III.3)**.

The defect in type II collagen distribution, particularly in the resting zone, is perhaps the most remarkable finding in our study because it implies that perturbing the interaction of resting chondrocytes with type II collagen matrix may impact the ability of cells to maintain their spatial organization and polarity, thereby disrupting cellular activities that underlie proliferation and differentiation of hypertrophic chondrocytes in cranial base synchondroses. Along these lines, we found that *Ddr2*-deficient synchondroses had disrupted chondrocyte polarization and altered organization of the Golgi apparatus, as demonstrated by abnormal distribution of GM130, a peripheral membrane protein associated with the cytoplasmic face of the Golgi apparatus. GM130 is required for maintaining Golgi structure, spindle assembly, cell cycle progression, and cytoskeletal dynamics (Colanzi and Corda 2007; Farquhar and Palade 1998; Liu et al. 2017; Sanders and Kaverina 2015; Wei et al. 2015). Disruption of GM130 in mitosis impairs spindle assembly and cell division (Wei et al. 2015). This suggests that a polarized GM130 structure is required for normal cell proliferation. Altered GM130 and reduced chondrocyte proliferation seen in our study is in agreement with previous studies. However, it is not clear whether *Ddr2* has a direct role in GM130 polarization. Interestingly, defects in the resting zone in costochondral cartilage of the rib cage is a prevailing histopathological feature of SMED, SL-AC patients, as firstly described by Borochowitz et al. (Borochowitz et al. 1993). Using toluidine blue staining, histological analysis showed abnormally distributed chondrocytes with noticeable dark staining in the surrounding matrix filling lacunar space (Borochowitz et al. 1993). While a defect in type II collagen was not specified in this study, the altered distribution of cartilage matrix

highlights the similarity between histopathological features of the patient sample and our results in *Ddr2*-deficient mice, and provide important insights into potential mechanisms underlying *Ddr2* regulation of cartilage extracellular matrix organization. Together, our data suggests that lineage-restricted expression of *Ddr2* in resting and proliferative zones of the synchondrosis is required for cells to receive regulatory signals from the type II collagen matrix necessary to control chondrocyte polarization, proliferation and maturation.

Indian Hedgehog (Ihh) signaling plays a critical role in cranial base development and function by regulating chondrocyte proliferation and maturation [reviewed in (Wei et al. 2016)]. Deletion of Ihh in mice caused delayed endochondral ossification due to chondrocyte disorganization, decreased chondrocyte proliferation and altered distribution of hypertrophic chondrocytes which occupied the central region as oppose to flanking sides of synchondroses (Young et al. 2006). These abnormalities were noticeable in the intersphenoid synchondrosis (ISS); however, spheno-occipital synchondrosis (SOS) was mostly unaffected. This was explained by a compensatory role of Sonic hedgehog (Shh) expressed from a residual notochord near the SOS (Young et al. 2006). The difference in phenotypic severity between ISS and SOS was also observed in *Ddr2*-deficient mice, raising the possibility of involvement of Ihh signaling in *Ddr2* regulation of cranial base growth and development. Activation of Ihh pathway requires Gli1, a transcriptional mediator of Ihh signaling. In support of this hypothesis, disruption of Ihh signaling was observed in calvarial osteoblast culture, and we found that *Ddr2*-deficient osteoblasts exhibited significant downregulation of Gli1. However, further studies are needed to understand *Ddr2* in context of Ihh signaling important for calvaria and cranial base development

Involvement of Ihh in craniofacial bone formation is proposed through its

regulation of Gli1+ stem cells in cranial sutures and bone formation at osteogenic fronts (Zhao et al. 2015). Sutural stem cells (SuSCs) have attracted significant attention due to their contribution to craniofacial bone formation and regeneration. Ablation of SuSCs could lead to craniosynostosis, a premature closure of cranial sutures resulting in arrest of skull growth (Durham et al., 2019; Zhao et al., 2015), while impaired cell proliferation and osteogenic differentiation of SuSCs could lead wide-open fontanels due to reduced or delayed bone growth (Goto et al., 2004; Qin et al., 2019). In view of co-expression of *Ddr2* and Gli1 in cranial sutures, we conditionally inactivated *Ddr2* in Gli1+ sutural cells at neonatal stage. Loss of *Ddr2* in Gli1+ cells faithfully recapitulated phenotypes of $Ddr2^{slie/slie}$ mice, including a wide opening in the frontal suture analogous to metopic suture in human, and mimicking wide-open fontanels seen in SMED, SL-AC patients. This suggests that *Ddr2* functions in Gli1+ sutural cells to regulate bone formation in the skull. Using calvarial osteoblast culture, *Ddr2*-deficient osteoblasts showed reduced osteoblast differentiation and downregulation of osteoblast-specific marker gene expression, thereby explaining impaired the calvaria bone formation associated with delayed suture formation in *Ddr2*-deficient mice (Ge et al. 2016). Intriguingly, our lineage tracing studies also identified Gli1 labeling beyond those previously reported in cranial sutures and in long bone metaphysis. As we show, Gli1 also marks chondrocyte lineages and co-localized with *Ddr2* in cranial base synchondroses during postnatal life. The similarity between *Ddr2* and Gli1 expression implies that these two genes are involved in the same biological processes.

Conditional knockout of *Ddr2* in chondrocytes using Col2-Cre resulted in abnormal chondrogenesis at the cranial base; however, this did not affect cranial sutures, suggesting that the contribution of *Ddr2* to endochondral bone formation is independent from its function in cranial sutures. An unexpected result in our study was

the thinning of intramembranous cranial bones resulting from *Ddr2* conditional knockout using a Col2-Cre, which was shown to be specific for early chondrogenesis (Ovchinnikov et al. 2000). Our results suggest that Col2-expressing cells contribute to non-chondrogenic skeletal lineages in calvarial bones. This is in agreement with a previous study targeting MT1-MMP, matrix metalloproteinase 14, in chondrocytes (Szabova et al. 2009). Examining endogenous *Col2* expression using in situ hybridization and COL2 immunohistochemistry showed staining in osteogenic lineages in the parietal bone of wild type mice (Szabova et al. 2009). Using a Col2a1-Cre transgene and an R26R-tdTomato reporter allele, lineage-tracing approach in prior work typically marked progenitors of the skeletal lineage contributing to canonical endochondral bone formation in the cranial base (Sakagami et al. 2017). However, Col2a1-Cre activity was also detected in osteoblasts and suture mesenchymal cells in the calvaria (Sakagami et al. 2017). This suggest that Col2 is expressed in skeletal cells of intramembranous bones, which could be responsible for reduced bone thickness in Col2-Cre; Ddr2fl/fl conditional knockout mice.

In summary, ECM signaling critically regulates skeletal development and growth, and has been implicated in a wide spectrum of human skeletal disorders, most of which involve craniofacial structures (Erlebacher et al. 1995; Kuivaniemi et al. 1997; Lu et al. 2011; Velleman 2000). Defects in cranial growth and development cause a wide range of disorders known to dramatically impact physical, social and emotional development of affected children. An understanding of the critical molecules and pathways necessary for the development of craniofacial skeleton is necessary to successfully treat these patients. Findings from this study established a critical function of *Ddr2* in skeletal progenitor cells and chondrocytes during postnatal development of craniofacial skeleton, and help advance our understanding of the roles of cell-matrix interactions in craniofacial

development by establishing the functions of a new collagen receptor.

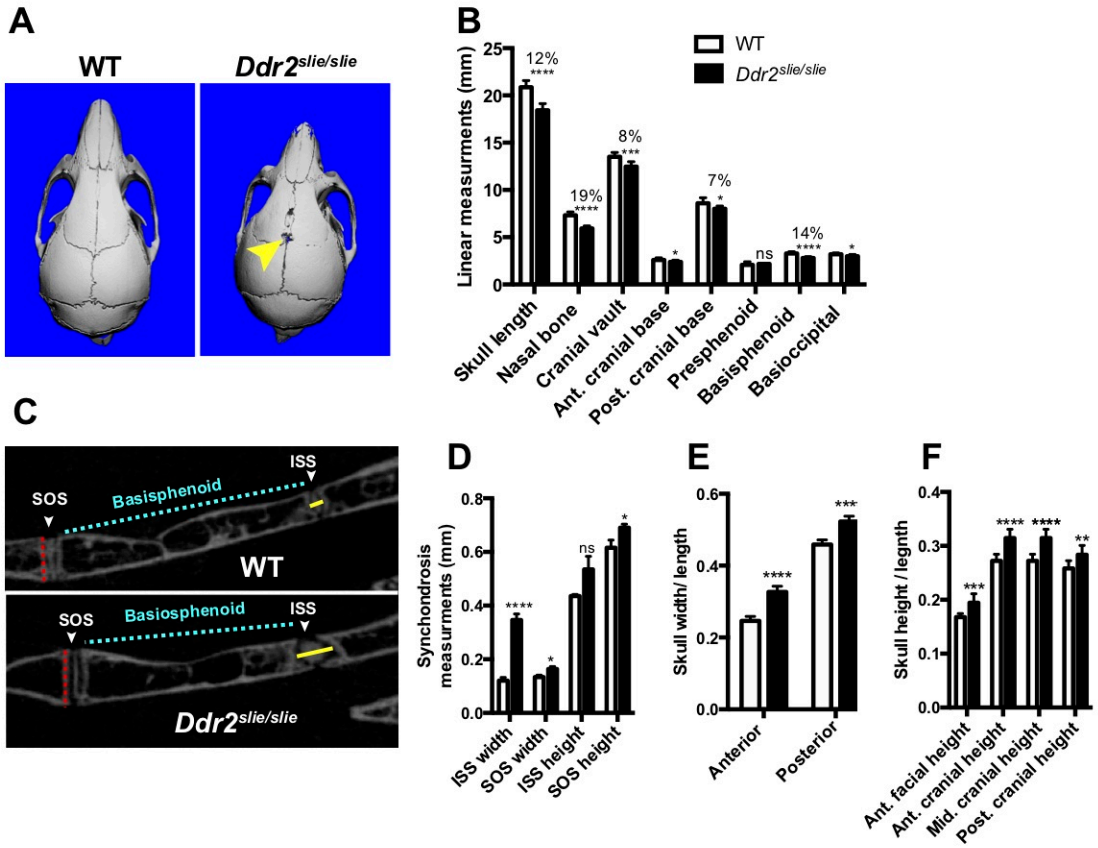

Figure II.1: Morphometric characterization of skulls from 3 month-old *Ddr2*$^{slie/slie}$ mice and WT littermates. (A) MicroCT scans of skulls show short skull length in *Ddr2*$^{slie/slie}$ mice. (B) Linear measurements along anteroposterior axis of skulls. (C) 2D microCT images of cranial bases show enlarged synchondroses: Intersphenoid (ISS) and spheno-occipital (SOS) synchondroses in *Ddr2*$^{slie/slie}$ mice (lower). (D) Quantification of width and height of cranial base synchondroses. (E) Quantification of anterior and posterior skull width in relation to skull length. (F) Quantification of anterior facial height and cranial heights in relation to skull length. n= 10 mice, **P*<0.05, ***P*<0.01, ****P*<0.001, *****P*<0.0001, ns, not significant.

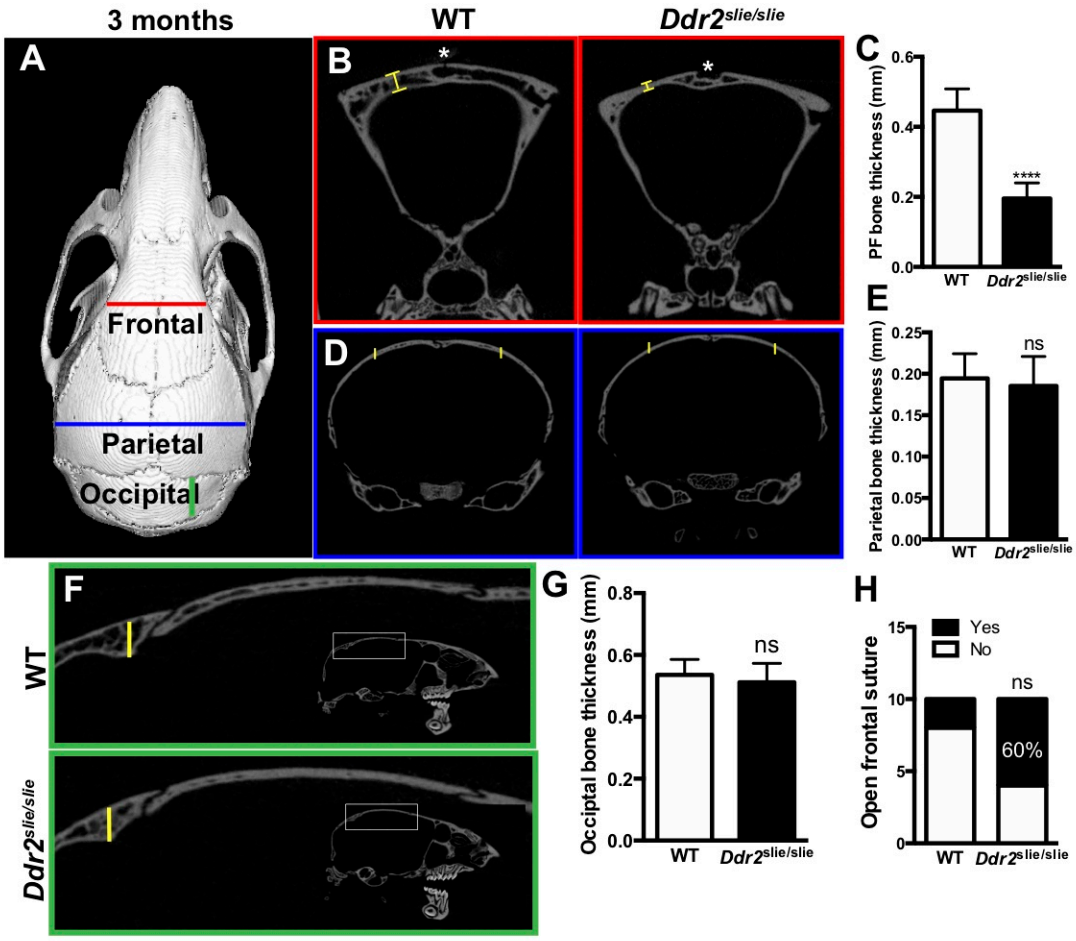

Figure II.2: Measurements of skull bone thickness. (A) Top view of a skull CT image constructed with MicroView software showing selected orthogonal planes used for measuring skull bone thickness. (B) The anterior coronal plane (red) shows a significant reduction in frontal bone thickness (yellow) in *Ddr2*$^{slie/slie}$ mice. (C) Quantification of frontal bone thickness made on both side of the frontal suture shows a significant reduction in *Ddr2*$^{slie/slie}$ mice. (D) The posterior coronal plane (blue) shows no aberrant changes in parietal bone thickness. (E) Quantification of parietal bone thickness made on both side of the sagittal suture (yellow lines). (F) The sagittal orthogonal plane (green) showing selected region used for measuring occipital bone thickness (yellow line). (G) Quantification of occipital bone thickness showing no changes in parietal bones in *Ddr2*$^{slie/slie}$ mice. (H) Frequency of open frontal suture defects in *Ddr2*$^{slie/slie}$ compared with WT. n= 10 mice, ****P<0.0001, ns, not significant.

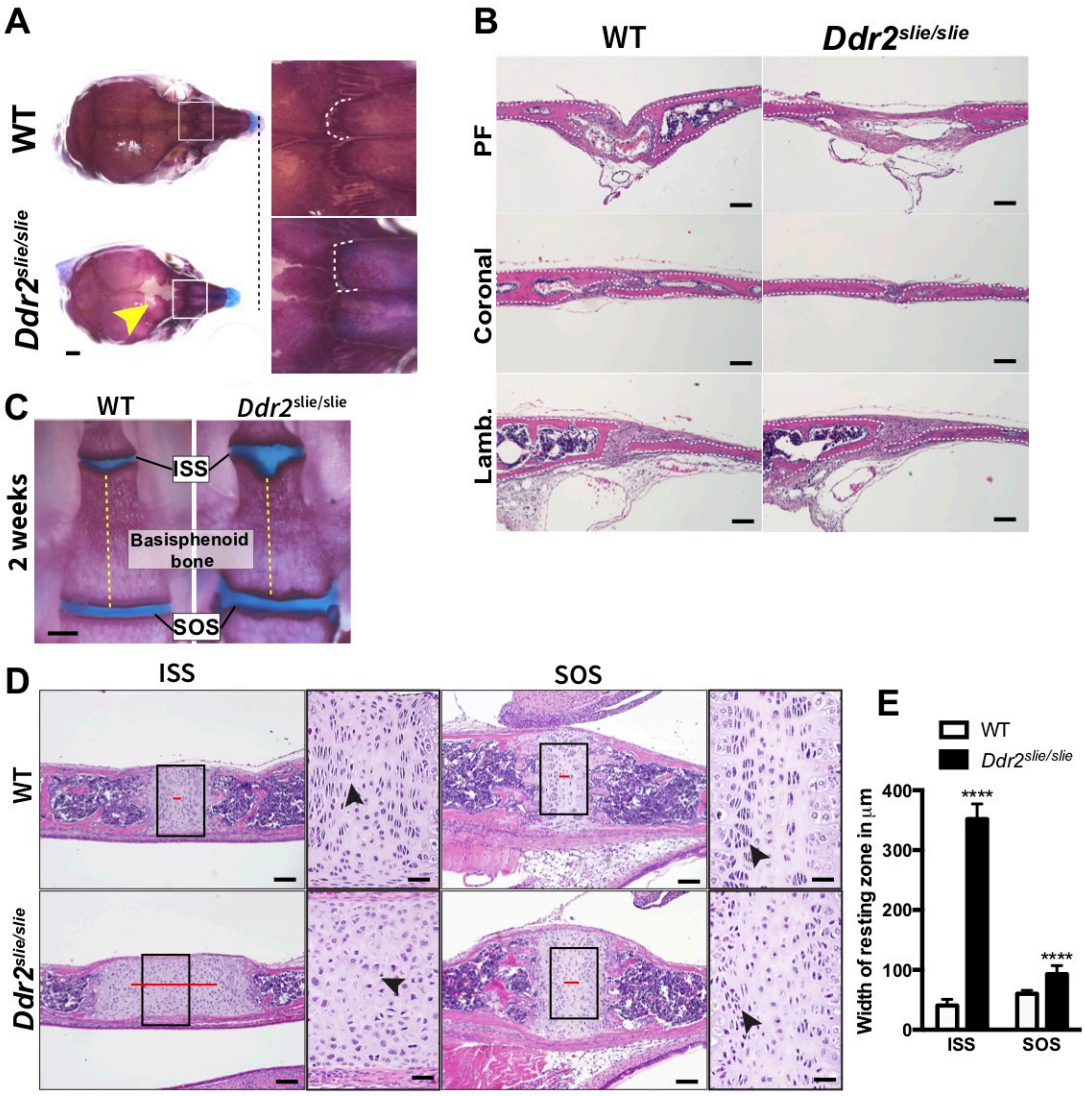

Figure II.3: Abnormalities in cranial sutures and cranial base synchondrosis in *Ddr2*$^{slie/slie}$ mice. (A) Alcian blue and alizarin red staining of 2 week-old mouse skulls shows delayed suture formation and abnormal suture morphology (dotted lines) in *Ddr2*$^{slie/slie}$. (B) Histological examination with hematoxylin and eosin (H& E) staining shows wide open prefrontal sutures (PF) in *Ddr2*$^{slie/slie}$ mice but transverse sutures, such as coronal and lambdoid (lamb.), were not affected. (C) Alcian blue and alizarin red of the cranial base shows abnormally enlarged cranial base synchondroses (blue) in *Ddr2*$^{slie/slie}$ mice (D) Representative images of cranial base synchondrosis stained with H&E showing abnormal chondrocyte organization and loss of columnar organization of proliferative chondrocytes. (E) Linear measurements of resting zone (red line) made on ISS and SOS. ISS: Intersphenoid synchondrosis, SOS: Spheno-occipital synchondrosis. Scale bar: 500 μm in (C), 100 μm in (A), (B), and (D, low magnification), and 50 μm in (D, high magnification). n=3, ****P<0.0001.

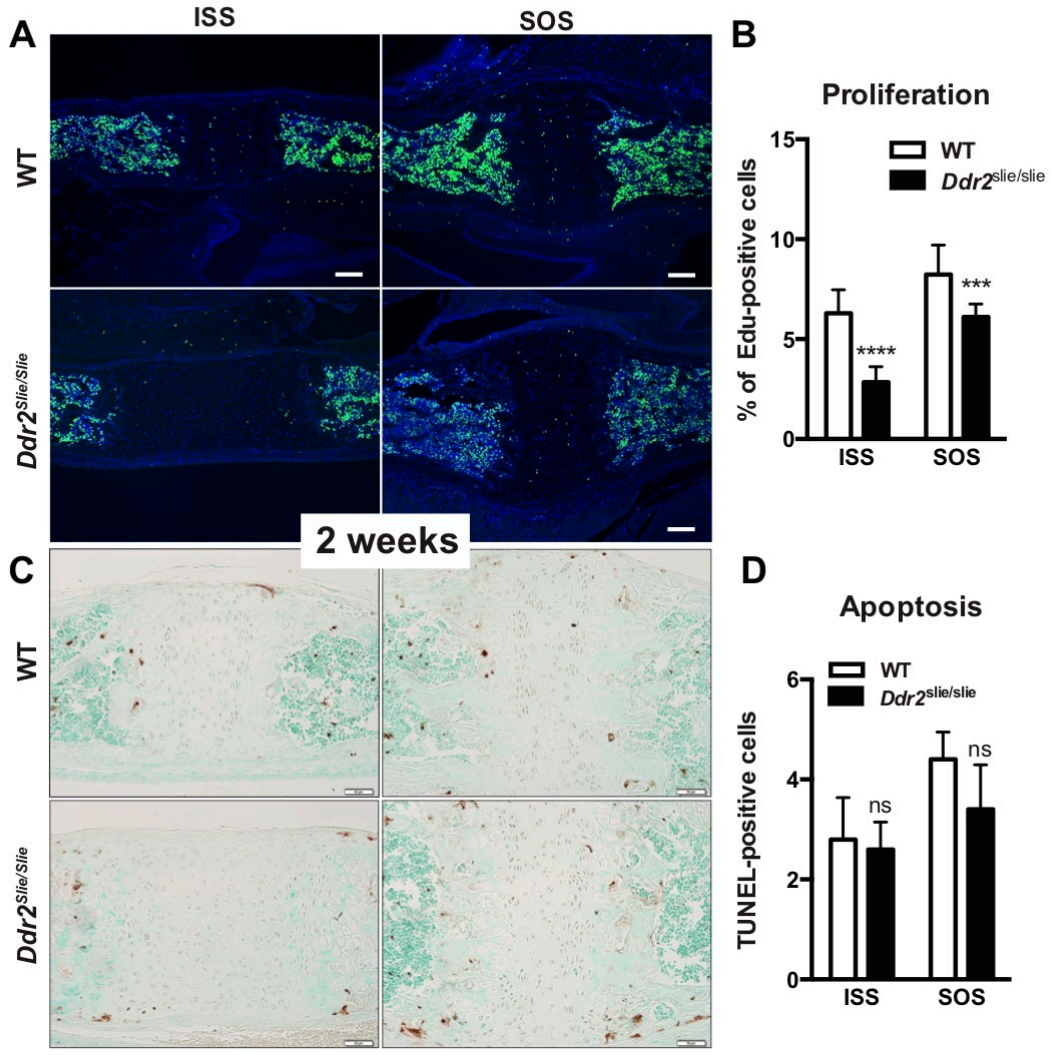

Figure II.4: Deficient chondrocyte proliferation in *Ddr2*$^{slie/slie}$ synchondroses. (A) EdU staining of cranial base synchondroses (green) shows reduction in EdU+ cells in *Ddr2*$^{slie/slie}$ mice compared with WT littermates. Cell nuclei were stained with DAPI (blue). (B) Quantification of chondrocytes stained with EdU in synchondrosis growth plate. (C) TUNEL staining (brown) shows no changes in apoptotic levels between *Ddr2*$^{slie/slie}$ mice and WT. Cell nuclei were stained with methyl green (green). (D) Quantification of TUNEL-positive cells in synchondrosis growth plate. n=3 mice/group. ***P<0.001, ****P<0.0001, ns, not significant. Scale bar: 100 μm in (A) and 50 μm in (C).

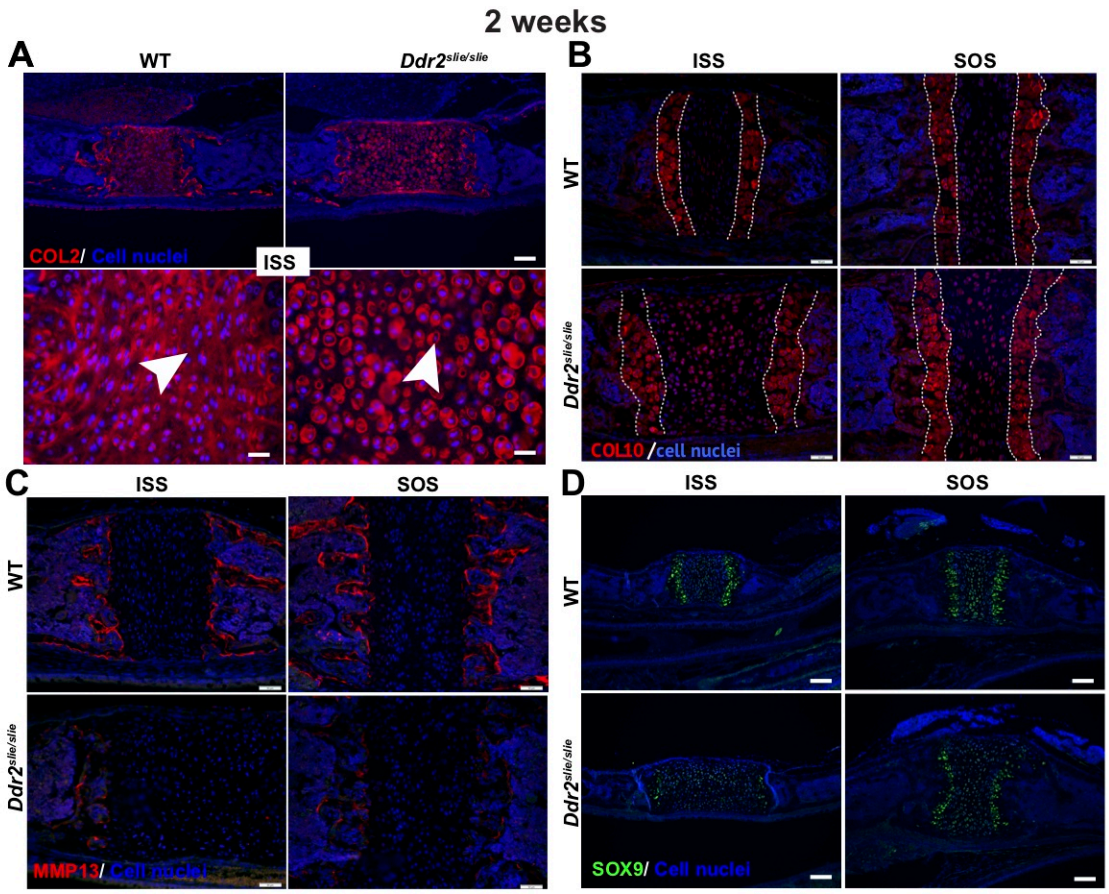

Figure II.5: Delayed endochondral ossification in synchondroses from *Ddr2*$^{slie/slie}$ mice. (A) COL2 immunostaining shows uneven distribution with rings-like staining around chondrocytes in *Ddr2*-deficient synchondrosis (high magnification in lower panel). (B) COL10 immunostaining shows no changes in expression pattern, but the hypertrophic zone of synchondrosis growth plate (dotted line) was slightly enlarged in *Ddr2*-deficient mice. (C) Shows decreased MMP13 immunostaining in *Ddr2*$^{slie/slie}$ sychondroses compared with WT controls. (D) Shows reduction of SOX9 immunostaining in *Ddr2*$^{slie/slie}$ sychondroses. Cell nuclei were stained with DAPI (blue). Scale bar: 200 μm in (D), 100 μm in (A, upper panel), 50 μm in (B) and (C) and 20 μm in (A, lower panel).

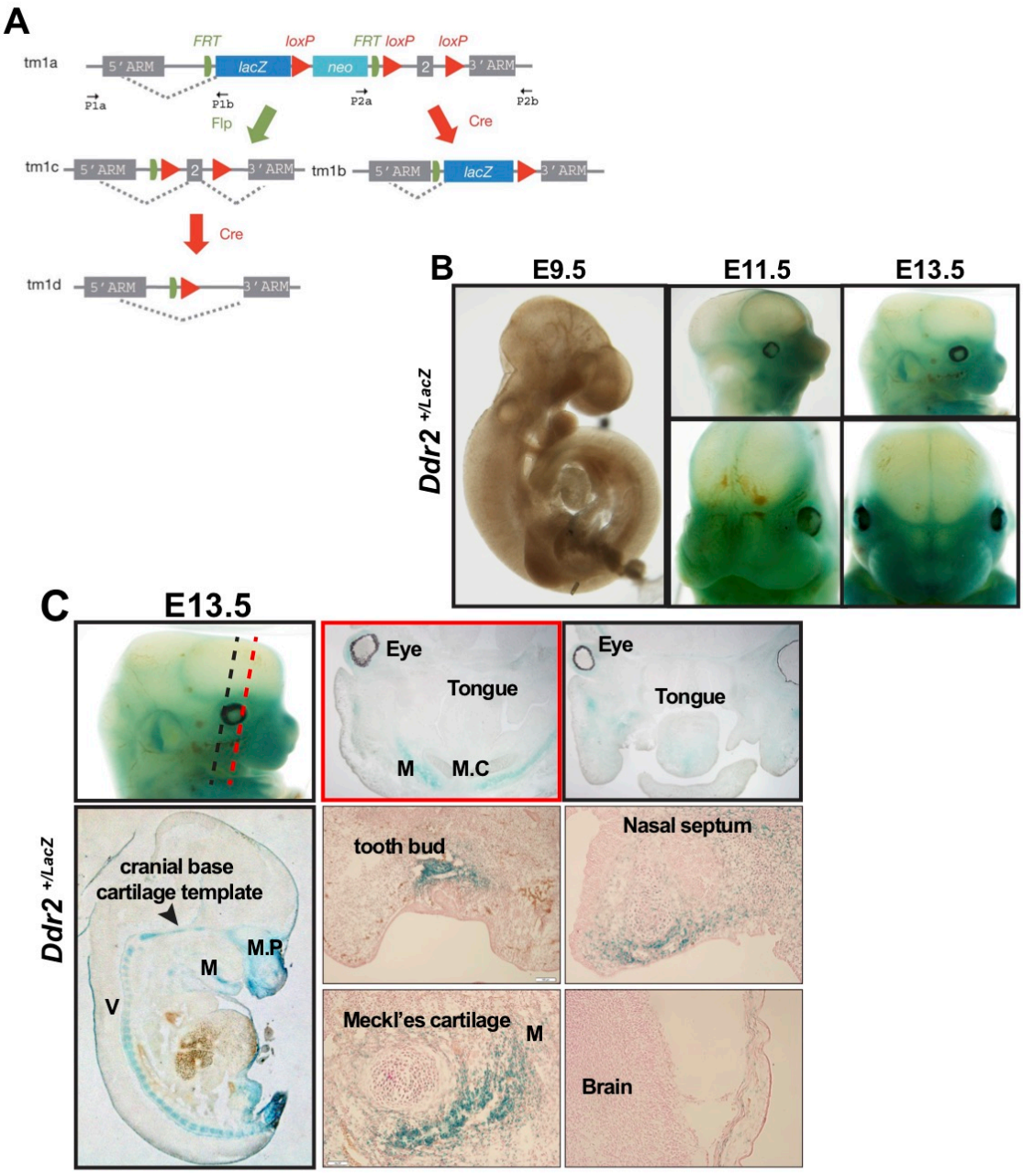

Figure II.6: Expression patterns of *Ddr2* during craniofacial development. (A) A schematic representation of the strategies used for generation of a Ddr2-LacZ knock-in and Ddr2 flox mice. (B) LacZ staining (green) shows a broad Ddr2 expression in nasal, maxillary and mandibular processes in Ddr2+/LacZ embryos at E11.5 and E13.5. (C) Tissue sections of E13.5 embryos show high Ddr2 expression in cartilage primordia of vertebrae (V), cranial base and Meckle's cartilage (M) in developing mandible, tongue and tooth buds, but no staining in brain.

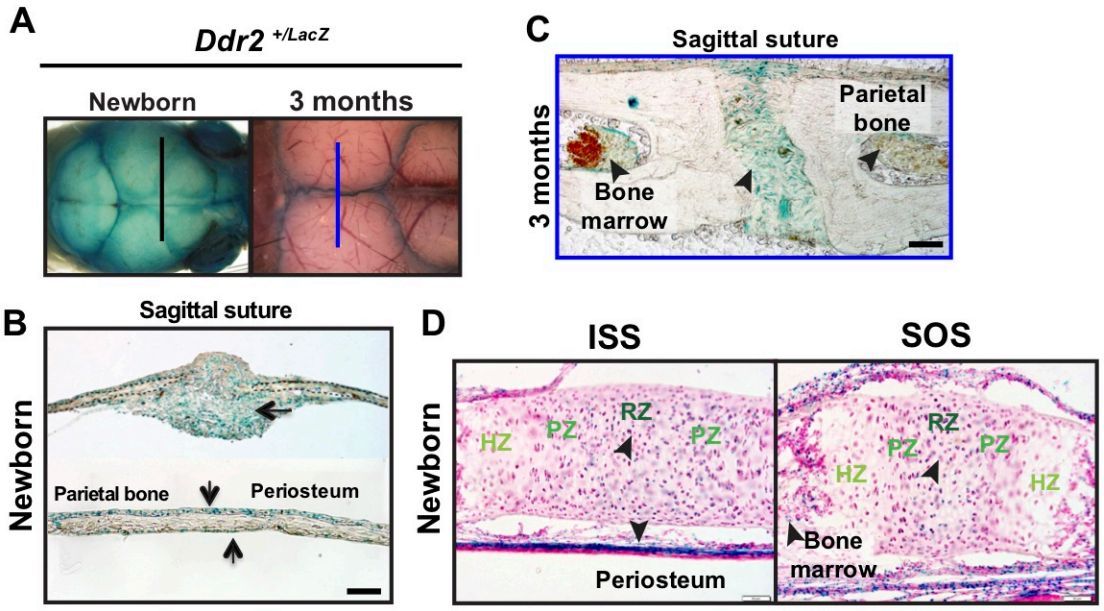

Figure II.7: *Ddr2* is expressed in cranial sutures, periosteum, dura, and cranial base synchondrosis. (A) Whole mount staining of skulls from $Ddr2^{+/LacZ}$ mice. (B) Frozen sections show Ddr2-LacZ staining (green) in suture mesenchyme, periosteum and dura (inner side) of flanking bone of $Ddr2^{+/LacZ}$ calvaria from newborn mice. (C) Frozen sections of 3 month-old calvaria show LacZ staining (green) mostly in suture mesenchyme, periosteum, dura and lining cells of bone. (D) Frozen sections of newborn cranial base showing LacZ staining in resting zone (RZ) and proliferative zone (PZ), but not in hypertrophich zone (HZ) of sychondrosis growth plate, and in periosteum and bone marrow. Scale bar: 50 μm in (B), (C) and (D).

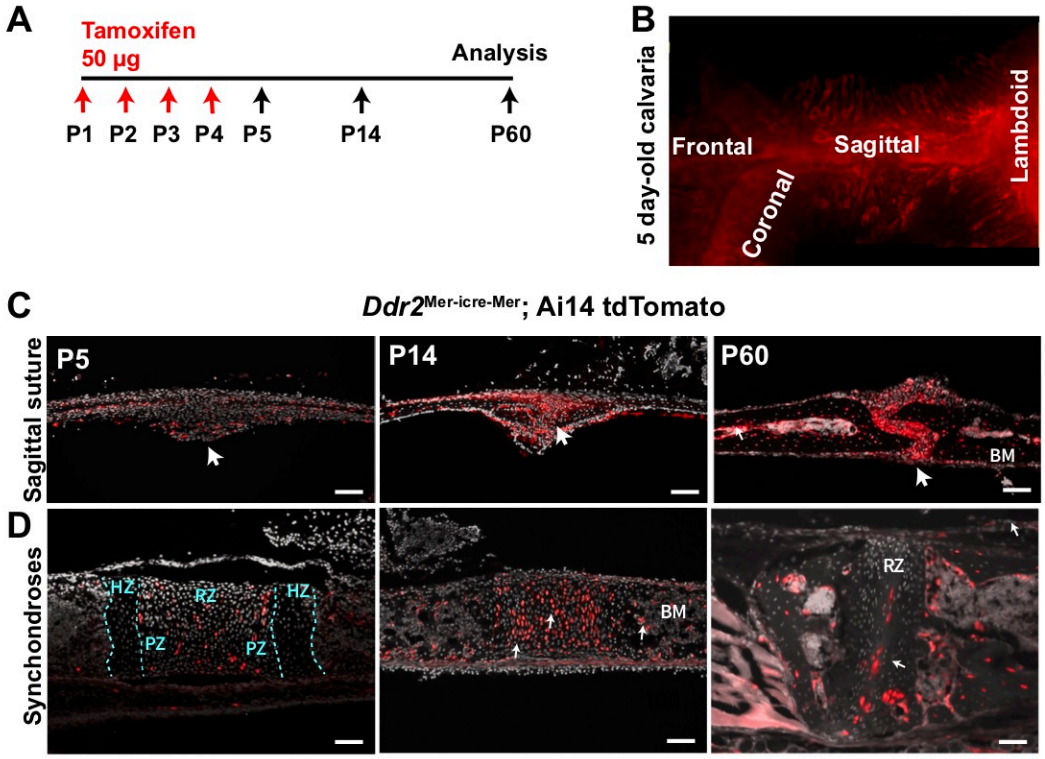

Figure II.8: *Ddr2*$^{mer\text{-}iCre\text{-}mer}$ marks progenitors of the skeletal lineage during postnatal craniofacial development. (A) Experimental approach used for induction of Cre-recombination and expression of tdTomato fluorescent protein (red) upon tamoxifen injection. (B) Whole calvaria from 5 day-old mice shows intense tdTomato labeling in cranial sutures. (C) Lineage tracing of suture cells. At P5 tdTomato+ cells are in suture mesenchyme, periosteum and dura of calvarial bones. The tdTomato labeling became intense in cranial sutures over 2 weeks and 2 months (P60), with positive cells expanding into osteocytes in calvarial bones and calvarial bone marrow. (D) Lineage tracing in the synchondrosis. At P5 tdTomato+ cells are in resting zone (RZ) and proliferative zone (PZ) of sychondrosis growth plate, but not in hypertrophic zone (HZ). Lineage trace at P14 shows an increase in tdTomato+ cells in sychondrosis and in associated bone marrow. After 2 months, tdTomato labeling is retained in resting zone and shows a single clone of tdTomato labeling in proliferative and hypetrophic chondocytes, but also it appears in the lining of bone marrow and in osteocytes of cortical bone. Scale bar: 100 µm in (C, P14 and P60), 50 µm in (C, P5).

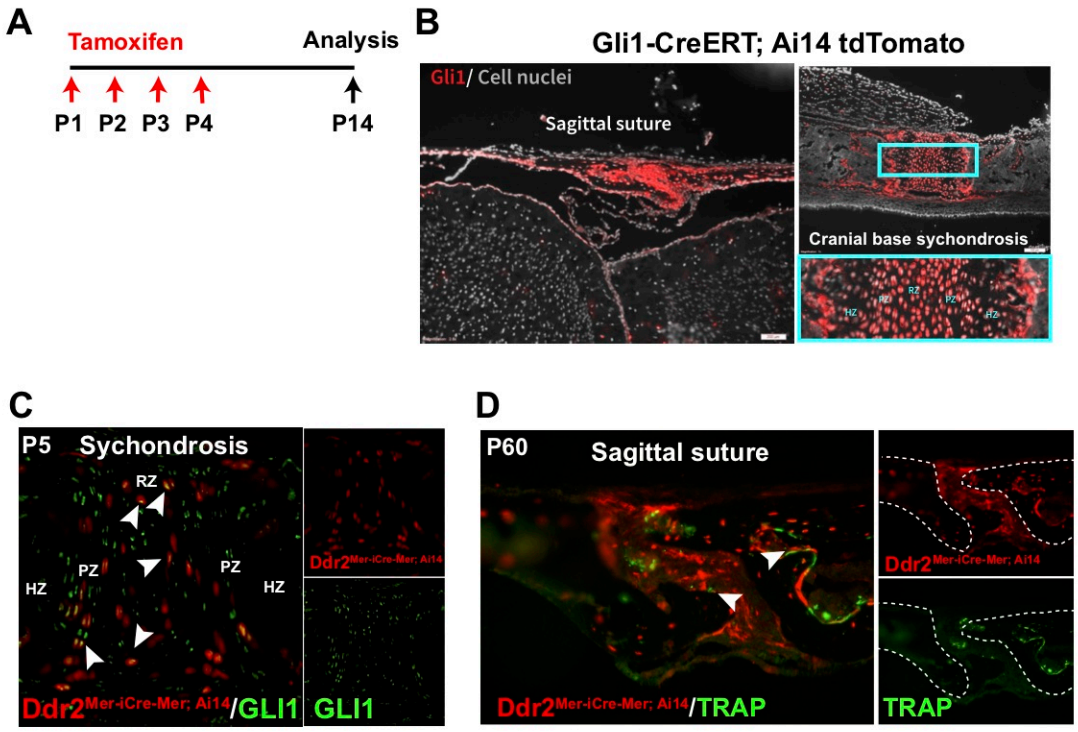

Figure II.9: *Ddr2*+ cells overlap with Gli1+ cell population, but not with osteoclasts. (A) Experimental approach used for induction Cre-recombination in Gli1-expressing cells (red) upon tamoxifen injections. (B) A P14 lineage trace shows tdTomato+ cells predominatelly in undedifferentiated cells in cranial sutures (left), and chondrocyte lineages in cranial base sychondroses (right). (C) Co-expression of *Ddr2*+ tdTomato cells with anti-Gli1 immunofluorescence in 5-day cranial base synchondrosis. (D) shows separate distribution of TRAP+ cells (green) from *Ddr2*+ tdTomato cells indicating that *Ddr2*$^{mer\text{-}iCre\text{-}mer}$ does not mark osteoclasts.

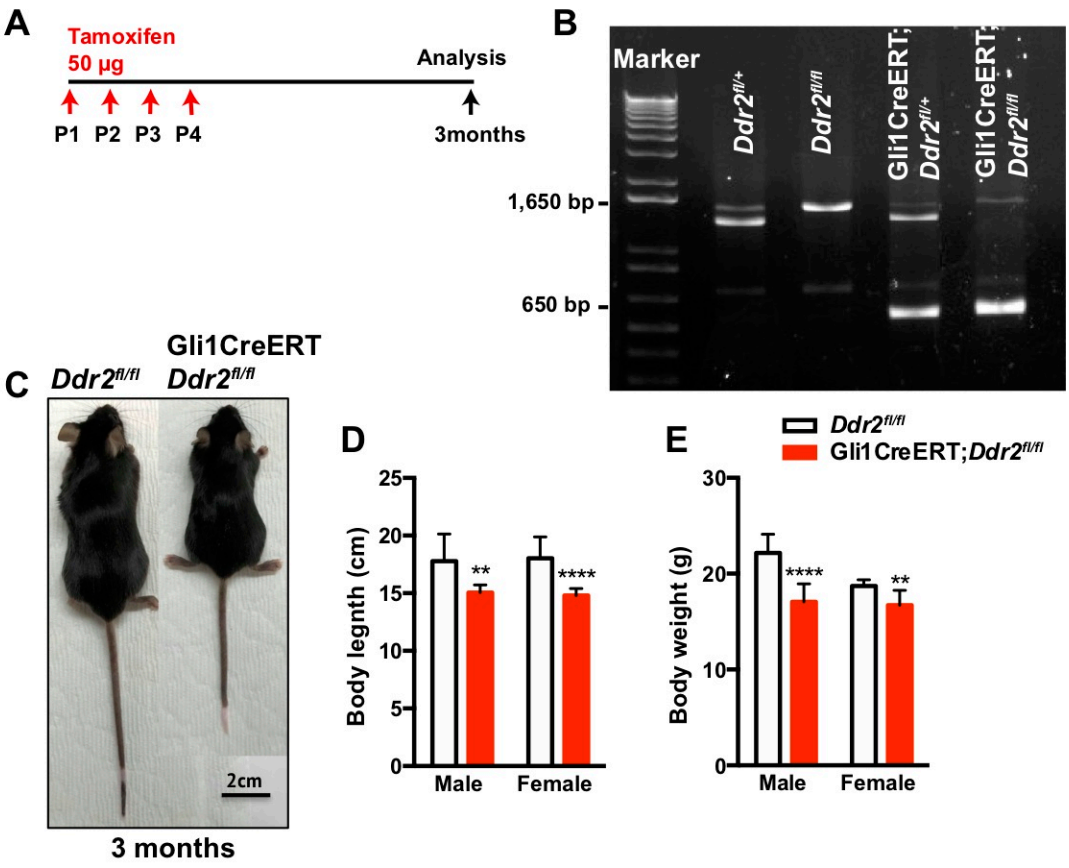

Figure II.10: Conditional knockout of *Ddr2* in Gli1-expressing cells results in dwarfism. (A) Experimental approach used for induction Cre-recombination to target a *Ddr2* allele in Gli1-expressing cells. (B) PCR analysis of genomic DNA extracted from ear punches to evaluate the efficiency of Cre recombination. (C) Gross appearance shows dwarfism in Gli1-CreER; $Ddr2^{fl/fl}$ conditional knockout mice. (D) Bar graph shows a significant reduction in body length in Gli1-CreER; $Ddr2^{fl/fl}$ mice both in males and females. (E) Bar graph shows a significant reduction in body weight in Gli1-CreER; $Ddr2^{fl/fl}$ mice compared with control littermates.

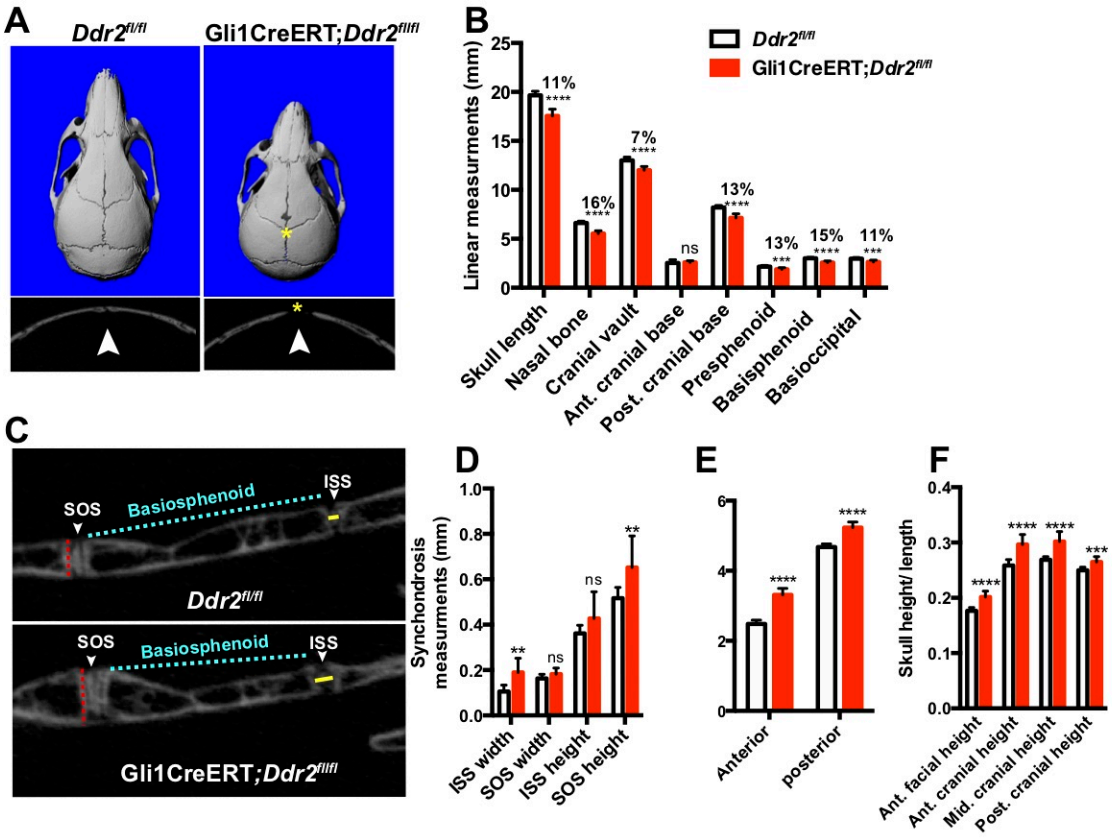

Figure II.11: Loss of *Ddr2* in Gli1-expressing cells resulted in a craniofacial phenotype similar to Ddr2$^{slie/slie}$ mice. (A) MicroCT scans of skulls showing shortening skull length in Gli1-CreER; *Ddr2*$^{fl/fl}$ mice associated with wide-open frontal sutures. (B) Linear measurements along anteroposterior axis of skulls. (C) 2D microCT images of cranial base showing enlarged synchondroses: intersphenoid (ISS) and spheno-occipital (SOS) synchondroses in Gli1-CreER; *Ddr2*$^{fl/fl}$ mice (lower). (D) Quantification of width and height of cranial base synchondroses. (E) Quantification of anterior and posterior skull width in relation to skull length. (F) Quantification of anterior facial height and cranial heights in relation to skull length. n= 10 mice, ***P*<0.01, ****P*<0.001, *****P*<0.0001, ns, not significant.

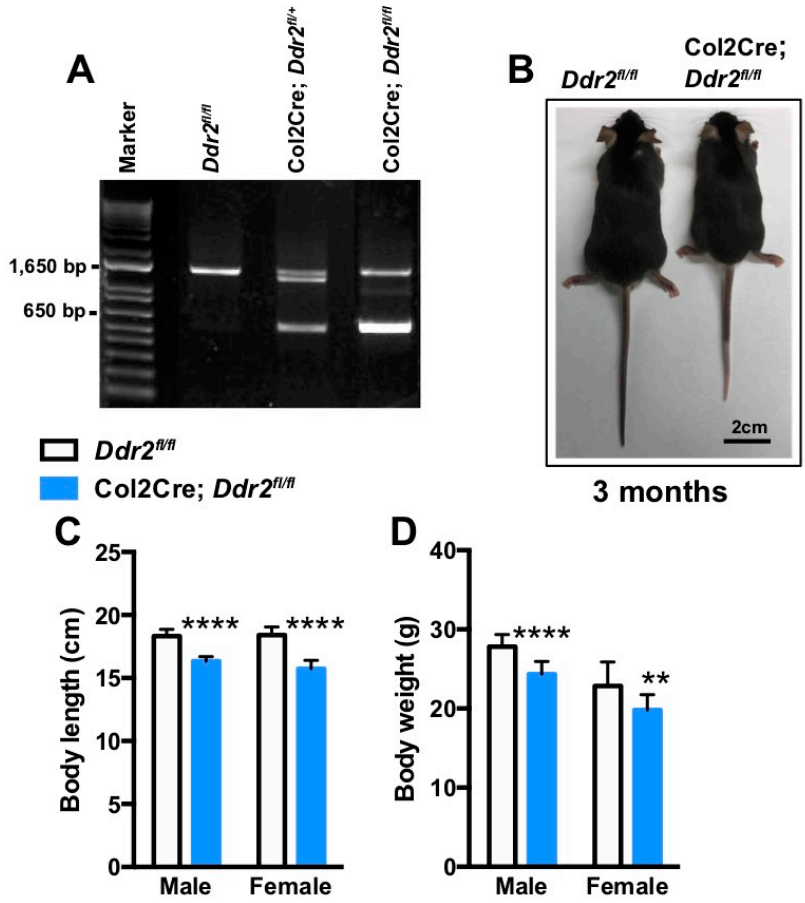

Figure II.12: Loss of *Ddr2* in Col2-expressing cells also resulted in dwarfism. (A) PCR analysis of genomic DNA extracted from ear punches to evaluate the efficiency of Cre recombination. (B) Gross appearance shows dwarfism in Col2Cre; *Ddr2*$^{fl/fl}$ conditional knockout mice. (C) Bar graph shows a significant reduction in body length in Col2Cre; *Ddr2*$^{fl/fl}$ mice both in males and females. (D) Bar graph shows a significant reduction in body weight in Col2Cre; *Ddr2*$^{fl/fl}$ mice compared with control littermates. ***P*<0.01, *****P*<0.0001.

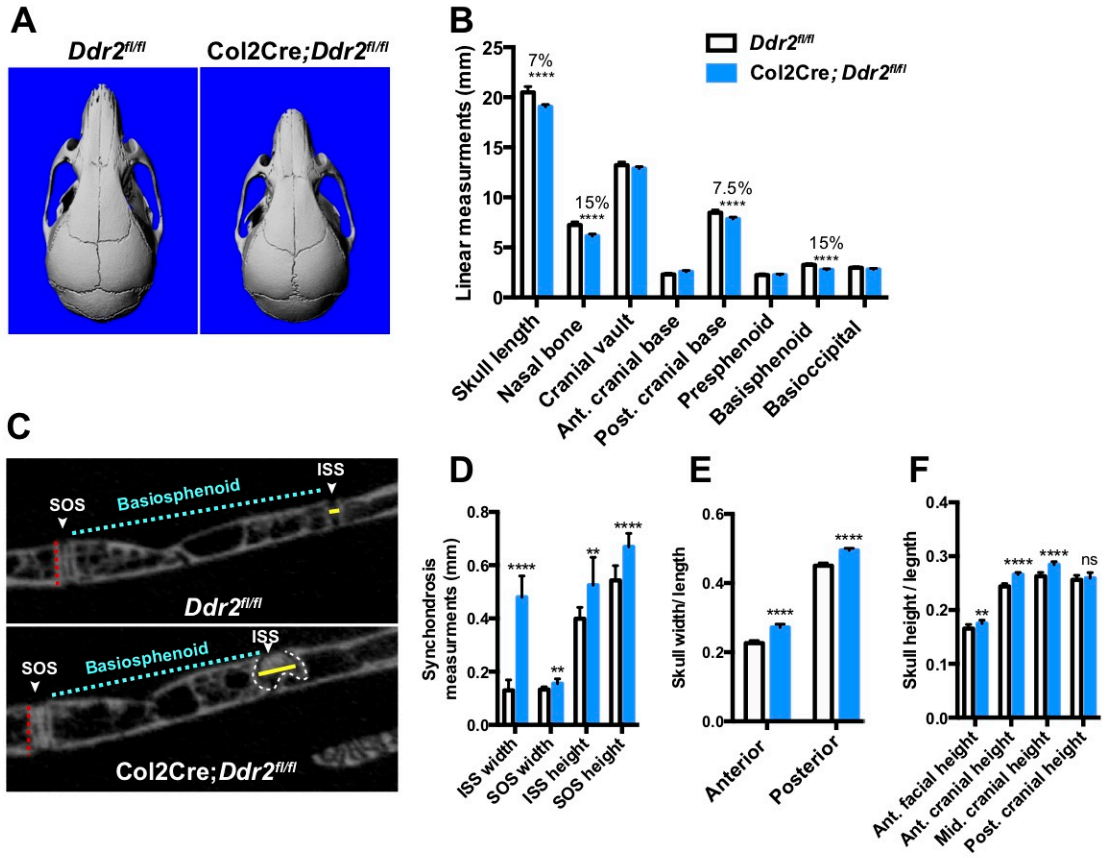

Figure II.13: *Ddr2* conditional knockout in Col2-expressing chondrocytes reduces skull length and alters synchondroses, but does not affect cranial sutures. (A) MicroCT scans of skulls showing shortened skull length in Col2Cre; *Ddr2*$^{fl/fl}$ mice but no effect on cranial sutures. (B) Linear measurements along anteroposterior axis of skulls. (C) 2D microCT images of cranial bases showing enlarged synchondroses: ISS and SOS in Col2Cre; *Ddr2*$^{fl/fl}$ mice (lower). (D) Quantification of width and height of cranial base synchondroses. (E) Quantification of anterior and posterior skull width in relation to skull length. (F) Quantification of anterior facial height and cranial heights in relation to skull length. n= 10 mice, ***P*<0.01, *****P*<0.0001, ns, not significant.

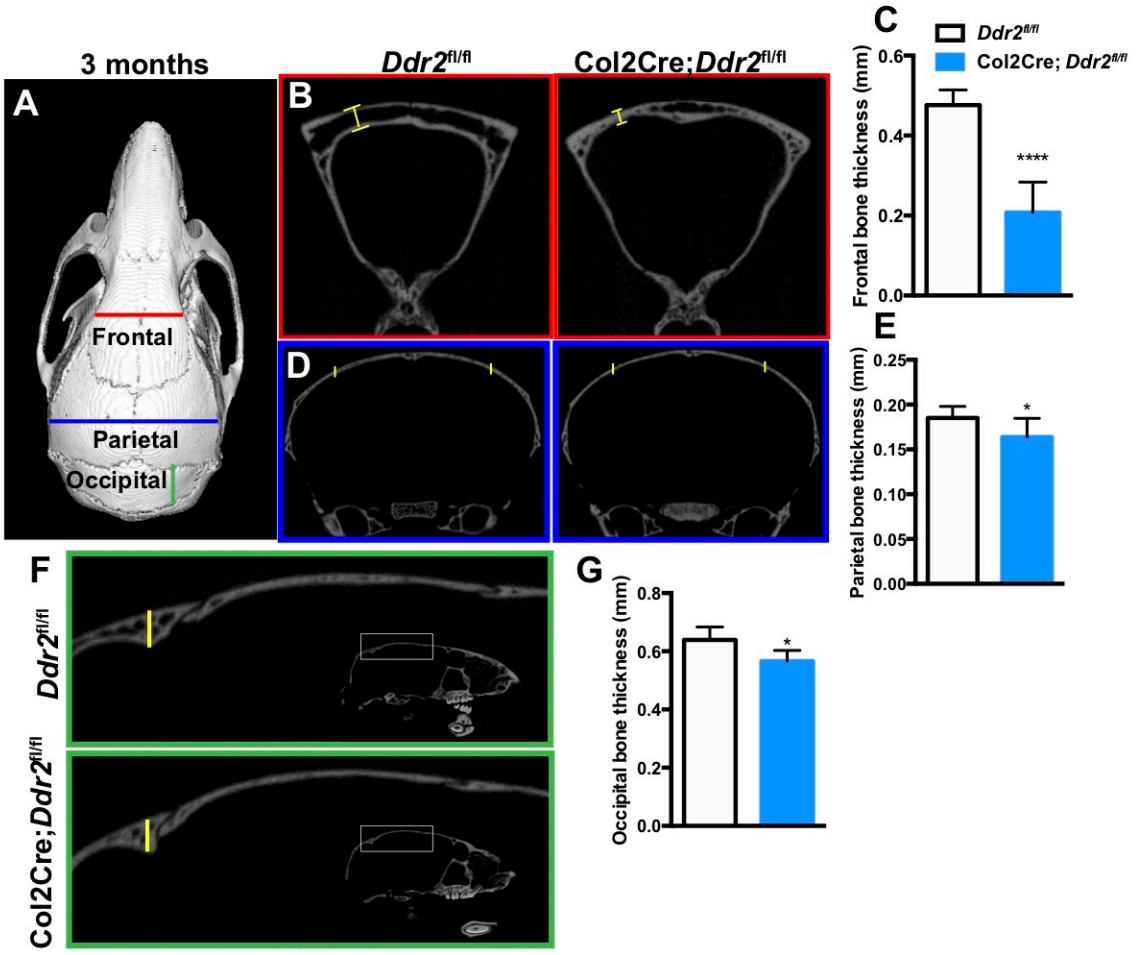

Figure II.14: Thinning of calvaria bones in Col2-Cre; *Ddr2*$^{fl/fl}$ mice. (A) Top view of a CT skull image constructed in MicroView software showing selected orthogonal planes used for measuring skull bone thickness. (B) The anterior coronal plane (red) shows a significant reduction in frontal bone thickness (yellow line) in Col2Cre; *Ddr2*$^{fl/fl}$ mice. (C) Quantification of frontal bone thickness made on both side of the frontal suture showing a significant reduction in Col2Cre; *Ddr2*$^{fl/fl}$ mice compared with control littermates. (D) The posterior coronal plane (blue) shows reduction in parietal bone thickness. (E) Quantification of parietal bone thickness shows an 11% reduction in occipital bone thickness. (F) The sagittal orthogonal plane (green) showing selected region used for measuring occipital bone thickness. (G) Quantification of occipital bone thickness shows an 11% reduction in occipital bone thickness in Col2Cre; *Ddr2*$^{fl/fl}$. n= 10 mice, **P*<0.05, *****P*<0.0001.

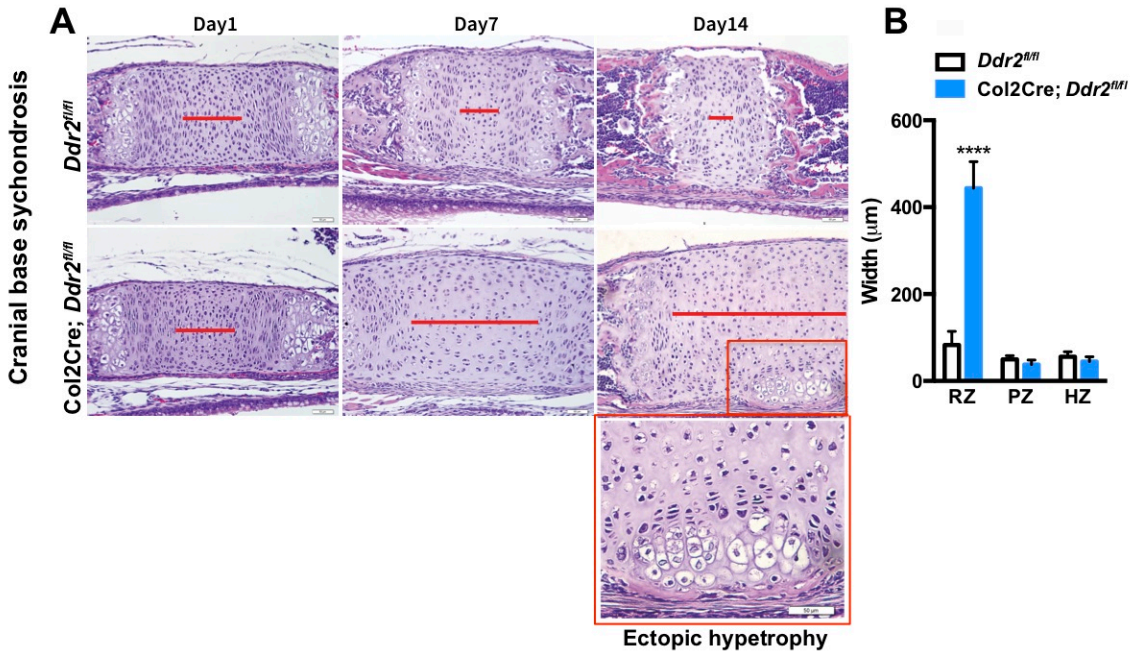

Figure II.15: Col2-Cre; *Ddr2*$^{fl/fl}$ mice exhibited time-dependent widening in resting zone, altered polarization and ectopic hypertrophy. (A) Time-course analysis shows no evident difference in histological structures of the ISS between Col2Cre; *Ddr2*$^{fl/fl}$ mice and their control littermates at P1, but during the first two weeks, the resting zone became abnormally wide (red lines) and exhibited ectopic hypertrophy on the ventral side of cranial base synchondrosis (red box). (B) Bar graph shows linear measurements of width of resting (RZ), proliferative (PZ) and hypertrophic (HZ) zones of synchondrosis growth plate. n= 5 mice, ****P<0.0001.

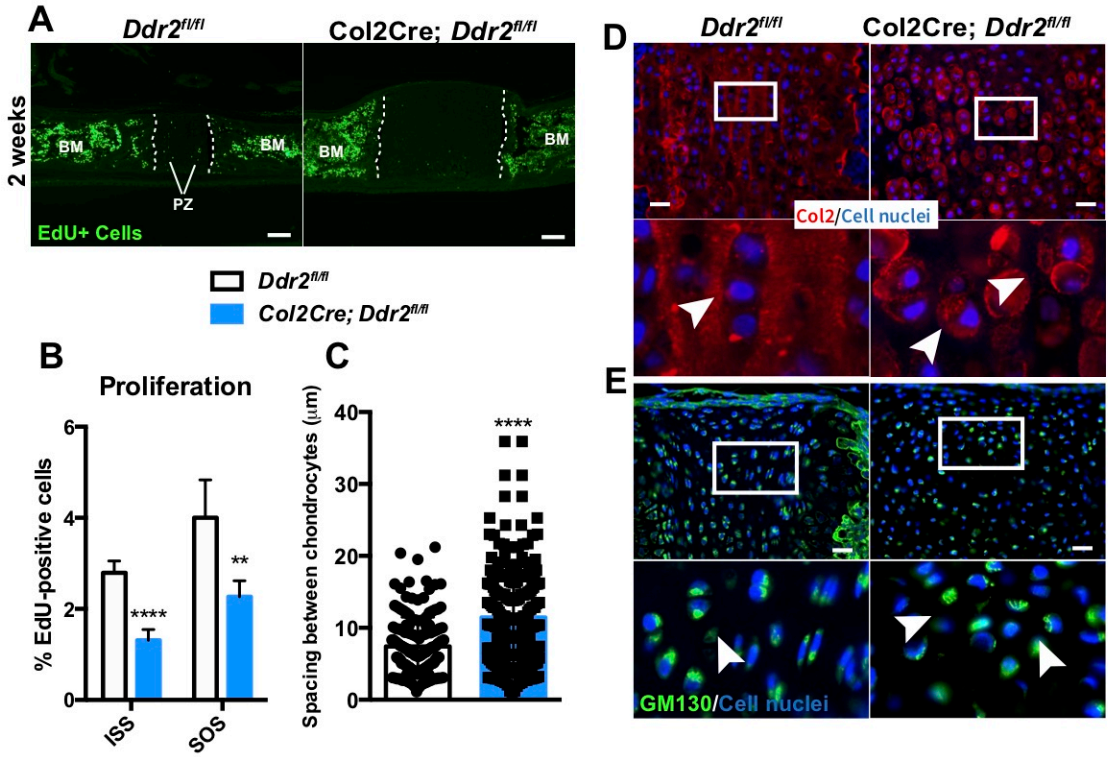

Figure II.16: Col2-Cre; *Ddr2*$^{fl/fl}$ synchondrosis exhibited deficient chondrocyte proliferation, abnormal type II collagen and disrupted polarization. (A) EdU staining (green) showed a significant reduction of chondrocyte proliferation in Col2Cre; *Ddr2*$^{fl/fl}$ synchondrosis. (B) Bar graph shows quantification of EdU-positive cells in cranial base synchondroses. (C) Bar graph shows increased spacing between chondrocytes in resting zone of mutant synchondroses. D) COL2 immunostaining shows altered type II collagen matrix in Col2Cre; *Ddr2*$^{fl/fl}$ mice. (E) GM130 immunostaining shows well-defined staining polarized to one side of cells in RZ of wild type synchondrosis, but in mutant synchondroses, GM130 immunostaining is diffuse and ill-defined indicating disturbed polarization. n= 3 mice, ***P*<0.01, *****P*<0.0001. Scale bar: 100 μm in (A), 20 μm in (D) and (E).

Table II.1: Primers used for genotyping

Ddr2 $^{slie/slie}$	
Primers	Oligonucleotide sequence **5`→ 3`**
oIMR1544	CACGTGGGCTCCAGCATT
oIMR3580	TCACCAGTCATTTCTGCCTTTG
oIMR9641	GAGAGATGGCTCAATCATTAAAGG
oIMR9642	AGCTGTGGGTTAGAAGATAAGATCC
TmoIMR0105	CCAATGGTCGGGCACTGCTCAA
TmoIMR0143	CAACCAAAATTAAGACAAAAACTCAAGGCA

Ddr2 flox	
Primers	Oligonucleotide sequence **5`→ 3`**
ARM1F	TCCCGCTGAAAGGTCATGAG
ARM1R	TTGTTTTCAAATACCACAGCAAGA
ARM2F	AAGATCCCGCTGAAAGGTCA
ARM2R	TTTCAAATACCACAGCAAGAAAGA
ARM3F	CTCCCATCTGAGCGGTTGTA
ARM3R	AAGGTGAGAGATGGGAGTCC

Ddr2-Lacz	
Primers	Oligonucleotide sequence **5`→ 3`**
KOF LacZ P1	GACGACTCCTGGAGCCCGTCAGTA
KOF LacZ P2	GGAAGAAGGCACATGGCTGAATATC

References

Abad V, Meyers JL, Weise M, Gafni RI, Barnes KM, Nilsson O, Bacher JD, Baron J. 2002. The role of the resting zone in growth plate chondrogenesis. Endocrinology. 143(5):1851-1857.

Afzal AR, Rajab A, Fenske CD, Oldridge M, Elanko N, Ternes-Pereira E, Tuysuz B, Murday VA, Patton MA, Wilkie AO et al. 2000. Recessive robinow syndrome, allelic to dominant brachydactyly type b, is caused by mutation of ror2. Nat Genet. 25(4):419-422.

Ahn S, Joyner AL. 2004. Dynamic changes in the response of cells to positive hedgehog signaling during mouse limb patterning. Cell. 118(4):505-516.

Al-Kindi A, Kizhakkedath P, Xu H, John A, Sayegh AA, Ganesh A, Al-Awadi M, Al-Anbouri L, Al-Gazali L, Leitinger B et al. 2014. A novel mutation in ddr2 causing spondylo-meta-epiphyseal dysplasia with short limbs and abnormal calcifications (smed-sl) results in defective intra-cellular trafficking. BMC Med Genet. 15:42.

Ali BR, Xu H, Akawi NA, John A, Karuvantevida NS, Langer R, Al-Gazali L, Leitinger B. 2010. Trafficking defects and loss of ligand binding are the underlying causes of all reported ddr2 missense mutations found in smed-sl patients. Hum Mol Genet. 19(11):2239-2250.

Borochowitz Z, Langer LO, Jr., Gruber HE, Lachman R, Katznelson MB, Rimoin DL. 1993. Spondylo-meta-epiphyseal dysplasia (smed), short limb-hand type: A congenital familial skeletal dysplasia with distinctive features and histopathology. Am J Med Genet. 45(3):320-326.

Brown KS, Cranley RE, Greene R, Kleinman HK, Pennypacker JP. 1981. Disproportionate micromelia (dmm): An incomplete dominant mouse dwarfism with abnormal cartilage matrix. J Embryol Exp Morphol. 62:165-182.

Carafoli F, Bihan D, Stathopoulos S, Konitsiotis AD, Kvansakul M, Farndale RW, Leitinger B, Hohenester E. 2009. Crystallographic insight into collagen recognition by discoidin domain receptor 2. Structure. 17(12):1573-1581.

Colanzi A, Corda D. 2007. Mitosis controls the golgi and the golgi controls mitosis. Curr Opin Cell Biol. 19(4):386-393.

Couly GF, Coltey PM, Le Douarin NM. 1993. The triple origin of skull in higher vertebrates: A study in quail-chick chimeras. Development. 117(2):409-429.

Cowling RT, Yeo SJ, Kim IJ, Park JI, Gu Y, Dalton ND, Peterson KL, Greenberg BH. 2014. Discoidin domain receptor 2 germline gene deletion leads to altered heart structure and function in the mouse. Am J Physiol Heart Circ Physiol. 307(5):H773-781.

Dy P, Wang W, Bhattaram P, Wang Q, Wang L, Ballock RT, Lefebvre V. 2012. Sox9 directs hypertrophic maturation and blocks osteoblast differentiation of growth plate chondrocytes. Dev Cell. 22(3):597-609.

Erlebacher A, Filvaroff EH, Gitelman SE, Derynck R. 1995. Toward a molecular understanding of skeletal development. Cell. 80(3):371-378.

Farquhar MG, Palade GE. 1998. The golgi apparatus: 100 years of progress and controversy. Trends Cell Biol. 8(1):2-10.

Ge C, Wang Z, Zhao G, Li B, Liao J, Sun H, Franceschi RT. 2016. Discoidin receptor 2 controls bone formation and marrow adipogenesis. J Bone Miner Res.

Jacome-Galarza CE, Percin GI, Muller JT, Mass E, Lazarov T, Eitler J, Rauner M, Yadav VK, Crozet L, Bohm M et al. 2019. Developmental origin, functional maintenance and genetic rescue of osteoclasts. Nature. 568(7753):541-545.

Kano K, Marin de Evsikova C, Young J, Wnek C, Maddatu TP, Nishina PM, Naggert JK. 2008. A novel dwarfism with gonadal dysfunction due to loss-of-function allele of the collagen receptor gene, ddr2, in the mouse. Mol Endocrinol. 22(8):1866-1880.

Kjaer I. 1990. Ossification of the human fetal basicranium. J Craniofac Genet Dev Biol. 10(1):29-38.

Kreiborg S, Marsh JL, Cohen MM, Jr., Liversage M, Pedersen H, Skovby F, Borgesen SE, Vannier MW. 1993. Comparative three-dimensional analysis of ct-scans of the calvaria and cranial base in apert and crouzon syndromes. J Craniomaxillofac Surg. 21(5):181-188.

Kuivaniemi H, Tromp G, Prockop DJ. 1997. Mutations in fibrillar collagens (types i, ii, iii, and xi), fibril-associated collagen (type ix), and network-forming collagen (type x) cause a spectrum of diseases of bone, cartilage, and blood vessels. Hum Mutat. 9(4):300-315.

Labrador JP, Azcoitia V, Tuckermann J, Lin C, Olaso E, Manes S, Bruckner K, Goergen JL, Lemke G, Yancopoulos G et al. 2001. The collagen receptor ddr2 regulates proliferation and its elimination leads to dwarfism. EMBO Rep. 2(5):446-452.

Lana-Elola E, Rice R, Grigoriadis AE, Rice DP. 2007. Cell fate specification during calvarial bone and suture development. Dev Biol. 311(2):335-346.

Le Douarin NM, Ziller C, Couly GF. 1993. Patterning of neural crest derivatives in the avian embryo: In vivo and in vitro studies. Dev Biol. 159(1):24-49.

Le Lievre CS. 1978. Participation of neural crest-derived cells in the genesis of the skull in birds. J Embryol Exp Morphol. 47:17-37.

Leitinger B, Hohenester E. 2007. Mammalian collagen receptors. Matrix Biol. 26(3):146-155.

Leitinger B, Kwan AP. 2006. The discoidin domain receptor ddr2 is a receptor for type x collagen. Matrix Biol. 25(6):355-364.

Lemmon MA, Schlessinger J. 2010. Cell signaling by receptor tyrosine kinases. Cell. 141(7):1117-1134.

Lieberman DE, Ross CF, Ravosa MJ. 2000. The primate cranial base: Ontogeny, function, and integration. Am J Phys Anthropol. Suppl 31:117-169.

Liu C, Mei M, Li Q, Roboti P, Pang Q, Ying Z, Gao F, Lowe M, Bao S. 2017. Loss of the golgin gm130 causes golgi disruption, purkinje neuron loss, and ataxia in mice. Proc Natl Acad Sci U S A. 114(2):346-351.

Lu P, Takai K, Weaver VM, Werb Z. 2011. Extracellular matrix degradation and remodeling in development and disease. Cold Spring Harb Perspect Biol. 3(12).

Madisen L, Zwingman TA, Sunkin SM, Oh SW, Zariwala HA, Gu H, Ng LL, Palmiter RD, Hawrylycz MJ, Jones AR et al. 2010. A robust and high-throughput cre reporting and characterization system for the whole mouse brain. Nat Neurosci. 13(1):133-140.

Mansouri M, Kayserili H, Elalaoui SC, Nishimura G, Iida A, Lyahyai J, Miyake N, Matsumoto N, Sefiani A, Ikegawa S. 2016. Novel ddr2 mutation identified by whole exome sequencing in a moroccan patient with spondylo-meta-epiphyseal dysplasia, short limb-abnormal calcification type. Am J Med Genet A. 170A(2):460-465.

Maruyama T, Jeong J, Sheu TJ, Hsu W. 2016. Stem cells of the suture mesenchyme in craniofacial bone development, repair and regeneration. Nat Commun. 7:10526.

McBratney-Owen B, Iseki S, Bamforth SD, Olsen BR, Morriss-Kay GM. 2008. Development and tissue origins of the mammalian cranial base. Dev Biol. 322(1):121-132.

McLeod MJ. 1980. Differential staining of cartilage and bone in whole mouse fetuses by alcian blue and alizarin red s. Teratology. 22(3):299-301.
Miettinen PJ, Chin JR, Shum L, Slavkin HC, Shuler CF, Derynck R, Werb Z. 1999. Epidermal growth factor receptor function is necessary for normal craniofacial development and palate closure. Nat Genet. 22(1):69-73.
Mizuhashi K, Ono W, Matsushita Y, Sakagami N, Takahashi A, Saunders TL, Nagasawa T, Kronenberg HM, Ono N. 2018. Resting zone of the growth plate houses a unique class of skeletal stem cells. Nature. 563(7730):254-258.
Mohamed FF, Franceschi RT. 2017. Skeletal stem cells: Origins, functions and uncertainties. Curr Mol Biol Rep. 3(4):236-246.
Nagy A, M. Gertsenstein, K. Vintersten, and R. Behringer,. 2007. Staining frozen mouse embryo sections for {beta}-galac- tosidase (lacz), activity. CSH Protoc. pdb.prot4726.
Noden DM. 1988. Interactions and fates of avian craniofacial mesenchyme. Development. 103 Suppl:121-140.
Ovchinnikov DA, Deng JM, Ogunrinu G, Behringer RR. 2000. Col2a1-directed expression of cre recombinase in differentiating chondrocytes in transgenic mice. Genesis. 26(2):145-146.
Pace JM, Li Y, Seegmiller RE, Teuscher C, Taylor BA, Olsen BR. 1997. Disproportionate micromelia (dmm) in mice caused by a mutation in the c-propeptide coding region of col2a1. Dev Dyn. 208(1):25-33.
Rice DP, Aberg T, Chan Y, Tang Z, Kettunen PJ, Pakarinen L, Maxson RE, Thesleff I. 2000. Integration of fgf and twist in calvarial bone and suture development. Development. 127(9):1845-1855.
Robin NH, Falk MJ, Haldeman-Englert CR. 1993. Fgfr-related craniosynostosis syndromes. In: Adam MP, Ardinger HH, Pagon RA, Wallace SE, Bean LJH, Stephens K, Amemiya A, editors. Genereviews((r)). Seattle (WA).
Rozovsky K, Sosna J, Le Merrer M, Simanovsky N, Koplewitz BZ, Bar-Ziv J, Cormier-Daire V, Raas-Rothschild A. 2011. Spondyloepimetaphyseal dysplasia, short limb-abnormal calcifications type: Progressive radiological findings from fetal age to adolescence. Pediatr Radiol. 41(10):1298-1307.
Sakagami N, Ono W, Ono N. 2017. Diverse contribution of col2a1-expressing cells to the craniofacial skeletal cell lineages. Orthod Craniofac Res. 20 Suppl 1:44-49.
Sanders AA, Kaverina I. 2015. Nucleation and dynamics of golgi-derived microtubules. Front Neurosci. 9:431.
Schwabe GC, Trepczik B, Suring K, Brieske N, Tucker AS, Sharpe PT, Minami Y, Mundlos S. 2004. Ror2 knockout mouse as a model for the developmental pathology of autosomal recessive robinow syndrome. Dev Dyn. 229(2):400-410.
Shrivastava A, Radziejewski C, Campbell E, Kovac L, McGlynn M, Ryan TE, Davis S, Goldfarb MP, Glass DJ, Lemke G et al. 1997. An orphan receptor tyrosine kinase family whose members serve as nonintegrin collagen receptors. Mol Cell. 1(1):25-34.
Smithson SF, Grier D, Hall CM. 2009. Spondylo-meta-epiphyseal dysplasia, short limb-abnormal calcification type. Clin Dysmorphol. 18(1):31-35.
Szabova L, Yamada SS, Wimer H, Chrysovergis K, Ingvarsen S, Behrendt N, Engelholm LH, Holmbeck K. 2009. Mt1-mmp and type ii collagen specify skeletal stem cells and their bone and cartilage progeny. J Bone Miner Res. 24(11):1905-1916.
Teddy Cendekiawan RWKWaABMR. 2010. Relationships between cranial base synchondroses and craniofacial development: A review
. The Open Anatomy Journal.67-75.

Thorogood P. 1988. The developmental specification of the vertebrate skull. Development. 103 Suppl:141-153.
Urel-Demir G, Simsek-Kiper PO, Akgun-Dogan O, Gocmen R, Wang Z, Matsumoto N, Miyake N, Utine GE, Nishimura G, Ikegawa S et al. 2018. Further expansion of the mutational spectrum of spondylo-meta-epiphyseal dysplasia with abnormal calcification. J Hum Genet. 63(9):1003-1007.
Velleman SG. 2000. The role of the extracellular matrix in skeletal development. Poult Sci. 79(7):985-989.
Vogel W, Gish GD, Alves F, Pawson T. 1997. The discoidin domain receptor tyrosine kinases are activated by collagen. Mol Cell. 1(1):13-23.
Vora SR, Camci ED, Cox TC. 2015. Postnatal ontogeny of the cranial base and craniofacial skeleton in male c57bl/6j mice: A reference standard for quantitative analysis. Front Physiol. 6:417.
Wei JH, Zhang ZC, Wynn RM, Seemann J. 2015. Gm130 regulates golgi-derived spindle assembly by activating tpx2 and capturing microtubules. Cell. 162(2):287-299.
Wei X, Hu M, Mishina Y, Liu F. 2016. Developmental regulation of the growth plate and cranial synchondrosis. J Dent Res. 95(11):1221-1229.
Wilk K, Yeh SA, Mortensen LJ, Ghaffarigarakani S, Lombardo CM, Bassir SH, Aldawood ZA, Lin CP, Intini G. 2017. Postnatal calvarial skeletal stem cells expressing prx1 reside exclusively in the calvarial sutures and are required for bone regeneration. Stem Cell Reports. 8(4):933-946.
Xu H, Raynal N, Stathopoulos S, Myllyharju J, Farndale RW, Leitinger B. 2011. Collagen binding specificity of the discoidin domain receptors: Binding sites on collagens ii and iii and molecular determinants for collagen iv recognition by ddr1. Matrix Biol. 30(1):16-26.
Young B, Minugh-Purvis N, Shimo T, St-Jacques B, Iwamoto M, Enomoto-Iwamoto M, Koyama E, Pacifici M. 2006. Indian and sonic hedgehogs regulate synchondrosis growth plate and cranial base development and function. Dev Biol. 299(1):272-282.
Zhang M, Xuan S, Bouxsein ML, von Stechow D, Akeno N, Faugere MC, Malluche H, Zhao G, Rosen CJ, Efstratiadis A et al. 2002. Osteoblast-specific knockout of the insulin-like growth factor (igf) receptor gene reveals an essential role of igf signaling in bone matrix mineralization. J Biol Chem. 277(46):44005-44012.
Zhang Y, Su J, Wu S, Teng Y, Yin Z, Guo Y, Li J, Li K, Yao L, Li X. 2015. Ddr2 (discoidin domain receptor 2) suppresses osteoclastogenesis and is a potential therapeutic target in osteoporosis. Sci Signal. 8(369):ra31.
Zhang Y, Su J, Yu J, Bu X, Ren T, Liu X, Yao L. 2011. An essential role of discoidin domain receptor 2 (ddr2) in osteoblast differentiation and chondrocyte maturation via modulation of runx2 activation. J Bone Miner Res. 26(3):604-617.
Zhao H, Feng J, Ho TV, Grimes W, Urata M, Chai Y. 2015. The suture provides a niche for mesenchymal stem cells of craniofacial bones. Nat Cell Biol. 17(4):386-396.

CHAPTER III

The Role of Discoidin Domain Receptor 2 in Tooth Development

Introduction

During tooth development, cell-extracellular matrix (ECM) interactions play an important role in cell adhesion, proliferation, differentiation and formation of dental structures (Chen et al. 2009; Fukumoto and Yamada 2005; Thesleff et al. 1989). Dysregulation of proteins mediating ECM interactions is implicated in several deformities affecting tooth structure and function (Mardh et al. 2002; Umemoto et al. 2012). Type I collagen is the core structural protein in the tooth dentin and bone where collagen-mediated signaling is critical for tissue differentiation and mineralization (Andujar et al. 1991; Nicholls et al. 1996; Thesleff and Hurmerinta 1981). Type I collagen organized into fiber bundles in periodontal ligaments (PDL) is important for tooth function during masticatory loads, proprioception, and regulation of alveolar bone volume (Andujar et al. 1991; McCulloch et al. 2000). Defects in PDL collagen fibers contribute to periodontal diseases, alveolar bone resorption, and tooth loss (Uitto and Larjava 1991). Therefore, proper collagen signaling is essential for development and maintenance of dental and periodontal tissues.

Two classes of receptors mediate cell-collagen interactions: β1-integrins and the discoidin domain receptors, DDR1 and DDR2 (Leitinger 2011). Unlike integrins, DDRs

have intrinsic tyrosine kinase activity and are selectively activated by triple-helical collagens (Shrivastava et al. 1997; Vogel et al. 1997). In addition, DDR1 preferentially binds to and is activated by type IV collagen while DDR2 is strongly activated by type I and III collagens found primarily in bones and teeth (Shrivastava et al. 1997; Vogel et al. 1997). Unlike DDR1, which is found primarily in epithelia, DDR2 is exclusively expressed in mesenchyme (Alves et al. 1995). DDR2 is essential for skeletal development in humans and mice. Patients carrying loss-of-function mutations in *DDR2* develop spondylo-meta-epiphyseal dysplasia (SMED), a rare, autosomal recessive disorder characterized by short stature, short limbs, and craniofacial anomalies (Bargal et al. 2009; Mansouri et al. 2016; Rozovsky et al. 2011). A similar phenotype is observed in *Ddr2*-deficient mice and associated with impaired postnatal bone growth, osteoblast differentiation, chondrocyte proliferation and maturation (Ge et al. 2016; Labrador et al. 2001; Zhang et al. 2011). While these studies uncovered a critical role for *Ddr2* in postnatal skeletal bone development, possible functions of *Ddr2* in teeth and associated structures has not been previously examined.

In this study, we define the tempo-spatial expression of *Ddr2* in dento-alveolar tissues and investigate the functional importance of DDR2 during postnatal development of teeth and surrounding periodontium using a *Ddr2*-deficient mouse model. These findings provide new insights into the role of cell-ECM interactions in the development of teeth and associated structures and may have important implications for understanding periodontal disease

Material and Methods

Mice

Generation and genotyping of *Ddr2*$^{slie/slie}$ mice and *Ddr2*-LacZ (*Ddr2*$^{+/LacZ}$) knock-in mice was previously described (Ge et al. 2018). *Ddr2*$^{fl/fl}$ mice in which exon 8 of the *Ddr2* gene is flanked by two LoxP sequences were generated from "knockout-first" ES cell clone *Ddr2*$^{tm1a(EUCOMM)Wtsi}$(EPD0607__B01; European Mutant Mouse Repository) as described in **(Figure II.6A)**. All mouse experimental procedures conformed to standards for the use of laboratory animals and were approved by the Institutional Animal Care and Use Committee (IACUC) of the University of Michigan. This study conforms to the Animal Research: Reporting In Vivo Experiments (ARRIVE) Guidelines.

Detection of β-gal (Lacz) Expression

Samples dissected from heterozygous *Ddr2-LacZ* (*Ddr2*$^{+/LacZ}$) mice were processed for X-gal staining using standard procedures. Frozen sections were stained with freshly prepared X-gal solution and counterstained with Vector® Nuclear Fast Red.

Tissue Preparation and Histological Analysis

Whole skulls were fixed in 4% paraformaldehyde and processed for paraffin sections. For immunofluorescence, histological sections were incubated with rabbit anti-periostin polyclonal antibody (Abcam, ab14041) and rabbit anti-RUNX2-S319-P (generated in the project laboratory (Ge et al. 2012) overnight at 4°C, and then with Alexa Fluor 488-conjugated donkey anti-rabbit IgG (Invitrogen A21206). For Picro Sirius Red (PSR) staining, paraffin sections were processed as previously described (Coleman 2011) and visualized under polarizing light using an Olympus BX51-P microscope.

Micro–Computed Tomography Analysis of Bone

After fixation in 10% formalin (Fisher), skulls were subjected to micro-computed tomography (μCT) analysis using with a Scanco Model 100 (Scanco Medical). Scan

settings were as follows: voxel size of 12 μm, 70 kVp, 114 μA, 0.5-mm aluminum filter, and integration time of 500 ms. To avoid examiner bias, the genotype of mice was not specifically highlighted during quantification analysis.

Cell Proliferation and TUNEL Assay

For proliferation assays, two week-old mice were intraperitoneally injected with 5-ethynyl-2'-deoxyuridine (EdU, Invitrogen) and sacrificed 4h after injection. Cells incorporating EdU were detected using Click-iT® EdU Alexa Fluor® 488 Imaging Kit (Invitrogen, # C10337). For TUNEL assays, sections were incubated in terminal deoxynucleotidyl transferase dUTP nick end labeling (TUNEL) reaction mixture according to the manufacturer instructions (Calbiochem).

Cell Culture, Transfection and In Vitro Differentiation

Periodontal ligament (PDL) and dental pulp stromal cells (DPSCs) were isolated as described (Balic and Mina 2010). The adenoviruses, Ad5-CMV-LacZ (AdLacZ) and Ad5-CMV-CRE (AdCre) at a titer of $1x10^{11}$ pfu/ml, were obtained from the Vector core, University of Michigan, and MOI of 100 particles/cells was used. Viral transduction did not affect cell viability, cell number or RNA yield (result not shown). Cells were stimulated for 21 days in α-MEM/10% FBS containing 50μg/mL ascorbic acid, 10mM β-glycerophosphate, and 10nM Dexamethasone (DPSCs only). For gene expression analysis, total mRNA was isolated using TRIzol (Invitrogen), cDNA was synthesized, and quantitative RT-PCR was performed on the following mRNAs: *Runx2*, *Col1a1*, *Ibsp*, *Bglap and, Postn* mRNA.

Statistical Analysis

All data was analyzed using the GraphPad Prism software version 6.0e, La Jolla California USA. Values were reported as mean ± SD. Student's *t* test was used for

statistical comparison between the two experimental groups. Differences were considered significant at $P < 0.05$. A sample size of five to seven mice (including both sexes) was used for experiments except where indicated. Cell culture experiments were done in triplicate and repeated at least twice.

Results

Ddr2 is Highly Expressed in Dentin-Forming Odontoblasts, PDL Fibroblasts and Alveolar Osteoblasts

As a prerequisite to examining possible *Ddr2* functions in teeth and associated structures, we examined its spatio-temporal expression pattern using a *Ddr2*-lacZ reporter mouse line. In this mouse, the bacterial LacZ gene is regulated by the endogenous *Ddr2* locus (Ge et al. 2018). *Ddr2*-LacZ expression assessed by X-gal staining was detected in developing and mature teeth of $Ddr2^{+/LacZ}$ mice at postnatal day 1 (P1), 3 (P3), 7 (P7) and 60 (P60) (Fig. 1). However, no X-gal staining was shown in wild-type (WT) littermates (data not show). At P1, X-gal staining was predominately found in the dental papilla mesenchyme and in surrounding dental follicle, which gives rise to cementum, PDL, and alveolar bone **(Figure III.1A and 1E)**. As the tooth continues to form, strong X-gal staining was observed in dentin-forming odontoblasts of the coronal dental pulp and in differentiating odontoblasts of developing molar roots at P3 and P7 **(Figure III.1B,F and 1C,G)**. Weak X-gal staining was found in mesenchymal cells around the Hertwig's epithelial root sheath (HERS) of developing molar roots **(Figure III.1C)**. Similar to molars, the mouse incisor also showed strong X-gal staining in dentin-forming odontoblasts along the incisor length with less evident staining in the proximal mesenchyme around the labial cervical loop at the incisor apex **(Figure III.1I-L)**. Consistent with the exclusive mesenchymal expression of *Ddr*2, no detectable X-gal

staining was seen in dental epithelial cells such as HERS and enamel-secreting ameloblasts. In addition to odontoblast-specific expression, *Ddr2*-LacZ expression was also evident in PDL-forming cells or fibroblastic cells aligned along PDL collagen fibers, and in putative alveolar bone-associated osteoblasts **(Figure III.1D,H)**. The odontoblast- and PDL-specific pattern of *Ddr2* expression was maintained after the completion of tooth formation and eruption into the oral cavity. From these results, we conclude that *Ddr2* is expressed throughout tooth and PDL development and suggest it may have important functions in these tissues.

Ddr2 is Important for Optimal Development of the Molar Root and Periodontium

To investigate the functional role of *Ddr2* in tooth formation, we used $Ddr2^{slie/slie}$ mice, which contain a spontaneous 150-kb deletion in the *Ddr2* locus resulting in an effective null (Kano et al. 2008). Our results showed that molar roots in $Ddr2^{slie/slie}$ mice were shorter than in their WT littermates **(Figure III.2A-D)**. The mean root length in $Ddr2^{slie/slie}$ mice was reduced by 26% at 2 weeks **(Figure III.2E)** and by 17% at 3 months of age **(Figure III.2F),** suggesting delayed root formation. In addition, crown height (from cusp tips to cemento-enamel junction-CEJ) **(Figure III.2G)** and crown width both increased by approximately 11% in 3 month-old $Ddr2^{slie/slie}$ mice **(Figure III.2I)**. When linear tooth measurements were normalized by expressing data as root length/crown height (root/crown ratio), an overall 25% decrease was observed in $Ddr2^{slie/slie}$ mice **(Figure III.2H)**.

Crown and root compositional changes were also seen in $Ddr2^{slie/slie}$ molars. These included a 3% decrease in crown dentin/total crown volume **(Figure III.2J)**, a 15% decrease in the mineralized portion of the root (dentin+cementum volume/total root volume, **Figure III.2K**) and a 46% increase in root pulp volume/total root volume **(Figure**

III.2L). No differences were observed in dentin+cementum mineral density **(Figure III.2M)** or enamel/total crown volume **(Figure III.2N)**. While incisor teeth were shorter in *Ddr2*$^{slie/slie}$ mice, no differences were observed in enamel volume and mineral density (data not shown). In addition to the tooth phenotypes, *Ddr2*$^{slie/slie}$ teeth exhibited a widened PDL space around molar roots **(Figure III.2O,2P)**. This was quantified by MicroCT analysis in 3 month-old mice, which showed that the PDL space adjacent to molars of *Ddr2*$^{slie/slie}$ animals was twice the width of WT controls **(Figure III.2Q)**. From these studies, we conclude that DDR2 signaling is required for optimal tooth morphogenesis and periodontal structure.

Ddr2 is Necessary for Proper PDL Collagen Organization

In addition to the wide PDL space, collagen fiber organization was abnormal in PDLs of *Ddr2*$^{slie/slie}$ teeth. For detailed analysis, we used PSR staining to visualize type I and III collagen fibers under bright-field and polarized light microscopy. This allowed us to assess collagen content, maturation and polarization **(Figure III.3A-D)**. PSR staining, quantified using NIH ImageJ software, revealed an increase (34%) in PDL collagen area in 3 month-old *Ddr2*$^{slie/slie}$ mice compared with WT littermates **(Figure III.3E)**. The data is presented as a percentage of collagen area to total area assessed using the thresholding function of ImageJ. Sharpey's fiber insertions into alveolar bone were also less evident in *Ddr2*$^{slie/slie}$ mice. Periostin is an abundant non-collagenous matricellular protein in the PDL matrix that binds type I collagen and is necessary for maintenance of periodontal health (Rios et al. 2008). We conducted immunofluorescence staining to determine if *Ddr2* status affected levels of this important PDL component. Periostin immunoreactivity was increased in PDLs of *Ddr2*$^{slie/slie}$ mice (320% increase, **Figure III.3J**) and was specifically localized in the PDL space surrounding the molar roots

(Figure III.3F-I). These findings suggest that DDR2 signaling may directly or indirectly regulate periostin expression and thus is important for periodontal integrity and function. Together, our data suggest that DDR2 signaling may determine the amount or integrity of collagen matrix required to maintain periodontal health.

Ddr2 Deficiency is Associated with Progressive Alveolar Bone Loss

To explore the role of *Ddr2* in alveolar bone, Micro-CT and MicroView software were used to assess bone parameters such as bone volume and bone volume fraction. *Ddr2*$^{slie/slie}$ mice displayed a statistically significant reduction (10%) in interradicular alveolar bone volume at 3 months that progressively increased as mice aged **(Figure III.4A-D and 3K)**. Notably, the interradicular alveolar bone between the roots in *Ddr2*$^{slie/slie}$ molars was also thinner (**Figure III.4A-D**, arrowheads in the sagittal view). With age, *Ddr2*$^{slie/slie}$ mice showed a progressive bone loss of about 26% after 5 months and 30% after 10 months (Fig. 4K). Transverse micro-CT views showed a widened PDL space and severe bone defects around the molar roots **(Figure III.4E-H,** arrows**)**. However, no sign of spontaneous tooth loss was observed at any of the ages examined. 3D reconstruction of the lower jaw of 10 month-old animals clearly showed severe alveolar bone loss in *Ddr2*$^{slie/slie}$ mice compared with WT **(Figure III.4I,J)**. Given the significant loss of alveolar bone volume, we performed tartrate-resistant acid phosphatase (TRAP) staining to assess whether *Ddr2* knockout affected osteoclast activity in the supporting alveolar bone. Our results revealed a significant increase in osteoclast numbers in 10-month-old *Ddr2*$^{slie/slie}$ mice **(Figure III.4L-P)**, suggesting that increased osteoclast activity contributes to alveolar bone resorption in knockout mice.

Ddr2 Signaling Regulates Differentiation Potential of Osteogenic and Odontoblastic Lineages of PDL and Dental Pulp Cells, Respectively

To further understand the function of *Ddr2*, we sought to elucidate its effects on cellular activities involved in root formation such as proliferation, differentiation, and apoptosis. To measure proliferation, we administered EdU to 2-week-old *Ddr2*$^{slie/slie}$ mice and the number of EdU+ cells was counted and reported as a percentage of EdU+ cells to the total cells (stained blue with DAPI). Our analysis of the first molars revealed positive EdU staining in PDL and mesenchymal cells surrounding the HERS of developing molar roots in *Ddr2*$^{slie/slie}$ and WT mice **(Figure III.5A-C)**. However, there was no significant difference in the percentage of EdU+ cells, suggesting the proliferation potential of dental cells in *Ddr2*$^{slie/slie}$ and WT teeth was not affected. In addition, no change in the number of apoptotic cells was seen between and *Ddr2*$^{slie/slie}$ and WT, as measured by TUNEL staining along the root dentin odontoblast and PDL regions **(Figure III.5D-F)**.

To assess the influence of *Ddr2* on the differentiation potential of relevant tooth-associated cells, we examined phosphorylation of RUNX2 at Serine 319, which at least in part mediates the effect of DDR2 on osteogenesis (Ge et al. 2016). Immunostaining of p-RUNX2 showed nuclear staining mostly in PDLs and mesenchymal cells around HERS at the apex of the developing roots **(Figure III.5G,H)**. *Ddr2*$^{slie/slie}$ teeth showed reduced levels of RUNX2 phosphorylation compared with WT controls **(Figure III.5I)**, suggesting that RUNX2 activity mediates DDR2 regulation of root development. We also generated cultures of incisor PDL cells (PDLs) and dental pulp stromal cells (DPSCs) from 3-month-old *Ddr2*$^{flox/flox}$ mice and examined differentiation after treatment with either AdLacZ or AdCre **(Figure III.6A)**. PCR analysis of DNA from cultured PDLs and DPSCs treated with AdCre confirmed the deletion of the floxed *Ddr2* allelle with generation of an

approx. 0.7 kb PCR product **(Figure III.6B)**. In addition, *Ddr2* mRNA levels were reduced by > 80%. Control cultures of both cell types mineralized and expressed typical osteoblast/odontoblast/PDL cell markers such as *Runx2*, *Col1a1*, *Bglap*, *Ibsp, and Postn.* For both cell types, *Ddr2* loss dramatically reduced differentiation as measured by expression of the differentiation markers, *Bglap*, *Ibsp, and Postn* **(Figure III.6E,F and 6J,K)**. Partial reduction of *Runx2* and *Col1a1* expression was also noted in dental pulp cultures at later culture times **(Figure III.6G,H)**. Taken together, these results show a clear requirement for *Ddr2* in the differentiation of PDL and dental pulp cells that may explain observed tooth and alveolar bone defects.

Discussion

Type I collagen, the core structural protein in tooth dentin, PDL and alveolar bone, plays an important role during tissue differentiation and mineralization (Andujar et al. 1991; Nicholls et al. 1996; Thesleff and Hurmerinta 1981). Previous studies largely focused on collagen-binding integrins as mediators of the response to this ECM component. However, bone-selective knockout of individual integrins resulted in relatively mild phenotypes (Bengtsson et al. 2005; Gardner et al. 1996; Holtkotter et al. 2002), suggesting the involvement of other collagen receptors. DDR2, a non-integrin collagen activated receptor tyrosine kinase, is critical for bone growth and development. The aim of this study was to examine the function of *Ddr2* in development of the tooth and associated periodontium.

Using LacZ staining, we localized *Ddr2* expression in developing and adult fully erupted teeth. *Ddr2* was expressed in undifferentiated cells in the dental papilla mesenchyme and subsequently in the dentin-forming odontoblasts and dental pulp. *Ddr2* was also highly expressed in the dental follicles during tooth development and in PDL

and alveolar bone of adult teeth. This *Ddr2* distribution suggests potential functions in formation of teeth and periodontium. However, the identity of *Ddr2*-expressing cells in the PDL needs to be determined.

Our analysis of *Ddr2*-deficient mice indicates that proper DDR2 signaling is required for optimal tooth morphogenesis and periodontal integrity. *Ddr2*$^{slie/slie}$ mice had short tooth roots and decreased root/crown ratio resulting in disproportionate tooth size. BMP/TGF-β and Wnt/β-catenin pathways play a critical role in tooth root formation and their disruption could cause a short root phenotype (Wang and Feng 2017). However, we do not know if either of these pathways are involved in DDR2 signaling. Mechanistically, our analysis suggests that RUNX2 phosphorylation mediates *Ddr2* regulation of root development as it does in bone (Ge et al. 2016; Zhang et al. 2011). In addition to the tooth phenotype, *Ddr2*-knockout mice exhibited a progressive alveolar bone loss first seen in the interradicular bone of 3 month-old mice and most dramatic after 10 months. This was accompanied by a dramatic increase in osteoclast numbers. This result was somewhat surprising in view of our previous work, which failed to detect any changes in osteoclast differentiation, tibial osteoclast surface or serum resorption markers in *Ddr2*-deficient mice (Ge et al. 2016). These discrepancies may be explained by the different bone regions being examined. For example, it is possible that the altered PDL structure seen with *Ddr2* deficiency **(Figure III.3)** may lead to changes in mechanical stability of the tooth accompanied by increased osteoclast-mediated bone resorption. Changes in periodontal structure could be a primary effect of *Ddr2* deficiency or be secondary to defects in alveolar bone formation due to impaired osteogenic differentiation of *Dd2*-deficient PDL cells. This would be consistent with the requirement for *Ddr2* in osteoblast differentiation of bone progenitors previously reported (Ge et al.

2016; Zhang et al. 2011). A direct demonstration that *Ddr2* specifically functions in PDL or alveolar bone in vivo will require cell-specific conditional knockout studies.

We also observed a widening of the PDL space in *Ddr2*-deficient mice; however, there was no evidence of PDL widening before tooth eruption (data not shown), suggesting that the PDL changes may require post-eruption occlusal loading. One interpretation of this observation is that loss of *Ddr2* may compromise PDL structure, which then fails when exposed to occlusal loads leading to PDL widening. Interestingly, there are anecdotal reports of tooth abnormalities in some SMED patients, although it is not known if the specific changes in tooth or PDL structure we describe in mice were present (Bargal et al. 2009).

Consistent with its effect on the periodontium, *Ddr2*$^{slie/slie}$ teeth also had atypical PDL collagen fibers associated with a significant increase in periostin immunostaining. However, periostin mRNA levels were significantly reduced in *Ddr2*-deficient PDL cells. This inverse correlation between periostin mRNA and protein is not understood. Periostin, a collagen-binding protein, is required to maintain PDL integrity and for proper collagen fibril formation and maturation (Rios et al. 2008). Aberrant PDL collagen fibers in *Ddr2* knockout could be due to impaired collagen fiber formation, crosslinking and/or maturation. A possible role of *Ddr2* in collagen crosslinking was previously demonstrated; these studies showed that *Ddr2* activation with type I collagen induces lysyl oxidase, the enzyme required for ECM crosslinking (Khosravi et al. 2014). Abnormalities in collagen deposition and/ or cross-linking have been reported in *Ddr2*-deficient heart and postnatal testicular tissues (Cowling et al. 2014; Zhu et al. 2015). Further studies will be required to resolve if *Ddr2* also controls collagen fibrillogenesis in dental structures.

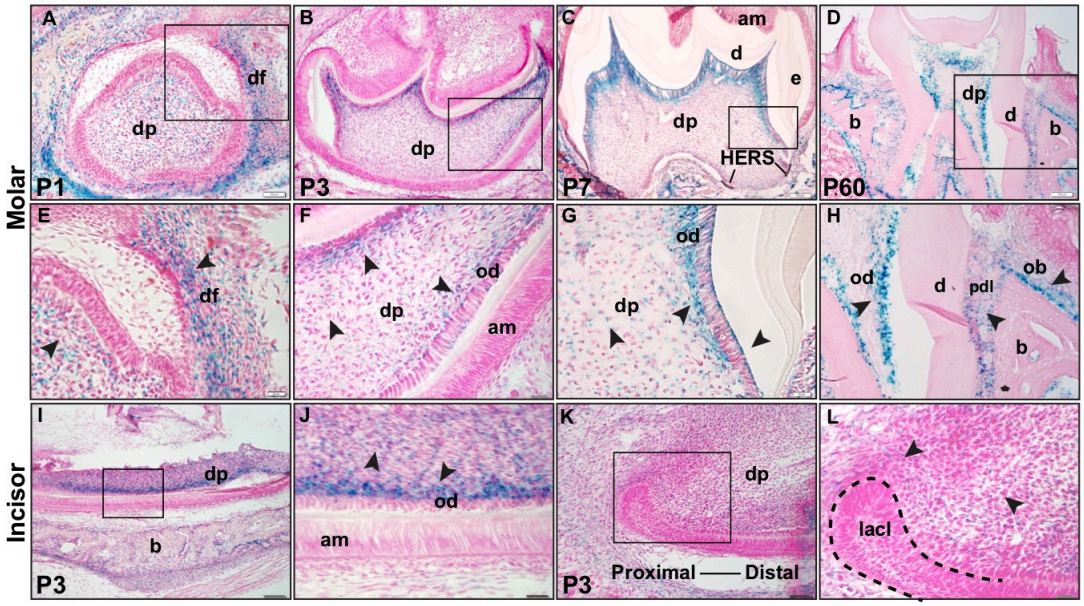

Figure III.1: Localization and expression of *Ddr2* in dental and periodontal tissues. (A-H) X-Gal staining of *Ddr2*$^{+/LacZ}$ mice reveals *Ddr2* expression in the molars during development through adulthood. (A) At P1, *Ddr2* expression is observed in dental papilla (dp) and surrounding dental follicle (df) in developing molars (high magnification in E). (B-D) *Ddr2*-LacZ expression is selectively high in dentin-producing odontoblasts (od) at P3, P7, and P60. (F,G) High magnification also reveals *Ddr2* expression in odontoblasts (od) and a subset of cells in dental pulp (dp). In a fully erupted molar (D,H), *Ddr2* is expressed in PDL cells (pdl) and putative alveolar bone-associated osteoblasts (ob). Black arrowheads point to the expression sites. (I,K) and high magnification (J,L) shows *Ddr2* expression in odontoblasts (od) of lower incisors, in dental pulp (dp) and around the labial cervical loop (lacl) at the proximal end of the incisor (dashed lines). No *Ddr2* expression was seen in molar (F) or incisor (J) ameloblasts (am). Scale bar: 100 μm in (A-D, K); 20 μm in (E-G, J, L).

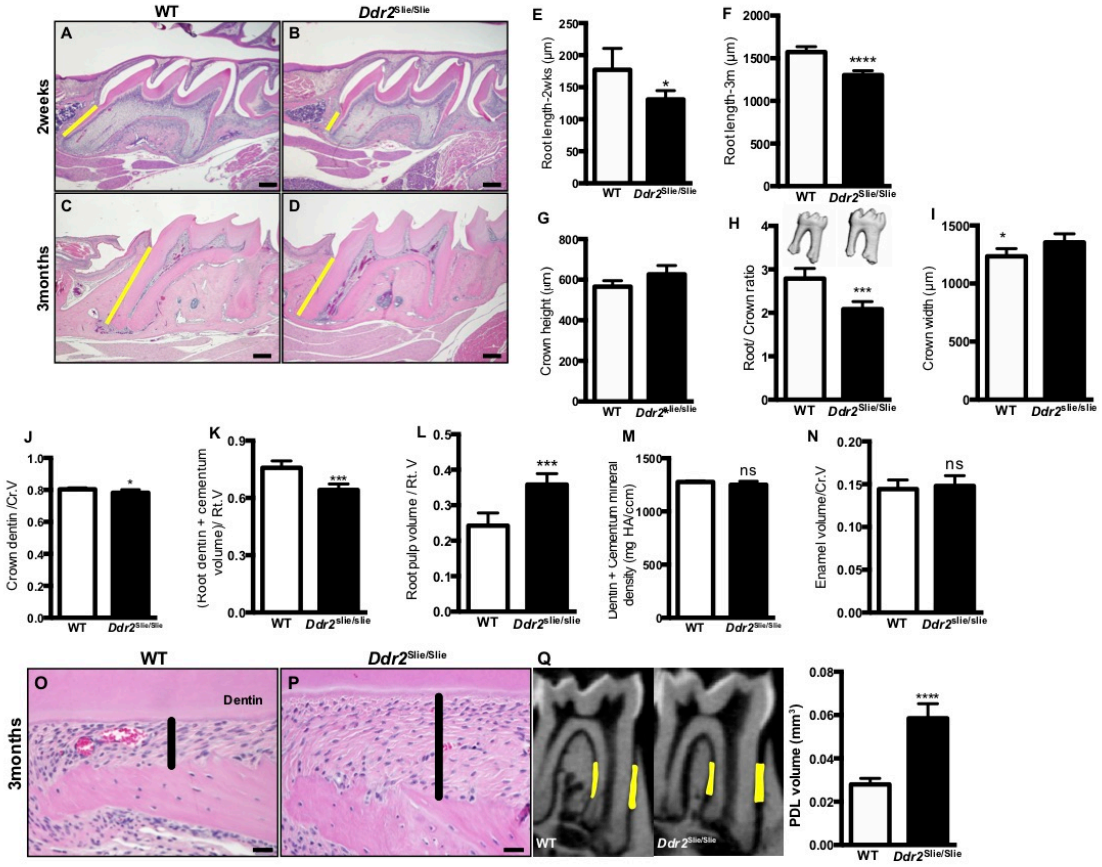

Figure III.2: Tooth and periodontal phenotypes in *Ddr2*-deficient mice. (A-D) Representative hematoxylin and eosin staining of teeth showing delayed molar root formation (yellow lines) in developing (B) and adult teeth (D) compared with WT. (E,F) Quantification of the molar root length at 2 weeks (E) and 3 months of age (F). (G-I) Quantification of the crown height, the molar root/crown ratio, and the crown width. (J-N) Quantification of crown dentin/crown volume (Cr.V), root dentin+cementum/ root volume (Rt.V), root pulp volume/Rt.V, dentin+cementum mineral density, the enamel volume/Cr.V in the first molar. (O,P) H&E staining shows wide PDL spacing (highlighted in black lines) in *Ddr2*$^{slie/slie}$ mice compared with WT. (Q) Quantification of wide PDL spacing in *Ddr2*$^{slie/slie}$ mice compared with WT littermates (right) and the region of interest (left). **P*<0.05, ****P*<0.001, *****P*<0.0001, ns, not significant. n=5-7 mice/group. Scale bar: 50 μm in (A, B); 200 μm in (C, D); 20 μm in (O,P).

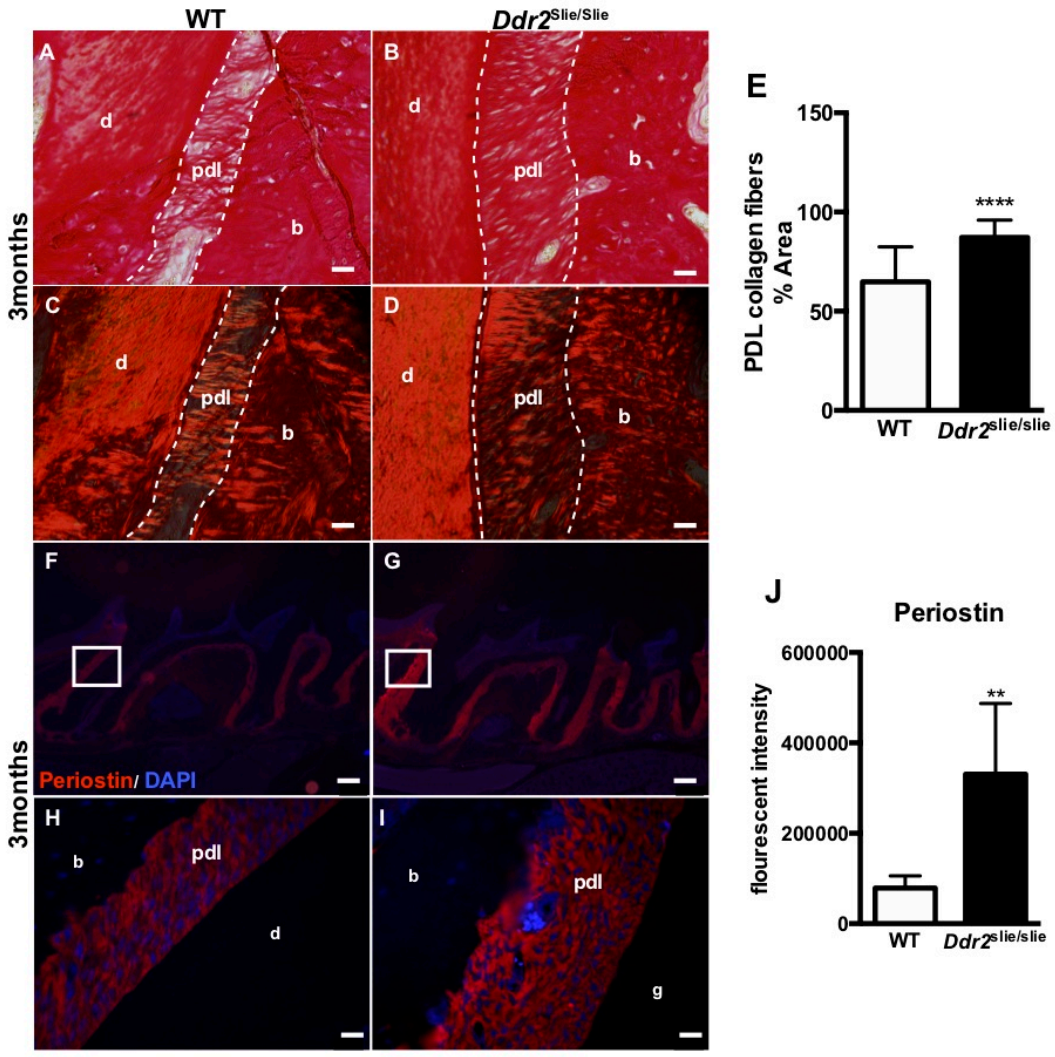

Figure III.3: *Ddr2*$^{slie/slie}$ teeth had atypical periodontal collagen fibers. (A-D) Picro-sirius red (PSR) staining of PDL collagen fibers in 3-month-old mice under a bright-field (A,B) and a polarizing (C,D) microscopy. (E) Quantification of the PDL collagen area stained with PSR, *n=3* mice, six measurements per mouse. (F-I) Immunostaining of periostin (red) with inserts (H,I) showing periostin expression in the PDL space surrounding the molar roots. The cell nuclei were stained with DAPI (blue). (J) Quantification of the fluorescent intensity of periostin immunostaining, n= 3 mice, five measurements per mouse. ***P*<0.01, *****P*<0.0001, ns, not significant. Scale bar: 200 µm in (F,G), 20 µm in (A-D, H,I).

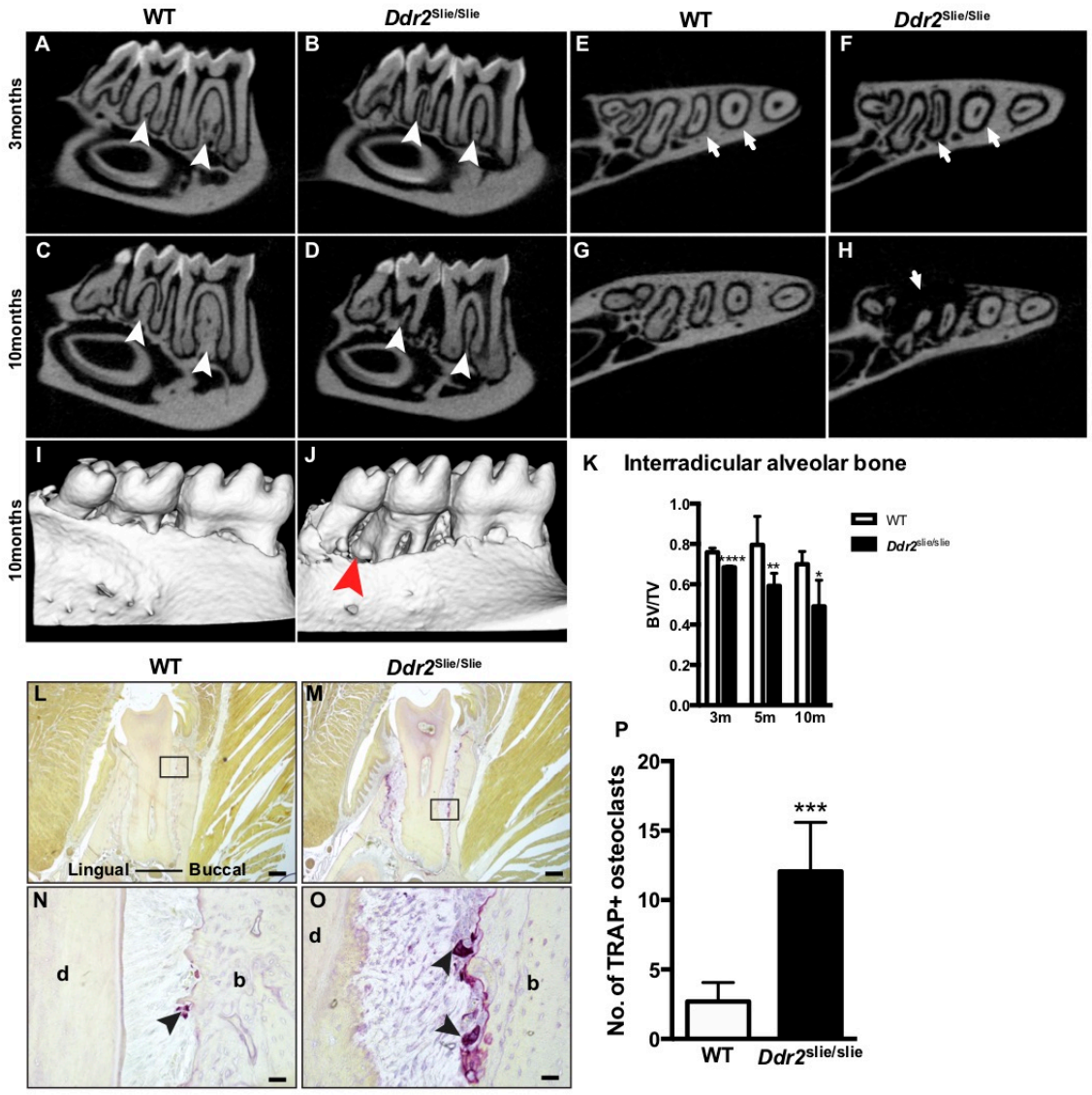

Figure III.4: Progressive alveolar bone loss in *Ddr2* knockout. (A-H) Representative micro-computed tomography (μCT) images showing alveolar bone defects (white arrowheads) and wide PDL spacing (white arrows) in *Ddr2*$^{slie/slie}$ mice at 3 (B,F) and 10 (D,H) months of age compared with WT. (I,J) Three-dimensional reconstruction of the lower jaw section showing severe bone defects (red arrowhead) around lower teeth at 10 months of age. (K) μCT analysis of bone volume/total volume of interradicular alveolar bone of the first and second molars (n=5-7 mice/group). (L-O) Representative TRAP staining images showing osteoclasts (purple color, arrowheads) along the alveolar bone surface at 10 months. (P) Quantification of TRAP+ osteoclasts. **P*<0.05, ***P*<0.01, ****P*<0.001, *****P*<0.0001. Scale bar: 200 μm in (L, M).

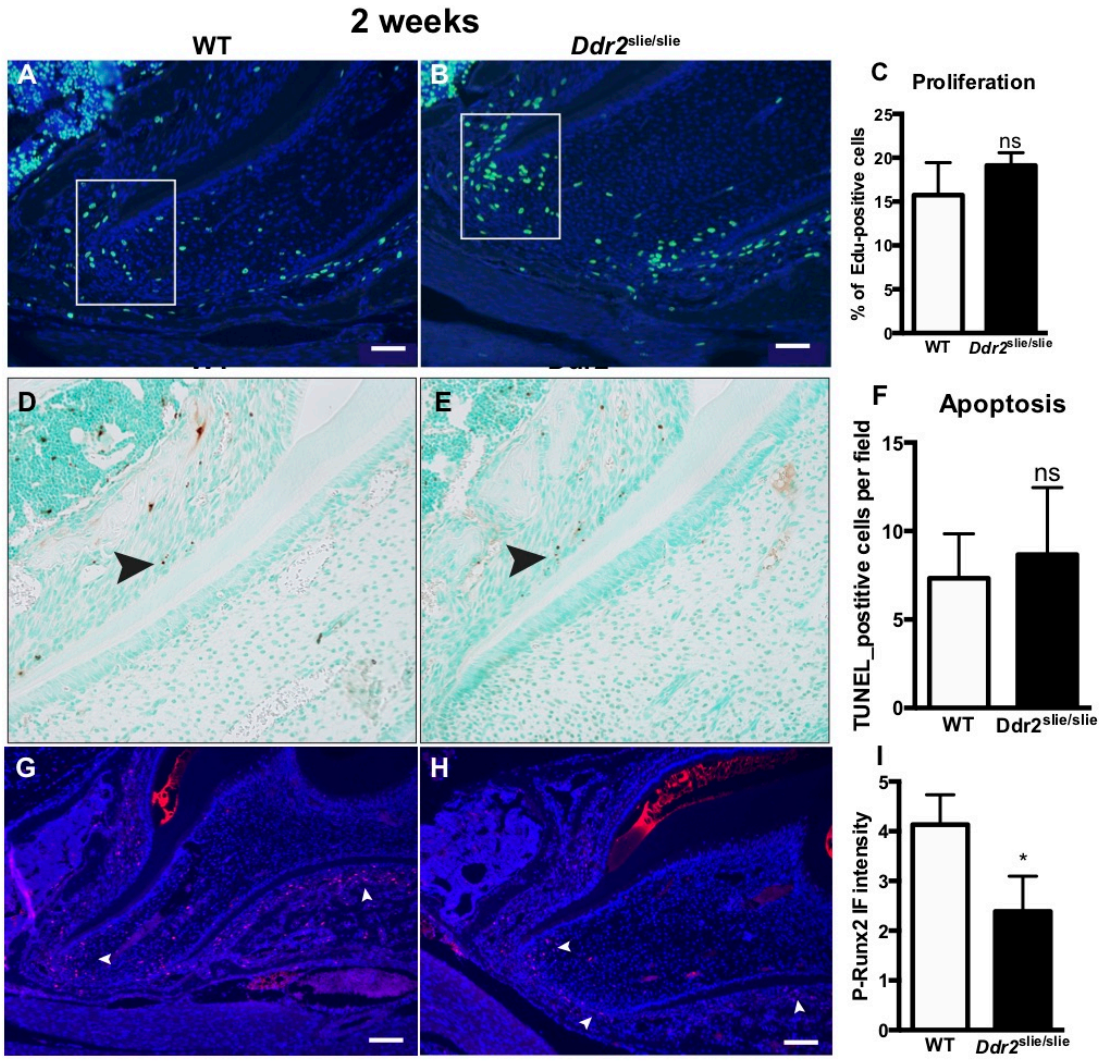

Figure III.5: *Ddr2*-knockout teeth showed reduced RUNX2 activity. (A,B) Representative images of EdU staining for labeling proliferating cells (green) and DAPI staining for cell nuclei (blue). (C) Quantification of the percentage of EdU-positive cells. (D,E) Representative images of TUNEL staining of the first molars in *Ddr2*$^{slie/slie}$ and WT mice. (F) Quantification of TUNEL-positive cells (brown) per field. Cell nuclei were stained with methyl green (green). (G,H) Representative images of p-RUNX2 immunostaining (red) in the nuclei of PDL cells and at the apex of developing root. (I) Quantification of the fluorescent intensity of p-RUNX2 immunostaining, n= 3 mice. **P*<0.05, ns, not significant. Scale bar: 50 μm in (A, B), 100 μm in (G, H).

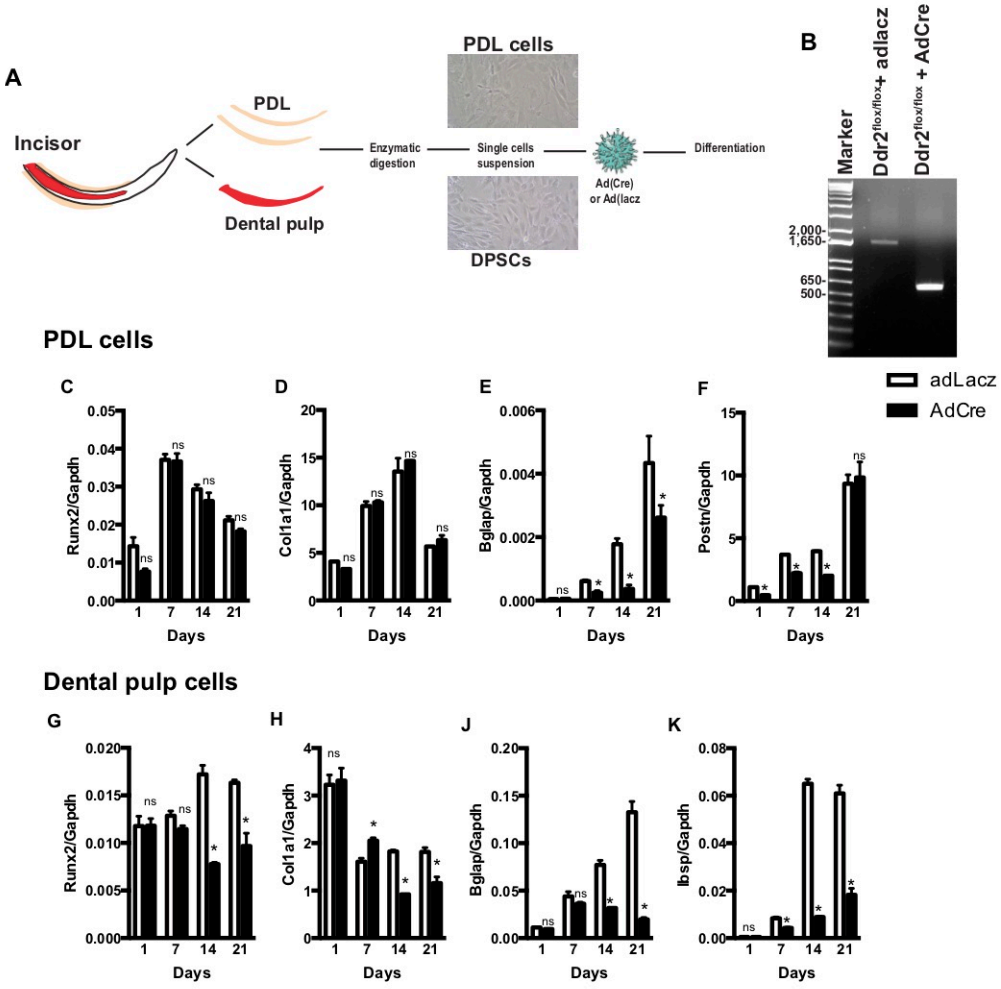

Figure III.6: *Ddr2* knockout exhibits decreased osteogenic and odontogenic differentiation of PDL and dental pulp cells, respectively. (A) Experimental design of cell isolation, viral transduction, and differentiation in vitro. (B) PCR analysis showing Cre-mediated recombination of the floxed Ddr2 alleles resulting in a PCR product of 600pb after treatment with AdCre. (C-F) Quantification of differentiation markers for PDL cells. (G-K) Quantification of differentiation markers for DPSCs after 21 days. **P*<0.05, ns, not significant, n = 3 cell cultures/group.

Table III.1: Probes used for qRT-PCR

Gene	Full name	Assay ID
Col1a1	Collagen, type I, alpha 1	Mm00801666_g1
Postn	Periostin, osteoblast specific factor	Mm00450111_m1
Runx2	Runt related transcription factor 2	Mm00501584_m1
Bglap	Bone gamma carboxyglutamate protein	Mm03413826_mH
Ibsp	Integrin binding sialoprotein	Mm00492555_m1
Gapgh	Glyceraldehyde-3-phosphate dehydrogenas	Mm99999915_g1

References

Alves F, Vogel W, Mossie K, Millauer B, Hofler H, Ullrich A. 1995. Distinct structural characteristics of discoidin i subfamily receptor tyrosine kinases and complementary expression in human cancer. Oncogene. 10(3):609-618.

Andujar MB, Couble P, Couble ML, Magloire H. 1991. Differential expression of type i and type iii collagen genes during tooth development. Development. 111(3):691-698.

Balic A, Mina M. 2010. Characterization of progenitor cells in pulps of murine incisors. J Dent Res. 89(11):1287-1292.

Bargal R, Cormier-Daire V, Ben-Neriah Z, Le Merrer M, Sosna J, Melki J, Zangen DH, Smithson SF, Borochowitz Z, Belostotsky R et al. 2009. Mutations in ddr2 gene cause smed with short limbs and abnormal calcifications. Am J Hum Genet. 84(1):80-84.

Bengtsson T, Aszodi A, Nicolae C, Hunziker EB, Lundgren-Akerlund E, Fassler R. 2005. Loss of alpha10beta1 integrin expression leads to moderate dysfunction of growth plate chondrocytes. J Cell Sci. 118(Pt 5):929-936.

Chen B, Goodman E, Lu Z, Bandyopadhyay A, Magraw C, He T, Raghavan S. 2009. Function of beta1 integrin in oral epithelia and tooth bud morphogenesis. J Dent Res. 88(6):539-544.

Coleman R. 2011. Picrosirius red staining revisited. Acta Histochem. 113(3):231-233.

Cowling RT, Yeo SJ, Kim IJ, Park JI, Gu Y, Dalton ND, Peterson KL, Greenberg BH. 2014. Discoidin domain receptor 2 germline gene deletion leads to altered heart structure and function in the mouse. Am J Physiol Heart Circ Physiol. 307(5):H773-781.

Fukumoto S, Yamada Y. 2005. Review: Extracellular matrix regulates tooth morphogenesis. Connect Tissue Res. 46(4-5):220-226.

Gardner H, Kreidberg J, Koteliansky V, Jaenisch R. 1996. Deletion of integrin alpha 1 by homologous recombination permits normal murine development but gives rise to a specific deficit in cell adhesion. Dev Biol. 175(2):301-313.

Ge C, Mohamed F, Binrayes A, Kapila S, Franceschi RT. 2018. Selective role of discoidin domain receptor 2 in murine temporomandibular joint development and aging. J Dent Res. 97(3):321-328.

Ge C, Wang Z, Zhao G, Li B, Liao J, Sun H, Franceschi RT. 2016. Discoidin receptor 2 controls bone formation and marrow adipogenesis. J Bone Miner Res.

Ge C, Yang Q, Zhao G, Yu H, Kirkwood KL, Franceschi RT. 2012. Interactions between extracellular signal-regulated kinase 1/2 and p38 map kinase pathways in the control of runx2 phosphorylation and transcriptional activity. J Bone Miner Res. 27(3):538-551.

Holtkotter O, Nieswandt B, Smyth N, Muller W, Hafner M, Schulte V, Krieg T, Eckes B. 2002. Integrin alpha 2-deficient mice develop normally, are fertile, but display partially defective platelet interaction with collagen. J Biol Chem. 277(13):10789-10794.

Kano K, Marin de Evsikova C, Young J, Wnek C, Maddatu TP, Nishina PM, Naggert JK. 2008. A novel dwarfism with gonadal dysfunction due to loss-of-function allele of the collagen receptor gene, ddr2, in the mouse. Mol Endocrinol. 22(8):1866-1880.

Khosravi R, Sodek KL, Faibish M, Trackman PC. 2014. Collagen advanced glycation inhibits its discoidin domain receptor 2 (ddr2)-mediated induction of lysyl oxidase in osteoblasts. Bone. 58:33-41.

Labrador JP, Azcoitia V, Tuckermann J, Lin C, Olaso E, Manes S, Bruckner K, Goergen JL, Lemke G, Yancopoulos G et al. 2001. The collagen receptor ddr2 regulates proliferation and its elimination leads to dwarfism. EMBO Rep. 2(5):446-452.

Leitinger B. 2011. Transmembrane collagen receptors. Annu Rev Cell Dev Biol. 27:265-290.

Mansouri M, Kayserili H, Elalaoui SC, Nishimura G, Iida A, Lyahyai J, Miyake N, Matsumoto N, Sefiani A, Ikegawa S. 2016. Novel ddr2 mutation identified by whole exome sequencing in a moroccan patient with spondylo-meta-epiphyseal dysplasia, short limb-abnormal calcification type. Am J Med Genet A. 170A(2):460-465.

Mardh CK, Backman B, Holmgren G, Hu JC, Simmer JP, Forsman-Semb K. 2002. A nonsense mutation in the enamelin gene causes local hypoplastic autosomal dominant amelogenesis imperfecta (aih2). Hum Mol Genet. 11(9):1069-1074.

McCulloch CA, Lekic P, McKee MD. 2000. Role of physical forces in regulating the form and function of the periodontal ligament. Periodontol 2000. 24:56-72.

Nicholls AC, Oliver J, McCarron S, Winter GB, Pope FM. 1996. Splice site mutation causing deletion of exon 21 sequences from the pro alpha 2(i) chain of type i collagen in a patient with severe dentinogenesis imperfecta but very mild osteogenesis imperfecta. Hum Mutat. 7(3):219-227.

Rios HF, Ma D, Xie Y, Giannobile WV, Bonewald LF, Conway SJ, Feng JQ. 2008. Periostin is essential for the integrity and function of the periodontal ligament during occlusal loading in mice. J Periodontol. 79(8):1480-1490.

Rozovsky K, Sosna J, Le Merrer M, Simanovsky N, Koplewitz BZ, Bar-Ziv J, Cormier-Daire V, Raas-Rothschild A. 2011. Spondyloepimetaphyseal dysplasia, short limb-abnormal calcifications type: Progressive radiological findings from fetal age to adolescence. Pediatr Radiol. 41(10):1298-1307.

Shrivastava A, Radziejewski C, Campbell E, Kovac L, McGlynn M, Ryan TE, Davis S, Goldfarb MP, Glass DJ, Lemke G et al. 1997. An orphan receptor tyrosine kinase family whose members serve as nonintegrin collagen receptors. Mol Cell. 1(1):25-34.

Thesleff I, Hurmerinta K. 1981. Tissue interactions in tooth development. Differentiation. 18(2):75-88.

Thesleff I, Vainio S, Jalkanen M. 1989. Cell-matrix interactions in tooth development. Int J Dev Biol. 33(1):91-97.

Uitto VJ, Larjava H. 1991. Extracellular matrix molecules and their receptors: An overview with special emphasis on periodontal tissues. Crit Rev Oral Biol Med. 2(3):323-354.

Umemoto H, Akiyama M, Domon T, Nomura T, Shinkuma S, Ito K, Asaka T, Sawamura D, Uitto J, Uo M et al. 2012. Type vii collagen deficiency causes defective tooth enamel formation due to poor differentiation of ameloblasts. Am J Pathol. 181(5):1659-1671.

Vogel W, Gish GD, Alves F, Pawson T. 1997. The discoidin domain receptor tyrosine kinases are activated by collagen. Mol Cell. 1(1):13-23.

Wang J, Feng JQ. 2017. Signaling pathways critical for tooth root formation. J Dent Res. 96(11):1221-1228.

Zhang Y, Su J, Yu J, Bu X, Ren T, Liu X, Yao L. 2011. An essential role of discoidin domain receptor 2 (ddr2) in osteoblast differentiation and chondrocyte maturation via modulation of runx2 activation. J Bone Miner Res. 26(3):604-617.

Zhu CC, Tang B, Su J, Zhao H, Bu X, Li Z, Zhao J, Gong WD, Wu ZQ, Yao LB et al. 2015. Abnormal accumulation of collagen type i due to the loss of discoidin

domain receptor 2 (ddr2) promotes testicular interstitial dysfunction. PLoS One. 10(7):e0131947.

CHAPTER IV

Conclusion and Future Directions

Conclusion

Extracellular matrix is a critical regulator of skeletal development and growth, and has been implicated in a wide spectrum of human skeletal disorders, most of which involve craniofacial structures (Erlebacher et al. 1995; Kuivaniemi et al. 1997; Lu et al. 2011; Velleman 2000). Defects in cranial growth and development cause a wide range of disorders known to dramatically impact physical, social and emotional development of affected children. An understanding of the critical molecules and pathways necessary for the development of craniofacial skeleton is necessary to successfully treat these patients. In this dissertation, we present in vivo studies for understanding the role of discoidin domain receptor 2 (DDR2) in craniofacial development, including tooth development. Using a *Ddr2*-LacZ knock-in mouse model, we demonstrate that *Ddr2* is expressed prenatally during craniofacial development in developing midface including the cranial base, tooth buds and mandible. *Ddr2* is expressed in suture mesenchyme, periosteum and dura mater of flanking calvaria bone, and has a lineage-restricted expression in resting and proliferative chondrocytes of cranial base synchondrosis. LacZ staining could not could detect *Ddr2* expression in osteocytes or hypertrophic chondrocytes, the terminally differentiated cells, suggesting a function in skeletal progenitor cells. Using a lineage-tracing approach, we demonstrate the contribution of *Ddr2*+ cells to skeletal elements in the cranial vault and cranial base. Our findings

suggest that functions of *Ddr2* in the craniofacial skeleton are mainly due to actions in chondrocyte and osteoblast lineages, but not in osteoclasts. We also demonstrate overlapping expression between *Ddr2* and Gli1-expressing cells, previously characterized stem cells in craniofacial and long bones (Shi et al. 2017; Zhao et al. 2015). Our study also demonstrates, for the first time, that Gli1 is expressed in the cranial base synchondrosis in addition to previously described region in cranial sutures and subchondral region in long bones (Shi et al. 2017; Zhao et al. 2015). Using conditional knockouts, we demonstrate that *Ddr2* functions in Gli1+ stem/progenitor cells in cranial sutures and the cranial base to regulate postnatal development of craniofacial skeleton, and that the function of *Ddr2* in cranial sutures is independent from its function in the synchondrosis growth plate. Together, our findings clearly establish an important function of *Ddr2* in skeletal progenitor cells and chondrocytes during postnatal development of craniofacial skeleton, and help advance our understanding of the roles of cell-matrix interactions in craniofacial development by establishing the functions of a new collagen receptor.

Future Directions

Our data indicate that *Ddr2* functions in skeletal lineage progenitors to regulate craniofacial bone formation. We demonstrate *Ddr2* expression in the suture mesenchyme, calvaria marrow and long bone marrow where undifferentiated cells reside. Also, lineage tracing of *Ddr2*+ cells is consistent with them being skeletal stem/progenitor cells. However, additional validation is important to further elucidate the identity of *Ddr2*+ cells using flow cytometry and immunofluorescence along with putative markers of sutural (Gli1, Axin2 and Prx1) and marrow skeletal stem/progenitor cells (Nestin, PDGFRα, CD51, Leptin R). To further assess potential stemness of *Ddr2*+ cells,

we could perform colony formation assays, which is one of the important criteria for characterizing skeletal stem cells. TdTomato+ cells will be sorted from tamoxifen-injected *Ddr2*^{Mer,iCre,Mer}; Ai14 tdTomato mice (from calvaria, synchondrosis and long bone growth plate) and will be plated at clonal density to analyze the ability of these cells to form tdTomato+ clones. Clonogenic cells that arise from a common progenitor or stem cell are known to be multipotent in terms of their ability to form cartilage, bone and fat. Complementary experiments using a lineage-tracing approach will be performed in vivo with a single tamoxifen injection to determine if individual *Ddr2*+ cells differentiate to skeletal cells as was suggested from our experiments. To identify the progeny of *Ddr2*+ cells, we will use specific markers, such as bone sialoprotein or osteocalcin for osteoblasts, perilipin for adipocytes, PDGFRα and Leptin receptor for marrow stromal cells. In the current study, our tracing experiments were conducted within a two-month window; however, longer tracing times are needed to determine the persistence of tdTomato+ cells, especially in tissues with low turnover rate, such as cranial sutures. Using LacZ localization, we showed that *Ddr2* expression appears during prenatal development even before chondrocyte differentiation and hypertrophy and the appearance of mature osteoblasts, which is additional evidence supporting our hypothesis of a putative function of *Ddr2* in progenitors of the skeletal lineage.

As a perquisite for understanding the contribution of putative *Ddr2*+ progenitors, it is important to use tracing analysis to mark *Ddr2*-expressing cells during early development at E12.5, and trace their progeny at E13.5 (appearance of hypertrophic chondrocytes), E14.5 (bone collar formation), and E18.5 (expanded long bone mineralization and cranial suture formation) and postnatal 2 months or 6 months. Concomitantly, analysis of the identity and contribution of *Ddr2*+ cells to tooth development will be investigated at indicated times. In Chapter 3, we showed that *Ddr2*-

deficient mice exhibit short tooth molar roots. To further understand mechanisms underlying root formation, we also will determine if *Ddr2* co-localizes with Gli1+ cells associated with molar roots, as it does in the cranial base and sutures. Teeth from Gli1-CreERT; *Ddr2*$^{fl/fl}$ will also be analyzed to ascertain the function of *Ddr2* in Gli1+ cells during tooth root formation.

In prior work, we showed that *Ddr2* is required for osteoblast differentiation and mineralization of bone marrow stromal cells and calvarial osteoblasts (Ge et al. 2016). We demonstrated that *Ddr2* regulates osteoblast differentiation by promoting ERK/MAPK-dependent RUNX2 phosphorylation and upregulation of osteoblast specific genes, such as bone sialoprotein and osteocalcin. In this thesis, we showed a requirement for *Ddr2* in odontogenic differentiation of dental pulp cells and osteoblast differentiation of periodontal ligament cells (PDLs). Our data suggests that *Ddr2* activation of RUNX2 phosphorylation may underlie the mechanism of osteoblast differentiation of PDLs. While our findings suggest a *Ddr2* requirement during early osteoblast differentiation, its function in mature osteoblasts cannot be excluded. In the future, we will perform additional conditional knockouts using Ocn-Cre or 2.3 Col1-cre to ascertain if *Ddr2* is required for differentiation/activity of mature osteoblasts or odontoblast in bone and tooth formation. Furthermore, our loss-of-function studies demonstrate that *Ddr2* knockout profoundly impacts the anterior craniofacial skeleton. Using LacZ staining, we show *Ddr2* expression initially in the anterior part of skull, which is typically derived from neural crest cells. Furthermore, disruption of *Ddr2* either in global or conditional knockouts had greater effects on anterior skull structures such as the ISS of the cranial base or nasal bones. This suggests that *Ddr2* is required for the development of neural crest-derived craniofacial structures. To address this, neural crest-specific conditional knockouts of Ddr2 using Wnt1-Cre or P0-Cre are needed.

Our work also highlights the importance of *Ddr2* in regulation of collage-rich extracellular matrix, since *Ddr2* knockout disrupted the distribution of type fibrillar type II collagen in cranial base synchondrosis and altered collagens in periodontal ligaments of teeth. As a result, *Ddr2* knockout disrupted chondrocyte organization and polarization as demonstrated by altered distribution of GM130, a marker for Golgi apparatus. We hypothesize that *Ddr2* regulates collagen fibrillogenesis, secretion and remodeling to support extracellular matrix function for maintaining spatial organization and cell polarization during cell proliferation and subsequent differentiation. Perhaps the most interesting finding of this study is the perturbed structure of GM130 in *Ddr2*-deficient mice. GM130 is tethered with the cytoskeleton and is required for mitotic spindle formation, cell cycle progression and directed cell migration and it is critical for growth and survival of mice (Colanzi and Corda 2007; Liu et al. 2017; Sanders and Kaverina 2015; Wei et al. 2015; Witkos and Lowe 2015). Knockout of GM130 results in significant growth retardation and reduced survival rate in mice (Liu et al. 2017). In view of these studies, we asked if *Ddr2* is involved in cytoskeleton organization and GM130 polarization. However, it is not known if there is a direct interaction between DDR2 and the cytoskeleton or if DDR2 has functions in maintaining cytoskeleton organization. Interestingly, the DS domain of DDR2 exhibits high homology to discoidin I-like domain of the slime mold Dictyostelium discoideum. The DS domain in Dictyostelium discoideum is important for cell adhesion and cytoskeletal organization. Whether *Ddr2* plays a role in maintaining cytoskeletal organization has not been explored in mammals. Together, this study suggests a direct role of extracellular matrix through collagen-mediated *Ddr2* signaling in regulation cell proliferation, differentiation and remodeling, maintaining collagen matrix and cell polarization, and thus normal development of craniofacial skeleton.

Reference

Colanzi A, Corda D. 2007. Mitosis controls the golgi and the golgi controls mitosis. Curr Opin Cell Biol. 19(4):386-393.

Erlebacher A, Filvaroff EH, Gitelman SE, Derynck R. 1995. Toward a molecular understanding of skeletal development. Cell. 80(3):371-378.

Ge C, Wang Z, Zhao G, Li B, Liao J, Sun H, Franceschi RT. 2016. Discoidin receptor 2 controls bone formation and marrow adipogenesis. J Bone Miner Res.

Kuivaniemi H, Tromp G, Prockop DJ. 1997. Mutations in fibrillar collagens (types i, ii, iii, and xi), fibril-associated collagen (type ix), and network-forming collagen (type x) cause a spectrum of diseases of bone, cartilage, and blood vessels. Hum Mutat. 9(4):300-315.

Liu C, Mei M, Li Q, Roboti P, Pang Q, Ying Z, Gao F, Lowe M, Bao S. 2017. Loss of the golgin gm130 causes golgi disruption, purkinje neuron loss, and ataxia in mice. Proc Natl Acad Sci U S A. 114(2):346-351.

Lu P, Takai K, Weaver VM, Werb Z. 2011. Extracellular matrix degradation and remodeling in development and disease. Cold Spring Harb Perspect Biol. 3(12).

Sanders AA, Kaverina I. 2015. Nucleation and dynamics of golgi-derived microtubules. Front Neurosci. 9:431.

Shi Y, He G, Lee WC, McKenzie JA, Silva MJ, Long F. 2017. Gli1 identifies osteogenic progenitors for bone formation and fracture repair. Nat Commun. 8(1):2043.

Velleman SG. 2000. The role of the extracellular matrix in skeletal development. Poult Sci. 79(7):985-989.

Wei JH, Zhang ZC, Wynn RM, Seemann J. 2015. Gm130 regulates golgi-derived spindle assembly by activating tpx2 and capturing microtubules. Cell. 162(2):287-299.

Witkos TM, Lowe M. 2015. The golgin family of coiled-coil tethering proteins. Front Cell Dev Biol. 3:86.

Zhao H, Feng J, Ho TV, Grimes W, Urata M, Chai Y. 2015. The suture provides a niche for mesenchymal stem cells of craniofacial bones. Nat Cell Biol. 17(4):386-396.